ISBN 978-82-326-1482-0 (printed version)
ISBN 978-82-326-1483-7 (electronic version)
ISSN 1503-8181

NTNU
Norwegian University of
Science and Technology

Doctoral Thesis

Andrés Codas Duarte

Doctoral theses at NTNU, 2016:72

Andrés Codas Duarte

Contributions to production optimization of oil reservoirs

Doctoral theses at NTNU, 2016:72

NTNU

NTNU
Norwegian University of
Science and Technology
Faculty of Information Technology,
Mathematics and Electrical Engineering
Department of Engineering Cybernetics

NTNU
Norwegian University of
Science and Technology

Andrés Codas Duarte

Contributions to production optimization of oil reservoirs

Thesis for the degree of Philosophiae Doctor

Trondheim, March 2016

Norwegian University of Science and Technology
Faculty of Information Technology,
Mathematics and Electrical Engineering
Department of Engineering Cybernetics

NTNU
Norwegian University of
Science and Technology

NTNU
Norwegian University of Science and Technology

Thesis for the degree of Philosophiae Doctor

Faculty of Information Technology,
Mathematics and Electrical Engineering
Department of Engineering Cybernetics

ISBN 978-82-326-1482-0 (printed version)
ISBN 978-82-326-1483-7 (electronic version)
ISSN 1503-8181

Doctoral theses at NTNU, 2016:72

Printed by Skipnes Kommunikasjon as

To those Saturday mornings with OMAPA

To those geriatric Saturday nights

Summary

This thesis covers methods for optimization of oil production in three time-scales. In the long-term perspective, years, it is desired to maximize the economic return of the field operation, or alternatively, it is desired to maximize the oil recovery factor. In the middle-term perspective, days, optimal scheduling and allocation of the production facilities are desired. In the short-term perspective, minutes, it is desired to maintain the process operating at a stable optimal set-point. The integration of the optimization solutions that tackle each of the layers independently is a formidable challenge. This requires the development of mathematical models and efficient optimization algorithms to deliver solutions in real-time.

This research focuses on efficient optimization algorithms and suitable simulation models for oil production optimization. The emphasis is on the integration of the decision process for different time-scales. To this end, this research studies each individual time-scale and proposes tools that lead to the desired integration. The work is divided into five parts.

Chapter 2 formulates and solves the reservoir control optimization problem applying the direct multiple shooting (MS) method. This method divides the prediction horizon into smaller intervals which can be evaluated in parallel. Further, output constraints are easily established on each interval boundary and as such hardly affect computation time. This opens new opportunities to include state constraints on a much broader scale than what is common in reservoir optimization today. However, multiple shooting deals with a large number of variables since it decides on the boundary state variables of each interval. Therefore, we exploit the structure of the reservoir simulator to conceive a variable reduction technique to solve the optimization problem with a reduced sequential quadratic programming algorithm. We discuss the optimization algorithm building blocks and focus on structure exploitation and parallelization opportunities. To demonstrate the method's capabilities to handle output constraints, the optimization algorithm is interfaced to an open-source reservoir simulator. Then, based on a widely used reservoir model, we evaluate performance, especially related to output constraints. The performance of the proposed method is qualitatively compared to a conventional method.

Chapter 3 solves a black-oil reservoir optimal control problem with MS. The black-oil fluid model, considering volatile oil or wet gas, requires a change of primary variables for simulation. This is a consequence of the absence of a fluid phase due to dissolution or vaporization. Therefore, reservoir simulators parametrize the states with an aug-

mented vector and select primary variables accordingly. However, the augmented state vector and the corresponding change of primary variables are not suitable for the application of MS because the optimization problem formulation must change according to the change of variables. Thus, we propose a minimal state-space variable representation that prevents this shortcoming. We show that there is a bijective mapping between the proposed state-space representation and the augmented state-space. The minimal representation is used for optimization and the augmented representation for simulation, thereby keeping the simulator implementation unchanged. Therefore, the proposed solution is not invasive. Finally, the application of the method is exemplified with benchmark cases involving live oil or wet gas. Both examples emphasize the requirement of output constraints which are efficiently dealt by the MS method.

The production life of oil reservoirs starts under significant uncertainty regarding the actual economical return of the recovery process due to the lack of oil field data. Consequently, investors and operators make management decisions based on a limited and uncertain description of the reservoir. Chapter 4 proposes a new formulation based on MS for robust optimization of reservoir well controls. This formulation exploits coherent risk measures, a concept traditionally used in finance, to deal with the uncertainty. A variable elimination procedure allows to solve this problem in a reduced space and an active-set method helps to handle a large set of inequality constraints. Finally, we demonstrate the application of constraints to limit the risk of water production peaks on a standard test case.

Chapter 5 addresses the middle-term perspective and develops a framework for integrated production optimization of complex oil fields such as Petrobras' Urucu field, which has a gathering system with complex routing degree of freedom, limited processing capacity, pressure constraints, and wells with gas-coning behavior. The optimization model integrates simplified well deliverability models, vertical lift performance relations, and the flowing pressure behavior of the surface gathering system. The framework relies on analytical models which are history matched to field data and simulators tuned to reflect operating conditions. A Mixed-Integer Linear Programming (MILP) problem is obtained by approximating these models with piecewise-linear functions. Procedures are developed to obtain simplified piecewise-linear approximations that ensure a given accuracy with respect to complex and precise models. Computational experiments show that the integrated production optimization problem can be solved sufficiently fast for real-time applications. Further, the operational conditions calculated with the simplified models during the optimization process match the precise models.

Chapter 6 studies the short-term problem and presents control and optimization of a network consisting of two gas-lifted oil wells, a common pipeline-riser system and a separator. The gas-lifted oil wells may be open-loop unstable. The regulatory layer stabilizes the system by cascade control of wellhead pressure measurements without needing bottom hole sensing devices. An economic Nonlinear Model Predictive Control (NMPC) based on MS is applied for optimization of the network operations. The optimization

layer thus provides optimal settings for the regulatory controllers. The control structure has been validated by using the realistic OLGA simulator as the process, and using simplified models for Kalman filtering and the NMPC design. The simplified models are implemented in Modelica and fit to the OLGA model to represent the main dynamics of the system. The proposed two-layer controller was able to stabilize the system and increase the economical outcome.

Preface

This thesis is submitted in partial fulfillment of the requirements for the degree of Philosophiae Doctor (PhD) at the Norwegian University of Science and Technology (NTNU). The research has been conducted at the Department of Engineering Cybernetics (ITK) from January 2012 to December 2015. The research enjoyed close cooperation with the Department of Systems and Automation Engineering (DAS), Federal University of Santa Catarina (UFSC), Florianópolis, SC, Brazil. Funding for the research has been provided by the Center for Integrated Operations in the Petroleum Industry (IO Center) and partly by the department, for which I am grateful.

First and foremost, I would like to express my sincere gratitude to my supervisor Professor Bjarne Foss. He was always patient and helpful when facing difficulties and kept me confident. Prof. Foss gave me full freedom to pursue my research on my way and pushed me forward when necessary.

I would like thank my co-supervisor Professor Eduardo Camponogara. Our discussions on the fundamentals of the optimization methods were key for the research. Moreover, his proof reading of our reports improved significantly the quality of the final documents.

I would like to thank my co-authors, students, and colleagues. They kept me motivated in all circumstances and encouraged me with interesting discussions in a broad range of topics.

The research in Chapter 4 was supported in part with computational resources at NTNU provided by NOTUR http://www.sigma2.no/. I'm very grateful for the support given by the attentive staff of the supercomputer Vilje.

Trondheim, February 2016

Andres Codas Duarte

Contents

List of Figures

Chapter 1

Introduction

This opening chapter motivates the development of oil production optimization strategies by discussing the importance of fossil-energy sources, and in particular oil, for Norway and the world. Then, the most relevant decisions taken during the oil field life cycle are presented in the context of Integrated Production Optimization. Finally, the research scope, contributions, and optimization tools explored in the following chapters are presented.

1.1 Background and Motivation

The world needs more energy to sustain its population and economic growth. The additional requirement of energy is critical in underdeveloped countries and emerging economies where the universal energy access is not guaranteed for all (The World Bank 2015). At the moment, it is estimated that 1.1 billion of the world population live without access to electricity. Thus, for a better future, to relieve energy poverty and to reduce the environmental impact of the population growth, we need clean and secure energy sources.

According to IEA (2014), fossil-energy sources, and in particular oil, have been the most important primary energy sources in the past, see Figure 1.1. However, the fossil-energy sources are not renewable and lead to the emission of greenhouse-gases. These facts spark the global conscience and led to initiatives to improve the efficiency and distribution of energy from renewable sources (The World Bank 2015). Figure 1.1 presents energy consumption forecasts by source according to a realistic New Policies Scenario (NPS) and a scenario which is consistent with the goal of limiting the global temperature increase. The later scenario is referred to as the 450 Scenario (450S) because it constrains the concentration of carbon dioxide in the atmosphere to 450 parts per million. Despite the initiatives to reduce fossil-energy consumption and the estimated increase of renewable energy sources, IEA (2014) forecasts the dominance of fossil-energy sources

in the next decades. Thus, as long as there is no other reliable and cleaner energy source, it is necessary to conscientiously use the available fossil-energy resources.

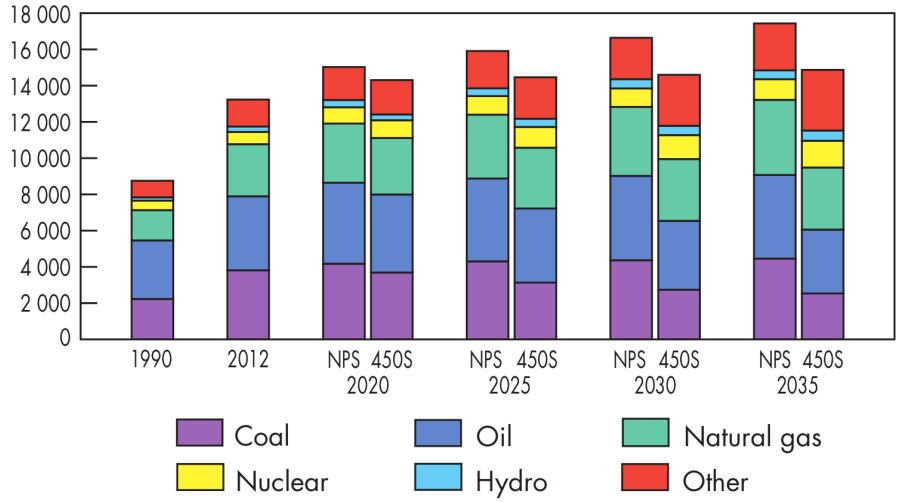

Figure 1.1: Total primary energy source outlook (in Mtoe) (IEA 2014).
NPS: New Policies Scenario. 450S: 450 Scenario.

This thesis investigates different alternatives for oil production optimization. The proposed tools aim to improve the profitability and extend the life of existing resources. Significant value can be added by applying technology to recover more oil from existing resources. Figure 1.2[1] shows the estimated lifetime of Norwegian petroleum fields according to different earlier forecasts. Although by 1992-1995 it was predicted that 6 out of the 7 considered fields would be out of operation by today (March 2016), all of the fields are still active. The life extension of the fields is partially supported by technological improvements and by economic conditions. The global demand of energy maintains high prices of hydrocarbons which allow the application of costly methods to recover more. In addition, the development of technology promotes the effectiveness and the efficiency of the recovery methods. Oil field life extension and improved recovery from existing fields are environmentally friendly endeavors because these activities delay the need to step into new discoveries.

Oil production starts under large uncertainty. The Ekofisk field is the most representative case in Norway to demonstrate the impact of the uncertainty and technology on an oil field operation. By 1965, oil exploration started in Norway, specifically in the northern region of the North Sea, motivated by the optimism after oil discoveries in the Netherlands in 1959. The first exploration well was drilled in 1966 and turned out to

[1]The content on the Norwegian Petroleum Directorate's webpages may be used in accordance with Norwegian License for Open Government Data (NLOD) http://data.norge.no/nlod/en/1.0.

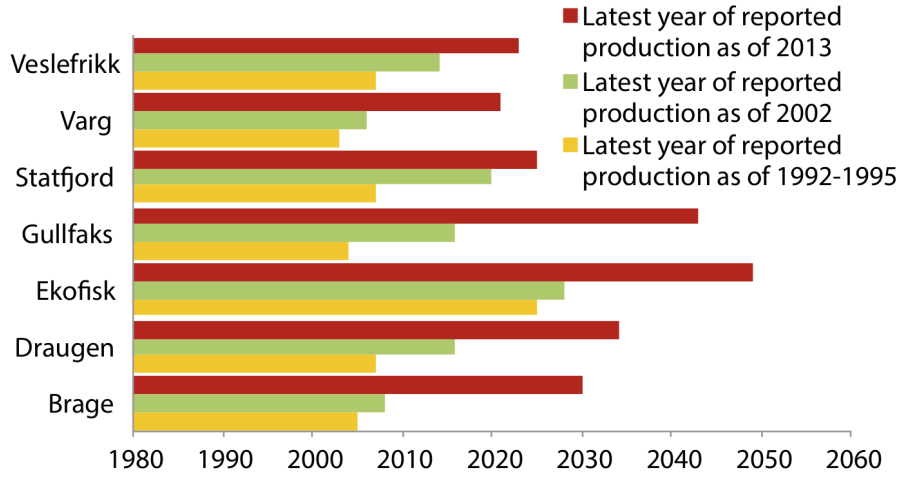

Figure 1.2: Lifetime of Norwegian petroleum fields (Tormodsgard 2014).

contain no profitable hydrocarbons. However, in 1969 the Ekofisk field was discovered and its production started in 1971. Figure 1.3 shows the oil reserve[2] increase when comparing recent production plans to the first plans for development and production (PDO). Observe that the first plans for development are decided under significant uncertainty due to lack of field data. Moreover, the initial plans can not rely on accurate predictions of technology development and the evolution of relevant economic indicators. Therefore, the average increase of oil reserves shown in Figure 1.3 is partially based by the application of technology to improve recovery (Ministry of Petroleum and Energy Norway 2011).

Ekofisk is the biggest and earliest discovery in Norway. In 1969, while drilling the first exploration well in Ekofisk, Ed Seabourn, the rig responsible said: "I can cover the North Sea from here to the North Pole with oil". Figure 1.4 shows a comparison of the base production scenario used for the field development plan and the actual production of several fields. Despite the initial optimism when drilling the first well for Ekofisk, the PDO expected a recovery factor of only 17% (Tormodsgard 2014). Large-scale water injection for improved oil recovery started in 1987 and boosted the production, see Figure 1.4. With these new technologies, the current expected recovery factor of Ekofisk is around 50%, *i.e.*, half of the resources will still be left after shut down.

So far around 44% of the Norwegian recoverable resources have been produced (Alveberg et al. 2013). Moreover, significant value can be added by increasing the recovery factor of existing fields. Figure 1.5 shows the distribution of produced oil, the reserves and the amount of resources estimated to be left over at abandonment. The current operational plans estimate an average recovery rate of 46% of oil and 70% of gas

[2]The oil reserve is the volume of oil expected to be produced economically using today's technology (IEA 2013).

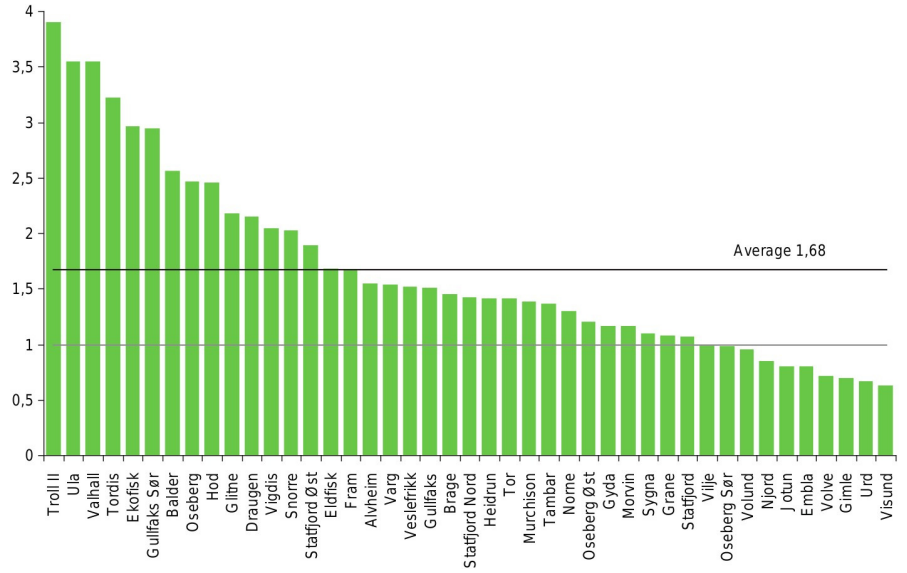

Figure 1.3: Oil reserve increase related to the first plan for development and operation (Ministry of Petroleum and Energy Norway 2011).

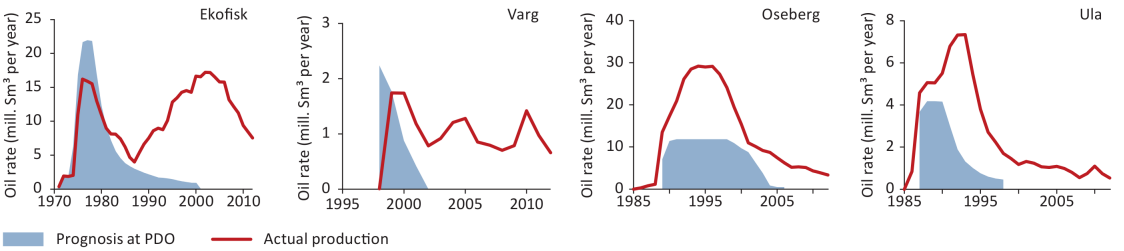

Figure 1.4: Production forecast used in PDO vs. Actual production. (Alveberg et al. 2013)

in the Norwegian Continental Shelf (Ministry of Petroleum and Energy Norway 2011). These estimates contrast with the global oil recovery rate which is around 22%. The ultimate recovery factor of a field depends on many variables accounting for the field characteristics and the economics. Moreover, the application of technology plays an important role in improving the recovery factor. These are some of the numerous alternatives that have been applied in the Norwegian Continental Shelf:

- Injection of water or gas for reservoir flooding and pressure maintenance. These techniques are extensively used in Norway. Alveberg et al. (2013) provides an overview of the application of these technologies by fields.
- Drilling of new wells. Around 50 billion NOK was spent in 2013 to drill 142 wells (Norwegian Petroleum Directorate 2014). Observe that this alternative required around 50% of the total field investments.

- Reservoir mapping by timed seismic data inversion to infer more about the geologic characteristics and the distribution of fluids. An accurate description of these characteristics leads to better decision-making of all the recovery strategies. Seismic interpretation was a key technology to locate Ekofisk in Norway (Ministry of Petroleum and Energy Norway 2011).
- Subsea compression to boost the production of gas and condensates, as done recently by Statoil in the Åsgard field (Tormodsgard 2014).
- Integrated operations which focus on the cross discipline cooperation and collaborative decision-making supported by information technology. Integrated operations lead to better operational practices supported by improved data accessibility and software functionality. (Ministry of Petroleum and Energy Norway 2011). Jansen et al. (2006) provides an analysis of the potential value of Integrated Operations in the Norwegian Continental Shelf.

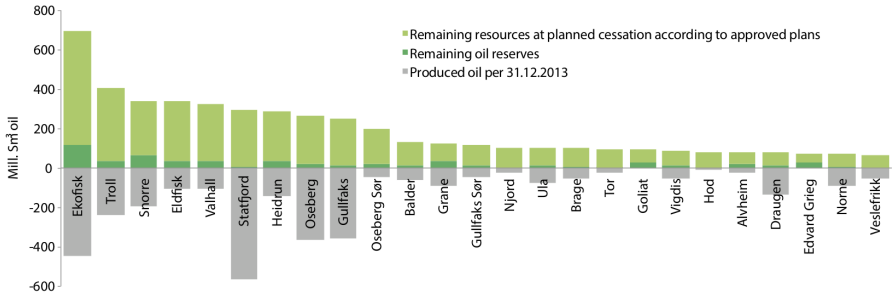

Figure 1.5: Distribution of produced oil, remaining oil reserves and remaining resources after close down (Tormodsgard 2014).

The application of the aforementioned technologies to improve oil recovery requires significant investments. A good example in Norway is the Ula oil field (Tormodsgard 2014), see Figure 1.4. From the beginning of its production in 1986 to 1998, the oil was produced initially by pressure depletion and followed by water injection. From 1998, water alternating gas injection has been used to improve oil recovery. All the produced gas is used with this aim, in addition to the gas from satellite fields. Moreover, oil production is assisted with gas-lift. These technologies for improved oil recovery require investments to install and operate the gas processing facilities. However, observe in Figure 1.4 that all these measures can not keep the oil production rate as high as the beginning of the operation. Thus, as the field ages the production profit decreases.

The trend observed in the Ula oil field is common and is reflected in the global supply of liquid fossil-fuels, see Figure 1.6. New wells in existing matured fields bring limited production compared to the operating costs, and the same trend is observed with other improved recovery methods. Thus, the exploration of new regions is encouraged, to

produce oil from fields yet to be found. For instance, Norway is analyzing the possibility to recover oil in the northern Barents Sea and in the area surrounding Jan Mayen (Tormodsgard 2014). The exploration of these areas requires a significant advance in technology for Marine Operations. Partly in response to this the Center for Autonomous Marine Operations and Systems at NTNU is educating people and developing technology. Thus, the current petroleum exploration activities and outlook yield value creation, welfare, and employment also in other economic sectors.

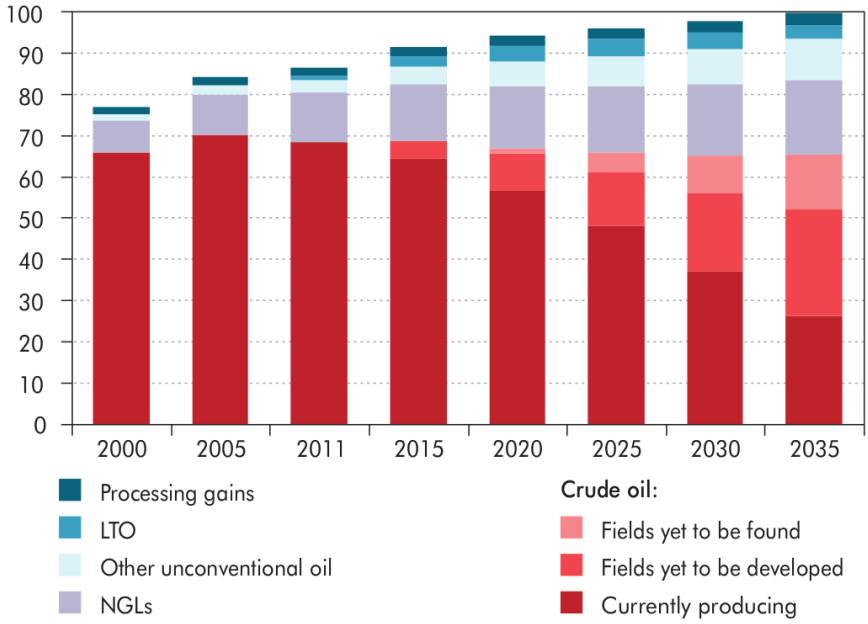

Figure 1.6: World liquid fossil-fuel supplies under the New Policies Scenario (in millions of barrels per day). (IEA 2013)

1.2 Integrated Production Optimization

Integrated production optimization refers to the optimization of decision-making processes taking into account methods and models from different disciplines in the oil industry. A typical example consists of the combined analysis of detailed reservoir models and detailed surface facility models for optimization of production processes (Litvak et al. 2002; Davidson et al. 2003). Campos et al. (2010) present fundamental design guidelines for integrated production models. These guidelines target a framework for multidisciplinary teams to support short-term decision-making, enhance production process perception and analyze the evolution of field life. Following an integrated modeling philosophy, Rahmawati (2012) proposed the direct integration of detailed commercial

simulation tools from upstream to downstream. Provided an economic model, Rahmawati (2012) showed the potential of derivative-free based optimization to increase the economical return of the oil field. However, the number of decision variables in the optimization problem were small, *e.g.*, less than 10 (Rahmawati et al. 2012), and the problems were unconstrained. Thus, there is a need of models and simulation tools that allow for efficient optimization procedures.

The impact of optimization tools to support decision-making processes may be analyzed from the perspective of the oil field life cycle. It involves multidisciplinary processes and decision-making activities in many domains. The oil field life cycle may be divided into the following activities (Jahn et al. 2008):

1. Licensing.

   The main decision during the licensing phase is related to the acquisition of the rights for exploration. This process entails negotiations with the local government to establish the area to be explored for a certain amount of time. Moreover, a petroleum fiscal regime is defined in this phase.

2. Exploration & Appraisal.

   The exploration phase executes geological and seismic surveys in the licensed area. Even if the outcome of these surveys is promising, the presence of hydrocarbons can be confirmed only by an exploration well. After confirming the presence of oil, further appraisal wells are drilled in the region aiming a better description of the size and producibility of the resources. The appraisal process continues until enough information is gathered to start the development of the field or to declare the area not profitable.

3. Development.

   The main goal of the development phase is to generate a PDO. The PDO defines a feasible recovery strategy. To this end, it specifies the subsurface and surface facilities to be installed, in addition to the operational requirements and investments cost. After the PDO is approved, the detailed design, fabrication and commissioning of the facilities follow.

4. Production.

   The production phase starts progressively as the facilities are installed. When the installation is complete, a production plateau is ideally reached and the field is produced at maximum capacity. This production is ideally sustained as long as possible, but the production declines as the field matures. This production trend was for instance observed in the Oseberg field, see Figure 1.4. Finally, the field remains in production during the decline phase as long as the cash-flow remains favorable. During the production phase, exploration & appraisal of nearby areas may be executed so as to re-utilize the installed infrastructure on minor fields.

Moreover, the facilities may be upgraded, *e.g.*, with gas-lifted wells, in order to keep the field in production for more time.

5. Decommissioning.

   In the decommissioning phase the facilities are disposed of in order to minimize environmental damage. The most important decisions in this phase are when to start decommissioning and what to do with the remaining facilities in the field.

Although every stage of the field life cycle may be thought to be independent of each other, the decisions on each stage have a great impact in the subsequent phases. Moreover, some of the steps may be repeated in a later stage, such as the re-development of parts of field during production.

The application of the Integrated Operations (IO) philosophy may improve the execution of the field life cycle activities (Ringstad et al. 2006; Ringstad et al. 2007). IO promotes multidisciplinary teamwork (Skjerve et al. 2010), therefore the problems are tackled from a broader perspective. IO is supported by an information technology infrastructure which allows the work to be performed independently of the physical location, thus it brings experts closer together. Moreover, the increased availability of real time data enables the development of technology for the automation of decision support tools. Thus, IO is an enabler for the development of optimization methodologies for the field life cycle activities.

The impact of IO may be assessed with a valuation framework (Strasunskas et al. 2012) along four dimensions: process, people, technology, and organization. The value of IO lies on an improved work process between the aforementioned dimensions. Strasunskas et al. (2012) affirm that advances in technology such as integrated decision support tools are a prerequisite for value creation due to IO. The aggregated value given by this technology is often intangible because it is not possible to assess precisely how the improved decisions impact the overall process. However, Teixeira et al. (2013) demonstrated quantitatively the aggregated value in a specific industrial setting.

The decisions in the life cycle may be seen from a control hierarchy perspective (Saputelli et al. 2006; Foss 2012), see Figure 1.7. This control hierarchy structure uses time-scales to classify data, models, and decisions. Within this framework, most of the decisions made for licensing, exploration & appraisal, development and decommissioning are classified as "Asset Management" decisions. These decisions aim to reduce the investments and minimize the risks of the field operation. The Asset Management decisions impact over years and the data required to make these decisions take months to acquire. On the contrary, the production operation requires faster feedback control operations and automation of decision processes:

- The reservoir management decisions aim to improve the field recovery factor. These decisions include water and gas injection for pressure support and oil sweep, production policies, and exact location of new wells to be drilled. These decisions are revised periodically, with a period of few months, typically less than a year.

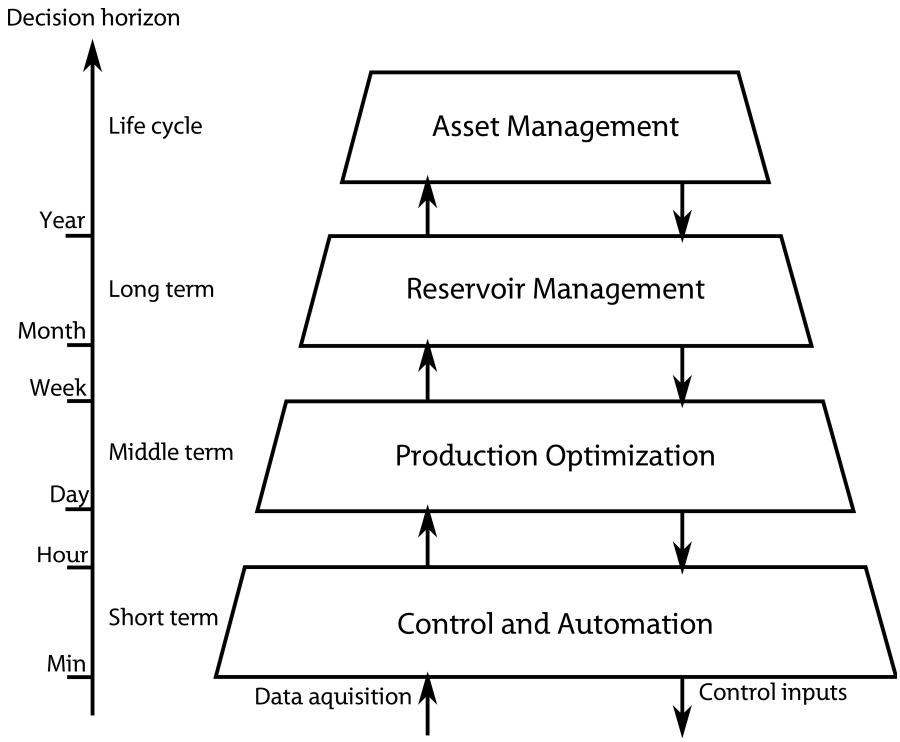

Figure 1.7: Control hierarchy in the oil & gas recovery context. Adapted from (Foss 2012).

The data gathered by the History Matching process (Oliver et al. 2008) is crucial for this phase. This procedure leads to plausible reservoir scenarios which must be analyzed to determine the impact of the operation activities. The periodical application of History Matching and Reservoir control Optimization is also known as Closed Loop Reservoir Management (CLRM) (Jansen et al. 2009).

- The production optimization decisions aim at the optimized utilization of the facilities, see (Bieker et al. 2007) for a comprehensive review and (Grimstad et al. 2016) for a recent application. These decisions include well-separator routing configurations, controller tunings and facilities operational set-points. The decision support tools for real-time production optimization often ignore the dynamics of the process. These tools rely on simple well models, typically disregarding the reservoir dynamics, and consider capacity constraints of the surface facilities. Thus, new well and processing facilities conditions require a review of these decisions. The data gathered by well tests (Gringarten 2006) is fundamental for this decision layer.

- The control & automation decisions aim to keep a stable operation, damp oscilla-

tions and reject disturbances. These procedures require feedback of field pressures, flow-rates and temperatures in a range from seconds to hours. These decisions include valve openings to keep pressure set-points in gas-lift systems (Camponogara et al. 2009) and pump speeds to regulate the production of sucker-pumping systems (Ordonez et al. 2009). The automation layer also contains emergency shutdown mechanisms that prevent the facilities to operate under dangerous conditions.

The time-scale separation as suggested in (Saputelli et al. 2006; Foss 2012) is a key to overcome the overwhelming computational challenge faced in the joint-model optimization approach (Rahmawati et al. 2012). The hierarchical control structure allows to divide the optimization problem in different time-scales. Moreover, when solving the problem on a given time-scale, the problems on the other scales are introduced with simplifications. In this way, when solving a reservoir management problem, the decision support tools may use a reservoir simulator and lump the models of the surface facilities to a single constraint equation. Opposed to the joint-model approach in (Rahmawati et al. 2012), the challenge is to generate representative simplified models for the surface facilities. Moreover, an additional challenge is the coordination of the different layers because the simplifications may lead to inconsistent models. Thus, data assimilation procedures are necessary to correct these simplifying assumptions and maintain the models tuned. Such application of data assimilation is performed by Van Essen et al. (2012) to maintain a two-layered control structure for reservoir water-flooding optimization and disturbance rejection.

The aforementioned time-scales are usually associated to different physical parts of the process, *e.g.*, the reservoir and the gathering facilities, which have time-scales of months and hours, respectively. However, the time-scales of these processes may overlap, see (Nennie et al. 2007; da Silva et al. 2015). Coupled reservoir and well models are required, for instance, to control and minimize the effects of gas coning (Leemhuis et al. 2008; Nennie et al. 2009) and to minimize wax deposition (Nennie et al. 2008). These are short-term effects which are typically disregarded when solving the long-term reservoir management problem due to the prohibitive simulation effort and uncertainty.

The wide spectrum of open challenges for modeling, simulation, and optimization of integrated oil production systems is the main motivation for the research in this thesis.

1.3 Research objective and scope

The seminal work of Saputelli et al. (2006) left many open challenges which must be solved in order to establish real-time oil field production optimization. Saputelli et al. (2006) suggested the following research activities:

- Develop algorithms for continuous feedback adjustments.
- Investigate useful models on each time-scale layer

- Propose methods to adjust these models to the actual field.
- Develop fast optimization tools for every decision layer.

In light of the many research directions left by previous work, the global objective of this thesis is:

Contribute to the development of integrated production optimization strategies.

New criteria for optimization arise with coupled models. The objective function of the joint problem can count on operational expenses taking into account the balance between short-term and long-term production goals. Examples of these operational expenses are separation process cost, gas compression energy consumption, allocation of facilities and maintenance. Furthermore, surface facilities constraints can be added to the inclusive formulation. When including surface facilities constraints, infeasible reservoir drainage schedules are avoided. In this way, the calculated optimal control laws, with respect to the coupled model, can be implemented without further conciliating iterations since it is feasible for all the modeling layers. However, these solutions require models and algorithms capable to solve the coupled problem in real-time.

It is clear that a fully integrated production optimization method requires many years of research of a multidisciplinary team. Thus, aiming at the global objective, this thesis follows a bottom-up project approach. Here, each individual time-scale is studied independently following guidelines from previous research activities. Moreover, we propose extensions leading to the integration of the decision process:

1. This thesis proposes a new method for simulation and optimization for the reservoir control optimization problem. This method promotes simulation parallelization and facilitates output constraints handling. These ingredients facilitate the incorporation of more details from the surface facilities into the reservoir management problem.
2. Aiming at the solution of the daily production optimization problem, this thesis develops a method to integrate simulators of surface facilities to optimization software. The use of adjusted surrogate models instead of the simulators is a key to introduce specialized optimization algorithms. The reservoir models are incorporated to the optimization formulation through simple inflow performance relations for the wells. Moreover, additional constraints are added to the problem formulation to ensure stability in the control and automation layer.
3. This thesis proposes the structure of a two-layer controller coordinating the interaction between the control & automation layer and the daily production optimization layer. To this end, a simple oil gathering network is equipped with regulatory controllers which are commanded by a model predictive control algorithm. The regulatory controllers keep the stability of the process and the predictive control algorithm steer the system to improved operational points computed by the optimization layer.

A common axis in this research work is the validation of the proposed strategies on process simulators that are actively used in the industry. These simulators include OLGA (Schlumberger 2014) for dynamic multiphase flow, PIPESIM (Schlumberger 2009) for steady-state multiphase gathering networks, and MRST (Lie et al. 2011; Krogstad et al. 2015) for two-phase and three-phase black-oil reservoir models. The use of industrial simulators permits the analysis of the process at a realistic level of detail. Moreover, the intention is to promote collaboration with the industrial partners in the IO Center.

Summarizing, this research focuses on efficient optimization algorithms and suitable simulation models for oil production optimization. The emphasis is on the integration of the decision process for different time-scales. To this end, this research studies each individual time-scale and proposes tools that lead to the desired integration.

1.4 Optimization tools

This section aims to introduce Direct Single Shooting (SS) and Direct Multiple Shooting (MS) for the solution of nonlinear optimal control problems (OCP) on a fixed time horizon. Instead of providing a deep theoretical insight, this section gives a practical approach towards the integration of nonlinear programming (NLP) solvers and dynamic simulators. The target is to explain the motivation to use the less intuitive MS formulation instead of SS when dealing with numerical-intensive simulators. Special attention will be given to reservoir simulators because this is the main application of this thesis. For a more general overview of solution methods for OCPs, see (Binder et al. 2001; Albersmeyer 2010; Biegler 2010).

1.4.1 Background

OCPs may be solved with Direct Methods (DMs) or Indirect Methods (IMs). The IMs solve a set of equations consisting of boundary value problems resulting from the dynamical equations and the optimality conditions of the OCP. The optimization of these equations leads to an optimal control function in time, which later must be discretized to be applied to the process. Therefore, this approach is known as first optimize and then discretize. Although IMs have been applied for optimization of Enhanced Oil Recovery processes (Fathi et al. 1984; Fathi et al. 1986; Ramirez 1987), the DMs are currently preferred for reservoir control optimization (Jansen 2011; Hou et al. 2015). The main drawback of the IMs is the inability to deal with output inequality constraints (Biegler 2010). Thus, the IMs are out of the scope in this study.

Figure 1.8 illustrates a classification of the DMs. The key idea is the transformation of the OCP to an NLP. To this end, the control input function is parametrized with a finite set of control variables. Then, these control variables are the degrees of freedom to be optimized with an NLP solver.

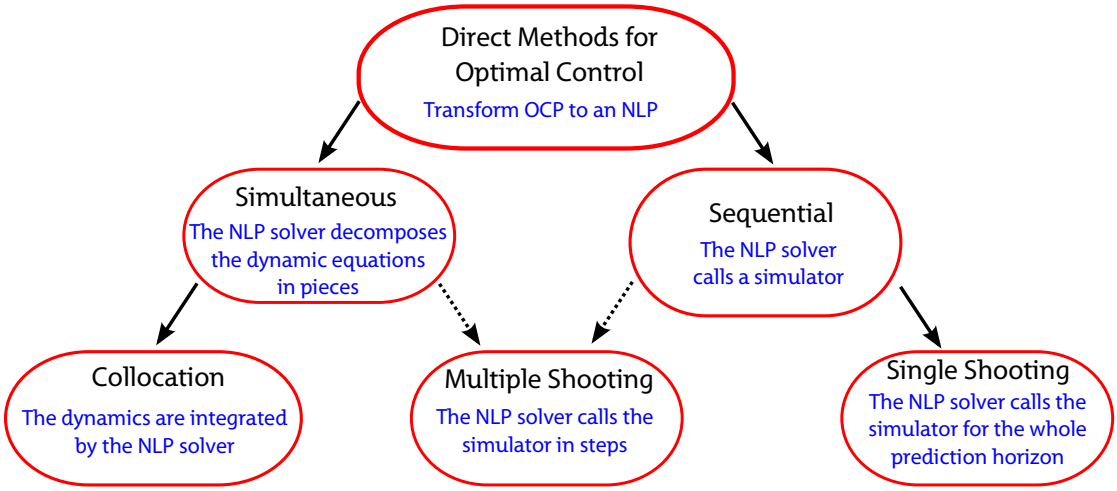

Figure 1.8: Direct methods for optimal control problems.

The DMs can be divided into sequential methods or simultaneous methods. On the one hand, the sequential methods embed a dedicated simulator which solves the differential equations. On the other hand, the simultaneous methods solve the differential equation with the NLP solver. The simulator function is instantiated either for the whole control time horizon for SS, or in pieces for MS. When the simulator function is called in pieces the convergence of the dynamical equations is controlled by the NLP, therefore, MS can be seen as a simultaneous approach. Simultaneous approaches solve the dynamical equations and optimize the control parametrization at the same time. As opposed to MS, Collocation does not require a dedicated simulator, but it instantiates the Runge-Kutta equations within the NLP solver to impose the dynamical equations directly.

This thesis does not investigate the use of Collocation for solving reservoir control optimization problems (Heirung et al. 2011). The author prefers to exploit the available simulators for this large-scale problem instead of studying how to equip the NLP solvers with this capability. Nevertheless, the customization of optimization algorithms based on the Collocation formulation is suggested for a future study after the application of MS.

Second-order derivative information may accelerate the convergence of NLP algorithms. Suwartadi et al. (2010) performed numerical studies using second-order derivatives for reservoir control optimization problems. The optimization algorithms that used second-order derivatives required less iterations to converge than the algorithms using first-order derivatives only. However, the overall computational time consumed by the algorithm using second-order information was higher. Moreover, the implementation effort for this type of algorithms is higher. Therefore, this thesis is limited to algorithms using only first-order gradient information.

1.4.2 Single Shooting and Multiple Shooting

Consider the following OCP which is already represented as an NLP:

$$\min_{D} \ \psi\left(\mathbf{x}, \mathbf{v}, \mathbf{u}\right) \tag{1.1a}$$

$$\text{s.t.}: \quad \mathbf{x}_k^{\mathrm{f}} - \mathbf{x}_{k+1} = 0, \quad k \in \mathcal{K}, \tag{1.1b}$$

$$\mathbf{v}_k^{\mathrm{f}} - \mathbf{v}_k = 0, \quad k \in \mathcal{K}, \tag{1.1c}$$

$$R_k\left(\mathbf{x}_k, \mathbf{x}_k^{\mathrm{f}}, \mathbf{v}_k^{\mathrm{f}}, \mathbf{u}_{\kappa(k)}\right) = 0, \quad k \in \mathcal{K} \tag{1.1d}$$

$$\mathbf{b}_l^{\mathrm{x}} \leq \mathbf{x} \leq \mathbf{b}_u^{\mathrm{x}} \tag{1.1e}$$

$$\mathbf{b}_l^{\mathrm{v}} \leq \mathbf{v} \leq \mathbf{b}_u^{\mathrm{v}} \tag{1.1f}$$

$$\mathbf{b}_l^{\mathrm{u}} \leq \mathbf{u} \leq \mathbf{b}_u^{\mathrm{u}}. \tag{1.1g}$$

where:

- $\mathcal{K} = \{1, \ldots, K\}$ is the set of time steps in the prediction horizon.
- $\mathcal{U} = \{1, \ldots, U\}$ is the set of control steps.
- $\kappa : \mathcal{K} \to \mathcal{U}$ is a function linking a simulation step to a control step.
- $\mathbf{x}_1$ is a constant parameter defining the initial state of the dynamic system.
- $\mathbf{x} = (\mathbf{x}_2, \ldots, \mathbf{x}_{K+1})$ are the predicted states of the dynamical system.
- $\mathbf{v} = (\mathbf{v}_1, \ldots, \mathbf{v}_K)$ are the predicted algebraic states of the dynamical system.
- $\mathbf{x}^{\mathrm{f}}$ and $\mathbf{v}^{\mathrm{f}}$ represent the output of the simulator for the state variables and the algebraic state variables, respectively.
- $\mathbf{u} = (\mathbf{u}_1, \ldots, \mathbf{u}_U)$ are the control variables.
- ψ is the objective function which must be minimized.
- R_k represents the simulator. For simplicity, it is assumed that R_k has a unique solution for $\mathbf{x}_k^{\mathrm{f}}$ and $\mathbf{v}_k^{\mathrm{f}}$ given $\mathbf{x}_k$ and $\mathbf{u}_k$ respecting their corresponding bounds. Moreover, it is assumed that $\left[\frac{\partial R_k}{\partial \mathbf{x}_k^{\mathrm{f}}}, \frac{\partial R_k}{\partial \mathbf{v}_k^{\mathrm{f}}}\right]$ is a full rank square matrix in an open ball around the point $\left(\mathbf{x}_k^{\mathrm{f}}, \mathbf{v}_k^{\mathrm{f}}\right)$ satisfying (1.1d).
- D represents the decision variables of the NLP solver. D is $\mathbf{u}$ in the SS formulation and $(\mathbf{x}, \mathbf{v}, \mathbf{u})$ in the MS formulation.
- Lower and upper bounds are given by $\mathbf{b}_l$ and $\mathbf{b}_u$, respectively, for the variables specified in the superscript. The inequality constraints (1.1e)-(1.1f) are regarded as output constraints because they constrain the simulator output and (1.1g) are referred to as input constraints for the analogous reason.

Problem (1.1) is a general formulation that appears in the next chapters of this thesis with some modifications according to the context. In this introductory chapter, it is used to compare solution algorithms, and to compare SS and MS. Observe that these formulations assume that the constraints (1.1d) are always satisfied. Therefore, $\left(\mathbf{x}_k^{\mathrm{f}}, \mathbf{v}_k^{\mathrm{f}}\right)$ are not independent variables but a function of D.

SS is particularly attractive when dealing with large-scale dynamical systems because the underlying simulator is loosely coupled to the NLP solver. The NLP solver decides on the control variables and the simulator provides with function evaluations and sensitivities of the objective and constraints. Therefore, the NLP formulation is small because it is independent of the size of $\mathbf{x}$ and $\mathbf{v}$. Thus, the general purpose NLP solvers can not be further developed for SS because the problem has no visible structure to be exploited. When dealing with a SS formulation, Problem (1.1) is better represented with the following formulation:

$$\min_{\mathbf{u}} \ \psi^{\mathrm{s}}\left(\mathbf{u}\right) \tag{1.2a}$$

$$\text{s.t.}: \quad \mathbf{b}_l^{\mathrm{x}} \leq \mathbf{x}^{\mathrm{s}}\left(\mathbf{u}\right) \leq \mathbf{b}_u^{\mathrm{x}} \tag{1.2b}$$

$$\mathbf{b}_l^{\mathrm{v}} \leq \mathbf{v}^{\mathrm{s}}\left(\mathbf{u}\right) \leq \mathbf{b}_u^{\mathrm{v}} \tag{1.2c}$$

$$\mathbf{b}_l^{\mathrm{u}} \leq \mathbf{u} \leq \mathbf{b}_u^{\mathrm{u}}. \tag{1.2d}$$

where ψ^{s}, $\mathbf{x}^{\mathrm{s}}$, and $\mathbf{v}^{\mathrm{s}}$ are equal to ψ, $\mathbf{x}$, and $\mathbf{v}$, respectively, when (1.1b)-(1.1d) are satisfied. The sequential calculation of $\left(\mathbf{x}_{k+1}^{\mathrm{s}}, \mathbf{v}_k^{\mathrm{s}}\right)$ from $k = 1$ to $k = K$ so that (1.1d) and then (1.1b)-(1.1c) are satisfied is regarded as forward simulation. In SS algorithms the forward simulation is typically run within the simulators without any interaction with the optimizer during the process. Finally, ψ^{s} can be calculated after the simulator returns $\mathbf{x}^{\mathrm{s}}$ and $\mathbf{v}^{\mathrm{s}}$ for all the time steps.

An important ingredient for NLP algorithms is a procedure to compute gradients. Kraaijevanger et al. (2007) provide a simple but comprehensive overview of gradient computation methods with applications to reservoir control optimization. The most efficient SS algorithms rely on the adjoint method for gradient computation. This method is attractive because the gradient computation of a real-valued function such as ψ^{s} requires at most the solution of K linear systems involving the transposed Jacobians $\left[\frac{\partial R_k}{\partial \mathbf{x}_k^{\mathrm{f}}}, \frac{\partial R_k}{\partial \mathbf{v}_k^{\mathrm{f}}}\right]^\top$. The computational burden is considered independent of the number of control inputs but increases linearly with the number of outputs. However, observe that it is possible to avoid repeated calculations when computing gradients of several real-valued functions, *e.g.*, the preconditioners for the linear systems may be computed only once.

The ability to handle output constraints is an essential feature for OCPs. For instance, $\mathbf{x}_k^{\mathrm{s}}(\mathbf{u})$ may not respect (1.2b) and therefore it may provoke simulation failures. In particular, for reservoir control optimization problems, it is required to define output constraints to prevent flow reversal in wells if these are controlled by pressure. However, the inclusion of these constraints requires more adjoint gradient computations in many

NLP solvers, *e.g.*, SNOPT (Gill et al. 2005) and IPOPT (Wächter et al. 2005). Therefore, specialized methods using a single adjoint based on the Augmented Lagrangian penalty (Chen et al. 2010; Chen et al. 2012) and heuristic methods (Kourounis et al. 2014) have been suggested to handle output constraints efficiently. In practice not all of $\mathbf{x}_k^{\mathrm{s}}(\mathbf{u})$ and $\mathbf{v}_k^{\mathrm{s}}(\mathbf{u})$ require constraints, therefore, the corresponding bounds are relaxed and the constraints are not interfaced to the NLP solver.

The application of decomposition techniques to oil production optimization (Foss et al. 2015) and to more general optimization problems (Conejo et al. 2006) is a viable way to tackle large but structured problems. According to Foss et al. (2015), structure exploitation through the application of decomposition techniques improves the efficiency of the numerical solvers and increases the flexibility of the optimization problem. Problem (1.1) has no apparent structure besides the chained equations (1.1b) and (1.1d). However, the decomposition of problem (1.1) is motivated by computationally intensive simulators. If the constraints (1.1b) are relaxed, then all the simulation steps can be run in parallel. Moreover, if such a technique is applied, the NLP algorithms must directly decide the variables $\mathbf{x}$, so the satisfaction of the constraints (1.1e) is a trivial task. However, the NLP algorithms must guarantee the convergence of (1.1b).

The Augmented Lagrangian method (Bertsekas 1996; Bertsekas 1999) has been suggested to coordinate structured problems which are tackled with decomposition (Conejo et al. 2006; Tosserams et al. 2006; Tosserams et al. 2009). Moreover, the Augmented Lagrangian method has been applied successfully to the output-constrained reservoir control optimization problems formulated with SS (Chen et al. 2010; Chen et al. 2012). Therefore, a natural idea is to apply this method to decompose and solve (1.1). To this end, the following subproblem is defined:

$$\psi^{\star}(\lambda,\alpha) = \min_{\mathbf{x},\mathbf{v},\mathbf{u}} \psi\left(\mathbf{x},\mathbf{v},\mathbf{u}\right) + \sum_{k\in\mathcal{K}} \left(\lambda_k^{\top} \begin{bmatrix} \mathbf{x}_k^{\mathrm{f}} - \mathbf{x}_{k+1} \\ \mathbf{v}_k^{\mathrm{f}} - \mathbf{v}_k \end{bmatrix} + \frac{1}{2}\alpha \left\| \begin{matrix} \mathbf{x}_k^{\mathrm{f}} - \mathbf{x}_{k+1} \\ \mathbf{v}_k^{\mathrm{f}} - \mathbf{v}_k \end{matrix} \right\|^2 \right) \tag{1.3a}$$

$$\text{s.t.}: \quad \mathbf{b}_l^{\mathrm{x}} \leq \mathbf{x} \leq \mathbf{b}_u^{\mathrm{x}} \tag{1.3b}$$

$$\mathbf{b}_l^{\mathrm{v}} \leq \mathbf{v} \leq \mathbf{b}_u^{\mathrm{v}} \tag{1.3c}$$

$$\mathbf{b}_l^{\mathrm{u}} \leq \mathbf{u} \leq \mathbf{b}_u^{\mathrm{u}}. \tag{1.3d}$$

where λ and α are regarded as the Lagrange multipliers and the quadratic penalty, respectively. The algorithm iterates through the following steps:

1. Solution of the relaxed primal problem (1.3).
2. Update of λ and α.
3. Convergence checking.

The update of the multipliers λ is usually performed with the method of multipliers (Bertsekas 1999) whereas the penalty parameter α is left equal or increased according to heuristic rules.

Although all the simulations in (1.1d) are independent and can be run in parallel, solving problem (1.3) is still computationally expensive. Note that the number of variables is very high because $\mathbf{x}$ is a decision variable. Therefore, it is recommended to use loose convergence conditions on the first iterations and to use the Alternating Direction Method of Multipliers (Tosserams et al. 2006). However, the relaxation of the convergence tolerances of (1.3) may deteriorate the convergence rate of the overall algorithm if safeguard conditions are not appropriately tuned (Bertsekas 1999).

The Reduced Sequential Programming (rSQP) method (Biegler et al. 1997; Nocedal et al. 2006) is an alternative approach to problem (1.1). Instead of including the constraints (1.1b)-(1.1c) as a penalty, the rSQP method exploits the structure of these constraints. Consider the following reformulation of problem (1.1):

$$\min_{D} \ \psi\left(D\right) \tag{1.4a}$$

$$\text{s.t.}: \quad 0 = c(D) \tag{1.4b}$$

$$\mathbf{b}_l \leq D \leq \mathbf{b}_u \tag{1.4c}$$

where $D = (\mathbf{x}, \mathbf{v}, \mathbf{u})$ is a guess to the optimal solution and c represents all the equality constraints, *i.e.*, $c^{\mathrm{x}} = \left(\mathbf{x}_1^{\mathrm{f}} - \mathbf{x}_2, \ldots, \mathbf{x}_K^{\mathrm{f}} - \mathbf{x}_{K+1}\right)$, $c^{\mathrm{v}} = \left(\mathbf{v}_1^{\mathrm{f}} - \mathbf{v}_1, \ldots, \mathbf{v}_K^{\mathrm{f}} - \mathbf{v}_K\right)$ and $c = (c^{\mathrm{x}}, c^{\mathrm{v}})$.

The Sequential Quadratic Programming (SQP) method (Nocedal et al. 2006, p. 531) finds an update to D with a Quadratic Programming (QP) problem. This QP is:

$$\min_{d} \ g^\top d + \frac{1}{2} d^\top W d \tag{1.5a}$$

$$\text{s.t.}: \quad 0 = c + A^\top d \tag{1.5b}$$

$$\mathbf{b}_l \leq D + d \leq \mathbf{b}_u \tag{1.5c}$$

where $d = (\Delta\mathbf{x}, \Delta\mathbf{v}, \Delta\mathbf{u})$, $g^\top = (\frac{\partial\psi}{\partial\mathbf{x}}, \frac{\partial\psi}{\partial\mathbf{v}}, \frac{\partial\psi}{\partial\mathbf{u}})$, and W is an approximation to the Hessian of the Lagrangian function $\psi + \lambda^\top c$. The linearization of c around D leads to a structured matrix A:

$$A^\top = \begin{bmatrix} \frac{\mathrm{d}\mathbf{x}^{\mathrm{f}}}{\mathrm{d}\mathbf{x}} - I & 0 & \frac{\mathrm{d}\mathbf{x}^{\mathrm{f}}}{\mathrm{d}\mathbf{u}} \\ \frac{\mathrm{d}\mathbf{v}^{\mathrm{f}}}{\mathrm{d}\mathbf{x}} & -I & \frac{\mathrm{d}\mathbf{v}^{\mathrm{f}}}{\mathrm{d}\mathbf{u}} \end{bmatrix} \tag{1.6}$$

Observe that building the matrix A is not practical for reservoir applications due to the high number of required gradient calculations and memory for storage. Instead of building A, the rSQP method relies on a matrix Z spanning the nullspace of $A^\top$ ($A^\top Z = 0$) and a matrix Y such that $[Y, Z]$ is square and full rank. Thus, d can be represented with two vectors p_y and p_z which parametrize the range-space and the nullspace solution of (1.5b), respectively:

$$d = Y p_y + Z p_z \tag{1.7}$$

Observe that (1.7) and (1.5b) lead to a unique solution for p_y:

$$p_y = -\left(A^\top Y\right)^{-1} c \tag{1.8}$$

And to the reduced QP problem:

$$\min_{p_z} \ \left(g^\top Z + w\right) p_z + \frac{1}{2} p_z^\top B p_z \tag{1.9a}$$

$$\mathbf{b}_l \leq D + Y p_y + Z p_z \leq \mathbf{b}_u \tag{1.9b}$$

where $w = p_y^\top Y^\top W Z$ and $B = Z^\top W Z$. This thesis uses the most popular choice of Z and Y (Biegler et al. 1997, p. 107):

$$Y = \begin{bmatrix} I_{\mathbf{x}} & 0 \\ 0 & I_{\mathbf{v}} \\ 0 & 0 \end{bmatrix}, \quad Z = \begin{bmatrix} -C^{-1} N \\ I_{\mathbf{u}} \end{bmatrix}, \quad C = \begin{bmatrix} \frac{\partial c}{\partial \mathbf{x}} & \frac{\partial c}{\partial \mathbf{v}} \end{bmatrix}, \quad N = \frac{\partial c}{\partial \mathbf{u}} \tag{1.10}$$

With this choice, the independent variables of the reduced problem (1.9) are the step on the control variables of the OCP, *i.e.*, $p_z = \Delta \mathbf{u}$. Observe that the invertibility of C follows from the non-singularity of $\left[\frac{\partial R_k}{\partial \mathbf{x}_k^{\mathrm{f}}}, \frac{\partial R_k}{\partial \mathbf{v}_k^{\mathrm{f}}}\right]$. This is a required condition for the construction of Z and the solution of p_y in (1.8).

The procedure to build and solve (1.9) has a great impact on the efficiency of the solution process. This requires the following calculations:

- The simulations in (1.1d) for the current solution guess D. Observe that these simulations can be performed in parallel. Moreover, $(\mathbf{x}, \mathbf{v})$ may be used as an initial guess for $(\mathbf{x}^{\mathrm{f}}, \mathbf{v}^{\mathrm{f}})$ in the iterative solvers for the implicit systems.
- The range-space solution p_y given by (1.8). This procedure requires one forward gradient propagation as explained in Section 2.A.
- A positive definite approximation for B. This may be instantiated using the actual value of the reduced Hessian $Z^\top W Z$ with a regularization if it is not positive definite. However, a procedure for this calculation is computationally costly or not available. Thus, Quasi-Newton approximations are typically used instead, which require the evaluation of two Lagrangian gradients.
- The cross-term w may be approximated following the recommendations in (Biegler et al. 1997). However, the algorithms in this thesis neglect w, *i.e.*, $w = 0$.
- Evaluations involving the matrix Z.

The construction of the matrix Z is performed indirectly evaluating vector-matrix multiplications ($l^\top Z$) or matrix-vector multiplications (Zr). Thus, Z can be constructed by iterating over each column of the corresponding identity matrix. The construction of the matrix Z requires a forward gradient propagation for each vector r or an adjoint

(backward) gradient propagation for each vector l. Observe that the matrix Z has as many columns as control variables and as many rows as state variables and algebraic state variables. Thus, the construction of Z using the adjoint method is not practical due to the high number of states in reservoir problems. However, if the dimension of the parametrization of the control input is low, the forward method is recommended.

In some cases, the construction of the matrix Z may be impossible due to the lack of memory for storage or may be inefficient due to the requirement of a large number of gradient calculations. Then, problem (1.9) can be solved without building explicitly Z. To this end, the violating constraints are incorporated on demand according to the following steps:

1. Estimate a subset J of the constraints that would be violated by the unconstrained solution of (1.9). This subset can be initialized with information from previous rSQP iterations.
2. Compute the rows of Z corresponding to J with the adjoint method .
3. Find a solution p_z^J for problem (1.9) considering only the constraints in J.
4. Compute Zp_z^J, which requires an additional forward gradient propagation, and check the feasibility of (1.9b).
5. If p_z^J is feasible, then p_z^J is a solution for (1.9). If p_z^J is infeasible, then include a subset of the violated constraints to J and repeat the procedure from the step 2.

Observe that problem (1.9) may be infeasible to solve. However, this provisional infeasibility may not imply that (1.4) is infeasible. Therefore, a reasonable step d may be found with an adaptation to problem (1.9). To this end, a slack variable can be included according to the algorithm developed in Chapter 2 or p_y may be damped according to the algorithm used in Chapter 4.

The MS formulation equipped with the rSQP algorithm can tackle the same problems as the SS formulation with a general SQP algorithm as described in (Nocedal et al. 2006). The main advantages of MS over SS as discussed here are:

- The opportunity to parallelize the execution of the simulation steps.
- The readily available initial guess for the simulation solvers.
- The different options to deal with Z and the constraints.

However, the rSQP method for MS deals with a more involved implementation than SS, in particular to provide the range space solution p_y which requires the computation of gradients in forward mode. Observe that the procedures to propagate gradients in forward mode are not usual in reservoir simulators. Moreover, it is not discussed if the overall convergence rate of the MS algorithm is affected by the infeasibility of the constraints (1.1b).

Albersmeyer (2010) and Albersmeyer et al. (2010) compare the lifted and nonlifted Newton methods which are equivalent to MS and SS, respectively. Albersmeyer et al.

(2010) indicate that MS is long known to outperform SS (Osborne 1969). Moreover, Albersmeyer et al. (2010) point as advantages the freedom for initialization of $\mathbf{x}$ and $\mathbf{v}$ in addition to the condition and block-sparsity structure of the linear systems in MS. However, Albersmeyer et al. (2010) show simple example cases where either SS or MS have better local convergence rate than each other.

1.5 Outline and contributions

The subsequent chapters of this thesis are articles that have been submitted or published in international journals and conferences. Consequently, the chapters are independent and the reader can choose the order to follow. However, they are sorted by topic and relevance. The chapters 2 to 4 deal with the reservoir optimization problem. It is recommended to read Chapter 2 first because the chapters 3 and 4 use concepts discussed in the former. Chapter 5 deals with daily production optimization and Chapter 6 with regulatory control and optimization. Finally, Chapter 7 provides concluding remarks and discusses future research directions.

The main contributions by chapter are:

2. The work in Chapter 2 was inspired by daily-production optimization problems where the gathering facilities operate continuously at the constraint limits. The initial research objective was to use decomposition techniques for tackling output constraints at each predicted step of the waterflooding control optimization problem. Therefore, Chapter 2 proposes a problem formulation which allows for the parallelization of simulations and inequality constraints at each predicted time step. However, this decomposition technique deals with the predicted time steps independently at the expense of a provisional inconsistency of the predictions. Thus, Chapter 2 proposes an optimization algorithm that ensures the consistency of the prediction at convergence. Finally, Chapter 2 solves waterflooding problems that are impossible to solve by applying a conventional SS framework. Although the Multiple Shooting formulation and the rSQP algorithms were previously developed, these tools have not been combined earlier to tackle the waterflooding optimization problem. Therefore, to the knowledge of the author, this work pioneers the application of a large-set of constraints and parallelization on this problem. This chapter is based on the paper (Codas et al. 2015).

3. The initial application of the Multiple Shooting formulation was limited to two-phase (oil-water) reservoirs. The direct extension to three-phase reservoirs containing fluids described by the black-oil model was not possible due to a change of primary variables for simulation. Therefore, Chapter 3 proposes a re-parametrization of the state variables that is valid for the black-oil model and the extended black-oil model. Moreover, it is shown that there is a bijective explicit transformation that permits the execution of simulations on the original variables space and the

optimization on the new parameters space. Therefore, the re-parametrization is not intrusive. Finally, Chapter 3 demonstrates the application of the formulation to benchmark cases dealing with volatile oil and wet gas. This chapter is based on (Codas et al. 2016a).

4. Chapter 4 extends the algorithms developed in the previous chapters to deal with uncertainty. Uncertainty plays a central role in the reservoir management problem due to the difficulty to measure and estimate the reservoir conditions. Chapter 4 formulates the robust reservoir control optimization problem with Multiple Shooting. Moreover, it applies coherent risk measures to handle output constraints. Thus, this framework allows for constraints on risk at all the predicted time steps. Besides the typical parallelization applicable for simulation of different scenarios, the simulation can be parallelized for the different predicted steps. In contrast to the previous rSQP algorithms which relied only on the forward method for gradient calculations, the algorithm presented in Chapter 4 relies on the adjoint method for gradient computation. This improvement diminishes the requirement of memory and is suitable for problems with a large number of control variables. The proposed framework is applied to a benchmark case considering several constraint scenarios. Finally, the capability of the algorithm to handle constraints on the risk of total field water production was shown. This chapter is based on (Codas et al. 2016b).

5. Chapter 5 deals with the daily production optimization problem. Algorithms for the daily production optimization problem have been extensively discussed in the literature. This work deals with a real onshore field which has a rather complicated gathering network structure. The overall goal was to develop a decision support tool that improves the well scheduling proposed by experienced production engineers. Therefore, an important task of the work was to identify all the available routing degrees of freedom. This work introduces a new parametrization for piecewise linear models of pipeline pressure drops. This surrogate model is better suited because it uses the same independent variables as the simulators used by the field engineers. Moreover, this work proposes simple algorithms to reduce the size of the surrogate models while respecting a threshold for accuracy. Finally, it is shown the quality of the optimal solution and the capability to compute optimal solutions in real-time. This chapter is based on (Codas et al. 2012b).

6. Chapter 6 deals with the regulatory control and the optimization of a simple oil gathering network. The objective is to study the interaction between the regulatory controllers and the nonlinear model predictive controller which steers the system to an optimal operational point. The gathering network is open loop unstable around the optimal operational point, thus a cascade Proportional-Integral controller is proposed to keep stability. The predictive controller obtains feedback of the current state from an Extended Kalman Filter and steers the system to the

steady-state optimal. The predictive controller uses the Multiple Shooting formulation which allows for the inclusion of output constraints. The contribution of this chapter lies on the control structure and the application of simplified models for closed-loop model predictive control. Numerical studies on the interaction of this two control layers were not available in the literature. This chapter is based on (Codas et al. 2016c).

In addition to the contributions listed above, the author contributed in the following publications during the PhD studies:

- Codas, A. et al. (2013). 'Differentiation Tool Efficiency Comparison for Nonlinear Model Predictive Control Applied to Oil Gathering Systems'. In: *9th IFAC Symposium on Nonlinear Control Systems, 2013*. Ed. by Tarbouriech, S., pp. 821–826. DOI: 10.3182/20130904-3-FR-2041.00069.
- Aguiar, M. A. et al. (2015). 'Systemwide Optimal Control of Offshore Oil Production Networks with Time Dependent Constraints'. In: *2nd IFAC Workshop on Automatic Control in Offshore Oil and Gas Production*. Vol. 48. 6. Elsevier Ltd., pp. 200–207. DOI: 10.1016/j.ifacol.2015.08.032.

The author co-supervised the following theses:

- Nalum, K. (2013). 'Modeling and Dynamic Optimization in Oil Production'. Master thesis. Norwegian University of Science and Technology.
- Aguiar, M. A. (2013). 'Optimal oil production network control using Modelica'. Final project work. Federal University of Santa Catarina.
- Lund, T. (2014). 'Non-linear model predictive control for an oil production network based on gas-lift'. Master thesis. Norwegian University of Science and Technology.
- Krogstad, J. A. (2015). 'Control-Switching Strategies for Reservoir Water-Flooding Management'. Master thesis. Norwegian University of Science and Technology.

This is a list of presentations to companies and dissemination of the research results:

- Long-Term & Short-term Production Optimization. Meeting at Kongsberg Oil & Gas. July 2012.
- Optimization Opportunities Using K-Spice. Meeting at Kongsberg Oil & Gas. October 2012.
- Dynamic Simulator Optimization. Meeting at Kongsberg Oil & Gas. October 2012.
- Dynamic Production Optimization. Technical Committee Meeting - IO Center. May 2013.
- Nonlinear Optimization Methods for Solving a Reservoir Multiple Shooting Control Formulation. Meeting at Petrobras. August 2013.

- Differentiation Tool Efficiency Comparison for Nonlinear Model Predictive Control Applied to Oil Gathering Systems. At 9th IFAC Symposium on Nonlinear Control Systems. September 2013.
- Dynamic Production Optimization. Technical Committee Meeting - IO Center. September 2013.
- Adjoint gradient calculation for a simple dynamical system simulated by Backward-Euler. Meeting at Kongsberg Oil & Gas. October 2013.
- Constraint handling & parallelization via Multiple Shooting applied to oil reservoir control optimization. Technical Committee Meeting - IO Center. May 2014.
- Simultaneous simulation & optimization for oil reservoir open-loop optimization. Technical Committee Meeting - IO Center. May 2014.
- Constraint handling & parallelization via Multiple Shooting applied to oil reservoir control optimization. At 3th Oil and Gas Production Optimization Conference - Petrobras. May 2014.
- Output Constraint Handling & Parallelization for Oil Reservoir Control Optimization via Multiple Shooting. Meeting at The Technical University of Denmark. August 2014.
- Output Constraint Handling & Parallelization for Oil Reservoir Control Optimization via Multiple Shooting. International Conference on Integrated Operations in the Petroleum Industry. September 2014. Poster presentation.
- Constraint handling & parallelization applied to reservoir control optimization. International Symposium on Advanced Petroleum Production (ISAPP). November 2015.

Chapter 2

Output Constraint Handling and Parallelization for Oil Reservoir Control Optimization by Means of Multiple Shooting

This chapter is based on (Codas et al. 2015):

Codas, A. et al. (2015). 'Output-Constraint Handling and Parallelization for Oil-Reservoir Control Optimization by Means of Multiple Shooting'. In: *SPE Journal* 20.04, pp. 856–871. ISSN: 1086-055X. DOI: 10.2118/174094-pa.

Abstract

We propose to formulate and solve the reservoir control optimization problem with the direct multiple shooting method. This method divides the optimal control problem prediction horizon in smaller intervals which can be evaluated in parallel. Further, output constraints are easily established on each interval boundary and as such hardly affect computation time. This opens new opportunities to include state constraints on a much broader scale than what is common in reservoir optimization today. However, multiple shooting deals with a large number of variables since it decides on the boundary state variables of each interval. Therefore, we exploit the structure of the reservoir simulator to conceive a variable reduction technique to solve the optimization problem with a reduced sequential quadratic programming algorithm. We discuss the optimization algorithm building blocks and focus on structure exploitation and parallelization opportunities. To demonstrate the method's capabilities to handle output constraints, the optimization algorithm is interfaced to an open-source reservoir simulator. Then, based on a widely used reservoir model, we evaluate performance, especially related to output constraints. The performance of the proposed method is qualitatively compared to a conventional method.

Is not included due to copyright

Chapter 3

Black-Oil Minimal Fluid State Parametrization for Constrained Reservoir Control Optimization

This chapter is based on (Codas et al. 2016a):

Codas, A. et al. (2016a). 'Black-oil minimal fluid state parametrization for constrained reservoir control optimization'. In: *Journal of Petroleum Science and Engineering* 143, pp. 35–43. ISSN: 0920-4105. DOI: 10.1016/j.petrol.2016.01.034.

Abstract

We propose to solve a black-oil reservoir optimal control problem with the Direct Multiple Shooting Method (MS). MS allows for parallelization of the simulation time and the handling of output constraints. However, it requires continuity constraints on state variables to couple simulation intervals. The black-oil fluid model, considering volatile oil or wet gas, requires a change of primary variables for simulation. This is a consequence of the absence of a fluid phase due to dissolution or vaporization. Therefore, reservoir simulators parametrize the states with an augmented vector and select primary variables accordingly. However, the augmented state vector and the corresponding change of primary variables are not suitable for the application of MS because the optimization problem formulation must change according to the change of variables. Thus, we propose a minimal state-space variable representation that prevents this shortcoming. We show that there is a bijective mapping between the proposed state-space representation and the augmented state-space. The minimal representation is used for optimization and the augmented representation for simulation, thereby keeping the simulator implementation unchanged. Therefore, the proposed solution is not invasive. Finally, the application of the method is exemplified with benchmark cases involving live oil or wet gas. Both examples emphasize the requirement of output constraints which are efficiently dealt with the MS method.

3.1 Introduction

The Direct Multiple Shooting Method (MS) is an effective technique to deal with output constraints in control optimization of two-phase reservoirs (Codas et al. 2015). However, the extension of this method to three-phase black-oil models is not trivial due to the reservoir grid-block state-space representation of the fluid saturation condition. This work extends the MS method in (Codas et al. 2015) to miscible black-oil fluid models including live oil and wet gas. Compared to immiscible models, the miscible black-oil model requires additional analysis of the fluid state during simulation to determine the fluid flow conditions appropriately.

Black-oil models are convenient due to their computational simplicity and their capability to approximate compositional models (Fevang et al. 2000). Black-oil models can be seen as a special case of compositional models with three components, water, oil, and gas, associated to three reservoir phases, aqueous, liquid and vapor, respectively. A component may be seen as an indivisible set of molecules which are transported within a fluid phase. A phase is a mixture of components, a homogeneous part of the fluid which is separated of other phases by a boundary surface. The oil and gas chemical components are typically defined as the composition of the liquid phase and vapor phase at standard conditions, respectively. Here, the water component is treated as an immiscible component found exclusively in the aqueous phase. Moreover, oil and gas are the main components of the liquid and vapor phases. However, oil and gas components may exist in both the liquid and vapor phases in the reservoir pressure and temperature conditions. Wet gas models consider a fraction of the oil components vaporized in the vapor phase, whereas live oil models consider a fraction of gas components dissolved in the liquid phase.

Depending on the components properties and reservoir conditions, a component may exist in the fluid mixture while its associated phase may be absent (Mattax et al. 1990; Chen et al. 2006). For instance, the gas and oil components may be completely dissolved in the liquid phase and in this case no vapor phase exists. In live oil models, there is a maximum amount of gas components that can be dissolved in the liquid phase at a given pressure and temperature condition. If the gas components found in the fluid do not reach this maximum amount then the fluid is regarded as under-saturated. In under-saturated conditions, no vapor phase is present. The vapor phase appears if and only if the liquid phase gets saturated of gas, for instance, as a consequence of a drop of pressure below the bubble point pressure. Analogously, wet gas models have an under-saturated and saturated state depending on the fluid conditions, and the existence of the liquid phase depends on the saturation condition.

Compared to compositional simulators, black-oil simulators dispense with the equations of state needed to define component mass fractions. During simulation, the fluid state is monitored and the set of equations describing the fluid flow is switched when a phase appears or disappears (Chen et al. 2006). Thus, any optimization procedure han-

dling this simulator must be capable to determine when the transition occurs and switch the set of equations and primary variables accordingly. Therefore, the optimizer inherits the simulator complexity. Further, since the state representation is discontinuous, MS optimizers face an additional complexity to estimate predicted states.

The application of optimal control to improve the economical return of oil reservoirs described by three-phase black-oil models is not new as Zakirov et al. (1996) applied the Conjugate Gradient method to solve this problem. A real field example considering a fluid model with gas soluble in the oil phase was optimized by Davidson et al. (2003) using the Sequential Quadratic Programming method. Recently, Krogstad et al. (2014) optimized a reservoir model including live oil with a line-search method and a heuristic control-switching method to handle output constraints. However, in the previous works the state variables are not explicitly available in the optimization method as in MS, therefore the specific representation of the state variables does not impose any problem. Key advantages that come with the explicit representation of the states are simulation parallelization opportunities and easy output-constraint handling (Codas et al. 2015).

This work aims to develop a MS formulation for control optimization of oil reservoirs modeled with the black-oil model including gas. In Section 3.2.1 we describe the reservoir model and Appendix 3.A presents a simplified procedure to solve it. Then, in Section 3.3 we develop a minimal state parametrization to represent the fluid state that is suitable for a MS optimal control problem formulation. In the following section we demonstrate the applicability of this new formulation to simple test cases. Finally, this work ends with a discussion of the results and a brief conclusion in sections 3.5 and 3.6, respectively.

3.2 Reservoir model

This works aims to develop a MS formulation which adapts tightly to black-oil reservoir simulators containing miscible hydrocarbons. This section briefly presents the equations being solved in such reservoir models. The solution procedure described in Section 3.A is taken from the Matlab Reservoir Simulation Toolbox (MRST) (Lie et al. 2011; Krogstad et al. 2015) which is later used in our test cases.

3.2.1 The miscible black-oil flow in porous media

The mass conservation principle, the capillary pressure phenomenon, the Darcy law and an empirical modeling of components miscibility given by the black-oil model lead to the differential equations describing three-phase flow in porous media (Chen et al. 2006, p. 283):

$$\frac{\partial}{\partial t}\left(\frac{\phi S_a}{B_a}\right) = -\nabla\cdot\left(\mathbf{T}_a\nabla\mathbf{\Phi}_a\right) + \frac{q_a}{B_a}, \tag{3.1a}$$

$$\frac{\partial}{\partial t}\left[\phi\left(\frac{S_l}{B_l} + \frac{R_v S_v}{B_v}\right)\right] = -\nabla\cdot\left(\mathbf{T}_l\nabla\mathbf{\Phi}_l + R_v\mathbf{T}_v\nabla\mathbf{\Phi}_v\right) + \frac{q_l}{B_l} + \frac{q_v R_v}{B_v}, \tag{3.1b}$$

$$\frac{\partial}{\partial t}\left[\phi\left(\frac{S_v}{B_v} + \frac{R_l S_l}{B_l}\right)\right] = -\nabla\cdot\left(\mathbf{T}_v\nabla\mathbf{\Phi}_v + R_l\mathbf{T}_l\nabla\mathbf{\Phi}_l\right) + \frac{q_v}{B_v} + \frac{q_l R_l}{B_l}, \tag{3.1c}$$

$$S_a + S_l + S_v = 1, \tag{3.1d}$$

$$p_{cla} = p_l - p_a, \quad p_{cvl} = p_v - p_l, \tag{3.1e}$$

$$\mathbf{\Phi}_\alpha = p_\alpha - \rho_\alpha \left\|\mathbf{g}\right\| z, \quad \mathbf{T}_\alpha = \lambda_\alpha \mathbf{k} = \frac{k_{r\alpha}}{\mu_\alpha B_\alpha}\mathbf{k}, \quad \alpha \in \{a, l, v\}\,; \tag{3.1f}$$

The nomenclature for (3.1) is presented in Table 3.1.

The gas solubility and the oil volatility determine the fluid miscibility and its saturation state. The gas solubility and oil volatility range from zero (for immiscible fluids) to a maximum value given by a saturation function, *i.e.*, $R_v \leq R_v^{\max}$ and $R_l \leq R_l^{\max}$. Furthermore, it is assumed that a phase can exist only if the reciprocal phase is saturated, *i.e.*, $S_v > 0 \rightarrow R_l = R_l^{\max}$ and $R_l < R_l^{\max} \rightarrow S_v = 0$ ($S_l > 0 \rightarrow R_v = R_v^{\max}$ and $R_v < R_v^{\max} \rightarrow S_l = 0$).

The saturation functions $R_v^{\max}$ and $R_l^{\max}$ are typically modeled as a function of the phase pressure.

The well flows q_α are not distributed over the reservoir, but concentrated at the well perforations, therefore well equations according to Peaceman (1983) are included with the Dirac δ function centered around the well perforations:

$$q_\alpha = \sum_{w\in\mathcal{W}}\sum_{m\in\mathcal{M}^w} W^{\mathrm{I}}_{w,m}\frac{k_{r\alpha}}{\mu_\alpha}\left(p^w_{\mathrm{bh}} - p_\alpha\right)\delta\left(\mathbf{x} - \mathbf{x}^{w,m}\right), \quad \alpha \in \{a, l, v\} \tag{3.2}$$

The nomenclature for (3.2) is presented in Table 3.1.

For simplicity, the well model described above does not include interactions between perforations of the same well due to the flow in the tubing. Therefore, the pressure difference due to the fluid gravity column is disregarded within the well. Moreover, the equations are written for the phases at reservoir conditions, but these equations are further manipulated to represent the flow at standard conditions.

Table 3.1: Nomenclature

Variable	Description
t	Time.
$\{a, l, v\}$	Set of phases (aqua, liquid and vapor).
$\{W, O, G\}$	Set of components (water, oil and gas).
ϕ	Rock porosity.
S_α	Saturation of the phase α.
B_α	Phase α's formation volume factor.
$q_{\beta s}$	Standard volumetric flow of component β injected or produced through the wells.
$k_{r\alpha}$	Phase α's relative permeability.
μ_α	Phase α's viscosity.
$\mathbf{k}$	Rock absolute permeability.
p_α	Phase α's absolute pressure.
ρ_α	Phase α's density.
$\|\mathbf{g}\|$	Gravity absolute value.
z	Height (increases in the same direction as the gravity).
p_{cla}	Liquid-aqueous capillary pressure.
p_{cvl}	Vapor-liquid capillary pressure.
R_v	Oil volatility in the vapor phase.
R_l	Gas solubility in the liquid phase.
$\mathbf{x}$	Space coordinates.
$\mathcal{W}$	Set of wells.
$\mathcal{M}^w$	Set of perforations of well w.
$W^{\mathrm{I}}_{w,m}$	Well index related to the perforation m of well w located at $\mathbf{x}^{w,m}$.
p^w_{bh}	Bottom hole pressure of well w.
N_P	Number of phases.
N_C	Number of components.
χ	Five dimensional grid-block state variable $(p_l, S_a, S_v, R_l, R_v)$.
γ	Three dimensional grid-block state variable (p_l, S_a, r_H).
Γ	Transformation taking χ to γ.
(r_O, r_G, r_H)	See eq. (3.3).
$\mathcal{S}$	Saturation state, see Table 3.2.
ζ	Simulation primary variable, see Table 3.2.
(w_O, w_G)	Volume fraction of oil and gas at standard conditions.

3.3 Multiple Shooting applied to the reservoir optimal control problem

A MS formulation divides the control problem time horizon in several shooting intervals. Each shooting interval has independent initial condition variables. These are coupled to their neighboring shooting intervals through state equality constraints at the interval boundaries. Therefore, an important issue concerning the MS formulation and black-oil models is the parametrization of the states.

Fluid systems are fully characterized by their intensive variables which are pressure, temperature and concentration of the fluid phases. Therefore, a three-phase ($N_P = 3$) system with three components ($N_C = 3$) is characterized by twelve variables ($12 = (N_C + 1)\, N_P$), *i.e.*, compositions, pressure and temperature for each phase. However, in a reservoir simulator, the degrees of freedom are not twelve because it assumes fluids in thermodynamic equilibrium. According to Gibbs phase rule[1] (Danesh 1998), 10 constraints ($(N_C + 2)\,(N_P - 1) = 10$) are required to ensure consistent components potential, pressure and temperatures among phases. Furthermore, since we restrict this work to isothermal reservoirs, one further degree of freedom is lost since the temperature is fixed. Thus, only one variable $(N_C - N_P + 1) = 1$ is required to fully determined the intensive properties of such fluid systems. However, if the fluid does not form three phases, *i.e.*, if $N_P < 3$, more variables are needed.

Reservoir simulators also require extensive fluid properties, which are determined by the total grid-block void space and the saturations of the formed phases (Acs et al. 1985). The usual variable to describe the intensive properties is the liquid phase pressure, which also describes the void space after the rock compressibility function. In addition, $(N_P - 1)$ variables describe the saturations. Thus, $N_C = (N_C - N_P + 1) + (N_P - 1)$ describe all the desired properties.

The N_C variables for simulation may be selected according to the current phases in the fluid. For instance, for a three-phase black-oil fluid, the variables (p_l, S_a, S_v) fully characterize the grid-block state if $S_a > 0$ and $S_v > 0$, however these variables are not descriptive when the vapor phase is missing due to under-saturation. MRST resolves this issue by keeping more variables $\left(\chi \in \mathbb{R}^5\right)$ per grid-block during simulation and switching the set of primary variables and equations according to the saturation state. Therefore, MRST requires additional measures to keep consistency between the 5 variables and their saturation states.

The natural extension of a simulator to a MS optimal-control problem formulation uses the same state variables on the simulator and on the optimizer side. However, the black-oil simulator in MRST is not suitable for such extension due to the requirement of extra variables for simulation and the related extra consistency checks. Observe that

[1] The Gibb's rule for fluid systems in equilibrium is usually stated as $F = N_C - N_P + 2$, where F is the number of the degrees of freedom to fully describe the system.

the number of required extra variables and algebraic equations grows proportionally to the grid size times the simulated steps. Furthermore, an extension considering the actual simulated variables (p_l, S_a, ζ) is also not possible due to the discontinuity in ζ, see Appendix 3.A.

In this section we propose a new state parametrization that overcomes the aforementioned issues and enables the use of an efficient MS implementation. Furthermore, we show that it is possible to preserve the simulator because the states are easily transformed from the optimizer space to the simulator space.

3.3.1 State variables transformation

Consider the transformation $\Gamma : \mathbb{R}^5 \to \mathbb{R}^3$ taking the variables $\chi = (p_l, S_a, S_v, R_l, R_v)$ to the variables $\gamma = (p_l, S_a, r_H)$. The variable r_H is defined as:

$$r_O = \frac{S_l}{B_l} + R_v \frac{S_v}{B_v} \tag{3.3a}$$

$$r_G = \frac{S_v}{B_v} + R_l \frac{S_l}{B_l} \tag{3.3b}$$

$$r_H = \frac{r_G}{r_G + r_O} \tag{3.3c}$$

The dimensionless variables r_O and r_G are the standard volumes of the oil and gas components in the grid-block void space divided by the pore volume. Therefore, r_H is the ratio between standard volumes of the gas components and the hydrocarbons.

Besides possible physical bounds to r_H depending on the limits on pressures and saturation on the grid block, we easily observe that $0 \leq r_H \leq 1$.

The variable r_H is undefined when $(r_O + r_G) = 0$. However, this issue does not imply in any difficulty to the state representation because $S_a = 1 \leftrightarrow (r_O + r_G) = 0 \leftrightarrow r_O = 0,\ r_G = 0$. This means that the grid block is filled up with water and no hydrocarbon phase is present, thus r_H is not required to represent the grid block state. Any convention can be adopted to define a value for r_H in this case, *e.g.*, $r_H = 0$.

In order to use γ to represent the state χ it must exist a function $\Gamma^{-1} : \mathbb{R}^3 \to \mathbb{R}^5$ such that $\Gamma^{-1}(\Gamma(\chi)) = \chi$, for all the valid values of χ describing a reservoir state. A state representation χ is valid if, $0 < p_l$, $0 \leq S_a \leq 1$, $0 \leq S_v \leq 1$, $S_v + S_a \leq 1$, $R_l \leq R_l^{\max}$ and $R_v \leq R_v^{\max}$. We will show that Γ^{-1} exists by construction.

It is trivial to calculate p_l and S_a in χ from γ because these variables are equal, therefore we focus on how to calculate S_v, R_l and R_v.

The function Γ^{-1} relies on the values of p_l and r_H to calculate the fluid saturation state label. Given r_H it is possible to calculate the corresponding under-saturated values for R_l and R_v. These under-saturated values must be consistent with $R_l^{\max}$ and $R_v^{\max}$ according to Table 3.2, otherwise the fluid is not under-saturated. Thus, the procedure evaluates the following cases:

3.3.1.1 Case $\mathcal{S}^l$ (under-saturated liquid)

The remaining states can be obtained by:

$$S_v = 0 \tag{3.4a}$$
$$R_l = \frac{r_H}{1 - r_H} \tag{3.4b}$$
$$R_v = R_v^{\max} \tag{3.4c}$$

The transformation is valid if:

$$R_l \leq R_l^{\max} \tag{3.5}$$

3.3.1.2 Case $\mathcal{S}^v$ (under-saturated vapor)

The remaining states can be obtained by:

$$S_v = 1 - S_a \tag{3.6a}$$
$$R_v = \frac{1 - r_H}{r_H} \tag{3.6b}$$
$$R_l = R_l^{\max} \tag{3.6c}$$

The transformation is valid if:

$$R_v \leq R_v^{\max} \tag{3.7}$$

3.3.1.3 Case $\mathcal{S}^a$ (water)

The remaining states can be obtained by:

$$S_v = 0 \tag{3.8a}$$
$$R_v = R_v^{\max} \tag{3.8b}$$
$$R_l = R_l^{\max} \tag{3.8c}$$

The transformation is valid if:

$$S_a = 1 \tag{3.9}$$

3.3.1.4 Case $\mathcal{S}^s$ (saturated)

The remaining states can be obtained by:

$$S_v = \frac{r_H\left(1+R_l^{\max}\right)-R_l^{\max}}{B_l\left(\frac{r_H\left(1+R_l^{\max}\right)-R_l^{\max}}{B_l}+\frac{1-r_H\left(1+R_v^{\max}\right)}{B_v}\right)}\left(1-S_a\right) \tag{3.10a}$$

$$R_v = R_v^{\max} \tag{3.10b}$$

$$R_l = R_l^{\max} \tag{3.10c}$$

The transformation is valid if the fluid is not cast in any of the first three cases. An efficient classification for transformation is achieved by first computing $R_l^{\max}$ and $R_v^{\max}$, which are functions of p_l only, and then testing the conditions (3.4b)-(3.5), (3.6b)-(3.7) and (3.9). However, the transformation could fail if eq. (3.10a) provides S_v out of bounds. Theorem 3.1 shows that this situation is impossible:

Theorem 3.1. *Consider a valid state representation (p_l, S_a, r_H) such that $R_l^{\max} < \frac{r_H}{1-r_H}$, $R_v^{\max} < \frac{1-r_H}{r_H}$ and $S_a < 1$. Then, the value of S_v given in* (3.10a) *satisfies $0 \leq S_v \leq 1$.*

Proof. Observe that $0 < r_H\left(1+R_l^{\max}\right) - R_l^{\max}$:

$$0 < \frac{r_H}{1-r_H} - R_l^{\max} \tag{3.11a}$$

$$0 < r_H - R_l^{\max} + R_l^{\max} r_H \tag{3.11b}$$

$$0 < r_H\left(1+R_l^{\max}\right) - R_l^{\max} \tag{3.11c}$$

Furthermore, $0 < 1 - r_H\left(1+R_v^{\max}\right)$:

$$0 < \frac{1-r_H}{r_H} - R_v^{\max} \tag{3.12a}$$

$$0 < 1 - r_H - R_v^{\max} r_H \tag{3.12b}$$

$$0 < 1 - r_H\left(1+R_v^{\max}\right) \tag{3.12c}$$

Thus, the numerator and the denominator of (3.10a) are positive, therefore $S_v > 0$. The inequality $S_v < 1$ is easily confirmed after re-writing (3.10a):

$$S_v = \underbrace{\left(1+\frac{\overbrace{\frac{1-r_H\left(1+R_v^{\max}\right)}{B_v}}^{>0}}{\frac{r_H\left(1+R_l^{\max}\right)-R_l^{\max}}{B_l}}\right)^{-1}}_{<1}\underbrace{\left(1-S_a\right)}_{<1} < 1 \tag{3.13a}$$

Lastly, the transformation can be undetermined if simultaneously:

$$0 = \frac{r_H}{1 - r_H} - R_l^{\max} \tag{3.14a}$$

$$0 = \frac{1 - r_H}{r_H} - R_v^{\max} \tag{3.14b}$$

However, eq. (3.14) implies in $1 - R_l^{\max} R_v^{\max} = 0$ which is inconsistent in black-oil models (Trangenstein et al. 1989). This is a property that the fluid must fulfill by construction of the model. □

3.3.2 State variables transformation based on volume fractions

Another transformation candidate for a minimal representation is $\hat{\Gamma} : \mathbb{R}^5 \to \mathbb{R}^3$ taking the variables $\chi = (p_l, S_a, S_v, R_l, R_v)$ to the variables $\hat{\gamma} = (p_l, w_O, w_G)$. The variables w_O and w_G are defined as:

$$w_O = \frac{r_O}{r_W + r_O + r_G} \tag{3.15a}$$

$$w_G = \frac{r_G}{r_W + r_O + r_G} \tag{3.15b}$$

where $r_W = \frac{S_a}{B_a}$. This candidate is attractive because w_O and w_G are the volume fractions at standard conditions. Moreover, the construction of $\hat{\Gamma}^{-1}$ is possible following a similar procedure as presented in Section 3.3.1. However, $\hat{\Gamma}^{-1}$ additionally requires $w_O + w_G \leq 1$. Consequently, the optimization problem formulation developed in Section 3.3.3 requires more constraints to use $\hat{\Gamma}$. Therefore, we prefer the transformation Γ developed in Section 3.3.1.

3.3.3 Optimal control problem formulation

We extend the optimal control problem formulation in (Codas et al. 2015) aiming to solve black-oil problems with a MS formulation. Thus the problem formulation is:

$$\min_{\Theta_c} \psi_c(\Theta_c) \tag{3.16a}$$

$$\text{s.t.}: \quad \gamma_k^{\mathrm{f}} - \gamma_{k+1} = 0, \quad k \in \mathcal{K}, \tag{3.16b}$$

$$R\left(\Gamma^{-1}(\gamma_k), \Gamma^{-1}\left(\gamma_k^{\mathrm{f}}\right), \mathbf{v}_k, \mathbf{u}_{\kappa(k)}\right) = 0, \quad k \in \mathcal{K} \tag{3.16c}$$

$$\mathbf{b}_{l,k}^{\gamma} \leq \gamma_k \leq \mathbf{b}_{u,k}^{\gamma}, \quad k \in \mathcal{K} \tag{3.16d}$$

$$\mathbf{b}_{l,k}^{\mathrm{v}} \leq \mathbf{v}_k \leq \mathbf{b}_{u,k}^{\mathrm{v}}, \quad k \in \mathcal{K} \tag{3.16e}$$

$$\mathbf{b}_{l,i}^{\mathrm{u}} \leq \mathbf{u}_i \leq \mathbf{b}_{u,i}^{\mathrm{u}}, \quad i \in \mathcal{U} \tag{3.16f}$$

The optimization variables Θ_c consist of $\left(\gamma, \gamma^{\mathrm{f}}, \mathbf{v}, \mathbf{u}\right)$. The optimization time horizon is divided into K time frames where $\mathcal{K} = \{1, \ldots, K\}$. The state variables $\left(\gamma, \gamma^{\mathrm{f}}, \mathbf{v}\right)$ are indexed for each frame in $\mathcal{K}$. However, the control variables are indexed on the set $\mathcal{U} = \{1, \ldots, U\}$ and the function $\kappa : \mathcal{K} \to \mathcal{U}$ maps a control index for every time frame index. The continuity of the state variables across intervals is enforced by the constraints (3.16b) on the space of $\gamma = (p_l, S_a, r_H)$. The bijective transformation Γ enables to link the simulator state variables defined on $\chi = (p_l, S_a, S_v, R_l, R_v)$ to the state variables for optimization given by γ, as described by the constraints (3.16c). Output constraints can be imposed as bounds on the state variables γ and on the algebraic state variables $\mathbf{v}$, as described by the constraints (3.16d) and (3.16e), respectively. Furthermore, input constraints are imposed by the constraints (3.16f). The objective function ψ_c is defined on the space of Θ_c and may instantiate the Net Present Value (NPV) of the recovery process.

The formulation (3.16) is not suitable for general purpose NLP solvers due to the size of the Jacobian of (3.16c). However, this formulation is structured, decomposable and suitable for parallelism (Codas et al. 2015). The application of the reduction techniques requires the Jacobian $\left[\frac{\partial R_k}{\partial \gamma_k^{\mathrm{f}}} \frac{\partial R_k}{\partial \mathbf{v}_k}\right]$ to be non-singular. Observe that $\frac{\partial R_k}{\partial \gamma_k^{\mathrm{f}}} = \frac{\partial R_k}{\partial \mathbf{x}_k^{\mathrm{f}}} \frac{\partial \mathbf{x}_k^{\mathrm{f}}}{\partial \gamma_k^{\mathrm{f}}}$ and $\frac{\partial \mathbf{x}_k^{\mathrm{f}}}{\partial \gamma_k^{\mathrm{f}}}$ is full rank because Γ is bijective, therefore the rank of $\left[\frac{\partial R_k}{\partial \gamma_k^{\mathrm{f}}} \frac{\partial R_k}{\partial \mathbf{v}_k}\right]$ depends on the correct construction of the equations for simulation and is independent of the transformation Γ. This property guarantees the existence of implicit functions R^{γ} and $R^{\mathbf{v}}$ and allows for the reformulation of (3.16):

$$\min_{\Theta} \ \psi\left(\Theta\right) \tag{3.17a}$$

$$\text{s.t.}: \quad \gamma_{k+1} = R_k^{\gamma}\left(\gamma_k, \mathbf{u}_{\kappa(k)}\right), \quad k \in \mathcal{K}, \tag{3.17b}$$

$$\mathbf{v}_k = R_k^{\mathbf{v}}\left(\mathbf{x}_k, \mathbf{u}_{\kappa(k)}\right), \quad k \in \mathcal{K} \tag{3.17c}$$

$$\mathbf{b}_{l,k}^{\gamma} \leq \gamma_k \leq \mathbf{b}_{u,k}^{\gamma}, \quad k \in \mathcal{K} \tag{3.17d}$$

$$\mathbf{b}_{l,k}^{\mathrm{v}} \leq \mathbf{v}_k \leq \mathbf{b}_{u,k}^{\mathrm{v}}, \quad k \in \mathcal{K} \tag{3.17e}$$

$$\mathbf{b}_{l,i}^{\mathrm{u}} \leq \mathbf{u}_i \leq \mathbf{b}_{u,i}^{\mathrm{u}}, \quad i \in \mathcal{U} \tag{3.17f}$$

The decision variables Θ are reduced to γ, $\mathbf{v}$ and $\mathbf{u}$. Moreover, the objective ψ is derived from ψ_c assuming that (3.16b) holds. Finally, observe that auxiliary functions and variables may be instantiated within the equation structure $R^{\mathbf{v}}$. The additional variables may help to instantiate constraints in (3.17e).

3.4 Case and Results

In this section we perform a computational assessment of the MS method applied to black-oil problems including gas. To this end, we propose the solution of 2 problems

based on the benchmark cases SPE1 (Odeh 1981) and SPE3 (Kenyon et al. 1987). The optimizer source code and the parametrization of the cases are available in (Codas 2014). An overview of this optimization method is provided in Section 1.4.

The SPE1 case is a three-dimensional reservoir with 300 grid-blocks $(10 \times 10 \times 3)$ which considers dissolved gas in live oil, *i.e.*, gas components may be found in the liquid phase at reservoir conditions. Initially, the liquid phase is under-saturated of gas components, thus no vapor phase is found. The reservoir model has 2 wells, 1 injector controlled by gas flow rate and 1 producer controlled by oil production rate.

Constraints on the operation of the wells are set as specified in (Odeh 1981). The oil production rate is limited within $[1000, 20000]\ STB/day$, and the gas injection rate within $[1, 100]\ MMscf/day$. The minimum flowing bottom hole pressure for the wells is $1000\ psi$. Moreover, the liquid-pressure state bounds are set according to the minimum flowing bottom hole pressure and the maximum value given in the PVT tables, *i.e.*, $[1000, 9014.7]\ psi$. The aqua-saturation is bounded in $[5, 100]\ \%$ and the states corresponding to r_H are within $[0, 1]$.

The reservoir is simulated for $1200\ days$ with fixed steps of 5 days, *i.e.*, $K = 240$. Moreover, the control steps are divided in equal periods of $120\ days$, therefore $U = 10$.

The objective function models the Net Present Value (NPV) of the recovery. The NPV function of one reservoir realization is given by:

$$\text{NPV} = \sum_{k=1}^{K} \left(\frac{q_{o,k} r_o + q_{gp,k} r_{gp} - q_{wp,k} r_{wp} - q_{gi,k} r_{gi}}{(1+d)^{t_k/t_K}} \right) \Delta t_k \tag{3.18}$$

where $q_{o,k}$, $q_{gp,k}$, $q_{wp,k}$ and $q_{gi,k}$ represent the oil produced, the gas produced, the water produced and the gas injected, respectively, and r_o, r_{gp}, r_{wp} and r_{gi} are their corresponding prices. Moreover, d is the discount factor and t_k is the time at the end of the step time k. In our experiments $(r_o, r_{gp}, r_{wp}, r_{gi}) = (300, 0.1, 0.1, 0.1)\, 10^{-8}\ USD/sm^3$ and $d = 0$. Although the prices are not realistic, the ratio r_o/r_{gp} is realistic in the current market and the prices are scaled for algorithmic purposes.

Scaling plays an important role in non-linear optimization algorithms. In our approach, the intention of the scaling factors is to make the range of the variables comparable in modulus. Thus, the pressure is scaled by $100\ psi$, the water saturation by $1\ \%$, and r_H by 0.1. Moreover, the rates of oil and water are scaled by $100\ STB/day$ and the gas rates by $1\ Mscf$.

Figures 3.1 and 3.2 display the optimal well schedules and the corresponding predictions for the injector and producer in the SPE1 case. The oil production rate is kept at the maximum during the first $1080\ days$ and consequently it is observed a pressure drop at the bottom hole pressure of the well. The gas injection is kept around $4\ MMscf/day$ during the first $980\ days$ with the aim to maintain the reservoir pressure and push fluids towards the producer. Moreover, observe that the flowing bottom hole pressure constraint is active in the producer at several time instants while the oil production rate is

kept at its maximum. Therefore, we conclude that the pressure constraint feasibility is maintained by regulating the injector. Finally, during the last $120\ days$ it is observed a rapid increase of the gas-production rate and a substantial decrease of the oil production which is a consequence of a gas breakthrough and a low reservoir pressure. At the end of the production period all the reservoir grid-blocks are saturated, *i.e.*, the vapor phase is present. The vapor phase is formed due to the low reservoir pressure and the gas injected during production, see Figure 3.3. This solution is feasible and provides a NPV increase of $25\ \%$ compared to the initial schedule which applies $100\ MMscf/day$ and $20000\ STB/day$ of constant gas rate injection and oil rate production, respectively.

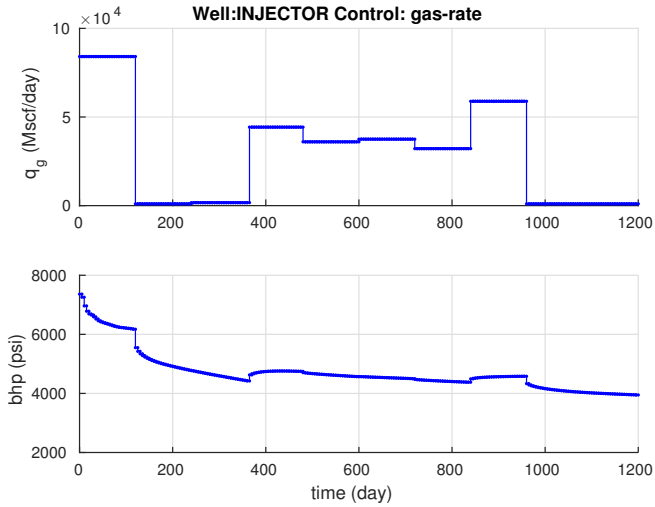

Figure 3.1: Optimal schedule for injector well of the SPE1 case.

The SPE3 case is a three-dimensional reservoir with 324 grid-blocks $(9 \times 9 \times 4)$. The rock properties of the reservoir, like porosity, permeabilities and thickness are constant for each of the 4 vertical layers. Moreover, it has 2 vertical wells which are positioned on the main diagonal. Thus, it is sufficient to model half of the reservoir due symmetry, however, we work with the full grid. Part of the task in (Kenyon et al. 1987) consisted of matching the PVT data from hydrocarbon laboratorial analysis, and therefore a unique PVT table is not provided. Therefore, we instantiate the model as provided in the MRST package to allow reproducibility of the results. This case considers the oil components completely dissolved in the vapor phase at the beginning of the production.

Both wells, the injector and the producer, are controlled by gas flow rate. The gas flow rate bounds are $[0, 4.7]\ \ MMscf/day$ and $[0, 6.2]\ \ MMscf/day$ for the well injector and producer, respectively. Moreover, the maximum flowing bottom hole pressure at the injector is $4000\ psi$ and the minimum flowing bottom hole pressure in the producer is set to $1050\ psi$. The bounds on the grid-block liquid pressure states are $[1215, 3600]\ \ psi$.

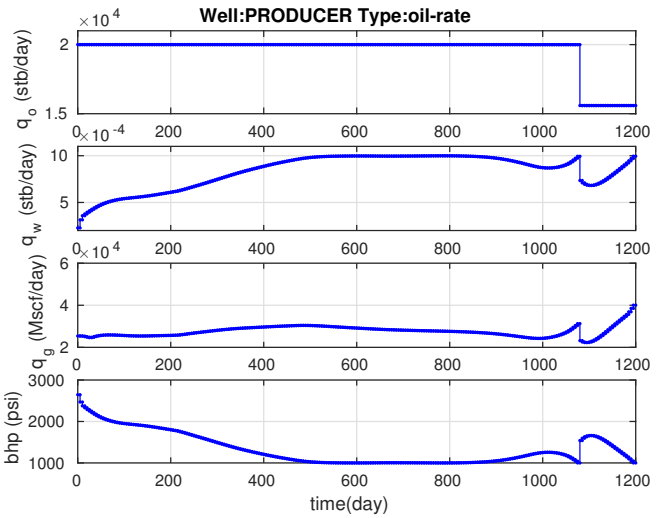

Figure 3.2: Optimal schedule for the producer well of the SPE1 case.

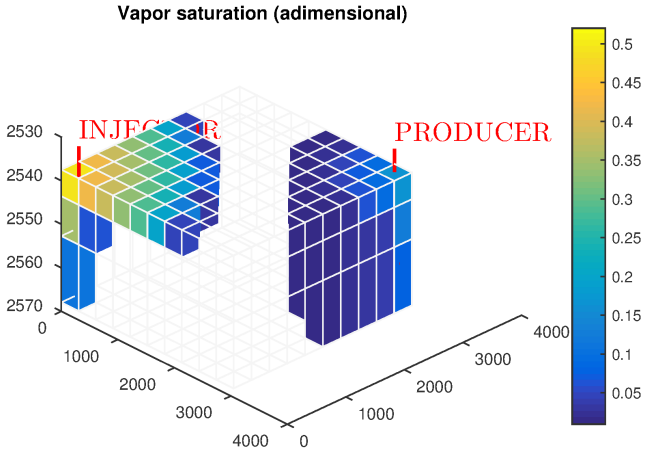

Figure 3.3: Predicted vapor saturation profile after 500 days of production for the SPE1 case. The transparent grid-blocks contain no vapor phase.

Moreover, the water saturations and r_H are bounded in $[0, 1]$.

The production process is predicted for $20\ years$ and each year is simulated with a sequence of fixed time steps given by $(1, 20, 70.25, 91.25, 91.25, 91.25)\ days$, therefore, $K = 120$. The shorter simulation time steps improve the simulation approximations after a control change and prevent simulator convergence failures. The control is divided in 20 equal periods of $1\ year$. Thus, $U = 20$. Finally, the objective value and the scaling

factors for optimization are identical as in the SPE1 case.

Optimal well schedules and well predictions for the SPE3 case are on display in the figures 3.4 and 3.5. The gas injection rate is kept at maximum for almost $5000\ days$ and then the well is closed. Through the bottom hole pressure in both wells we observe that the gas injector makes a good pressure maintenance during the first $4000\ days$. The producer starts with a production of around $350\ STB/day$ of oil which decays to around $0\ STB/day$ by the end of the production life. The gas flow rate in the producer is regulated around $4.5\ MMscf/day$ during the first $3000\ days$ and then ramped to the maximum in the last $10\ years$. Observe that the pressure constraints in the producer are active at the end of the production life. After $4000\ days$ of production the reservoir pressure drops significantly around the producer, therefore, the oil components condense and form the liquid phase, see Figure 3.6. This solution provided an NPV increase of 37% compared to the baseline schedule which required maximum injection and production during the whole production life.

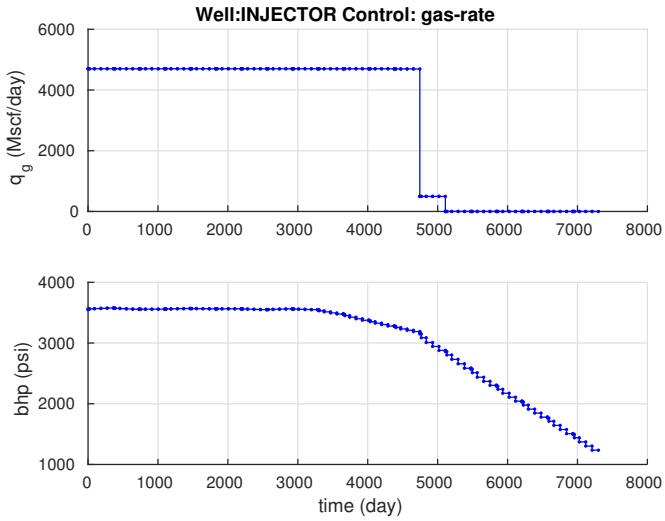

Figure 3.4: Optimal schedule for the injector well of the SPE3 case.

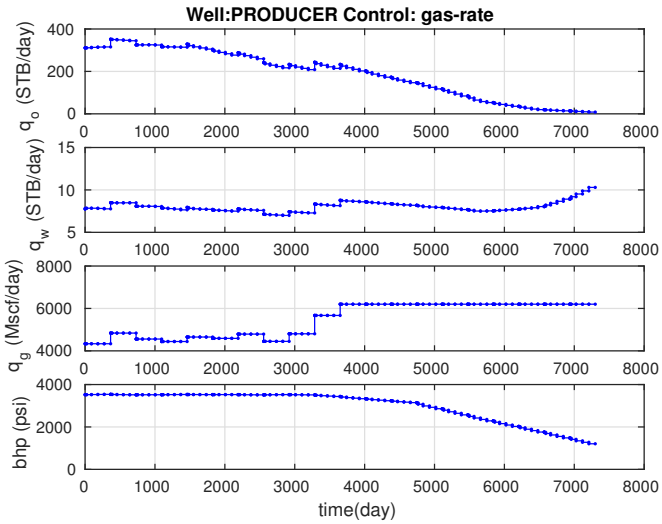

Figure 3.5: Optimal schedule for the producer well of the SPE3 case.

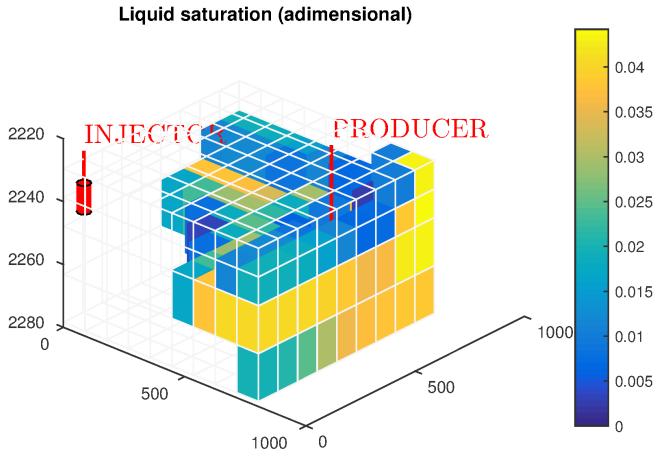

Figure 3.6: Predicted liquid saturation profile after 14 years of production for the SPE3 case. The transparent grid-blocks contain no liquid phase.

3.5 Discussion

Reservoir models with miscible black-oil fluids usually require a change of primary variables during simulation. For instance, this change of variables may be associated to the bubble-point pressure of the fluid. When the pressure is above the bubble-point pres-

sure, no gas phase is found and the gas solubility is used as a primary variable. However, when the pressure is below the bubble-point pressure, then the saturation of the gas phase is used as primary variable. This change of variables is not problematic for optimization methods considering only the control variables as decisions (Zakirov et al. 1996; Krogstad et al. 2015). However, the MS method requires additional equality constraints on the state variables, therefore, the change of variables is not suitable.

To resolve this problem, we propose an alternative representation that requires a minimal number of parameters to fully define the fluid state. This representation is capable to model the intensive and extensive properties of the fluid. It includes the oil pressure and a variable related to the mixture of hydrocarbons. These two variables are enough to represent the saturation state of the liquid phase and the vapor phase. Moreover, the water saturation provides the missing information to decode the extensive properties. This representation is proven minimal according to the Gibbs phase rule for fluids. Although, a semantically simpler representation based on standard volumes is also minimal, it requires additional constraints for its application in practice.

Although not investigated in this paper, alternative solutions to this problem may use more variables and equations. One possible alternative is provided in Section 3.3.2. This alternative is not encouraged because the number of inequality constraints of the MS method increases with the number of grid-blocks. Further, extensions of this algorithm to general compositional models may require all these extra variables to allow the solution of the equations of state. Here, only black-oil models are studied due to their simplicity, popularity and capability to approximate more general fluids.

The proposed state transformation is computationally efficient. The transformation is explicit, in the sense that it does not require to solve extra implicit equations. Moreover, two variables are directly obtained because they are common in both representations. The remaining variables are obtained from straightforward arithmetics. In addition, the reservoir simulator does not require modifications because the transformation is bijective. Therefore, this method is not invasive because the reservoir simulator is not changed for its application. However, this method inherits potential shortcomings related to discontinuities in the fluid property functions. Thus, at the problem formulation phase it is important to verify that the functions related to the fluid properties are sufficiently smooth, including on state transitions. MRST models the fluid properties using continuous piecewise linear functions from tabulated data properties. Thus, these functions are not continuously differentiable ($\mathcal{C}^1$) as needed to prove the first-order optimality conditions(Nocedal et al. 2006, p. 321). Nevertheless, a piecewise $\mathcal{C}^1$ function can be approximated with a $\mathcal{C}^1$ function with arbitrary accuracy. Therefore, if the optimization method experiences convergence issues due to evaluations of the fluid properties on the function break-points, then a smooth approximation may be needed.

In contrast to traditional methods as in (Zakirov et al. 1996; Krogstad et al. 2015) which only require an initial guess for $\mathbf{u}$, MS also requires an initial guess for γ and $\mathbf{v}$. In (Codas 2014) these initial guesses are obtained by solving (3.17b) and (3.17c)

sequentially for $k = 1$ to $k = K$. If this procedure provides an infeasible initial guess regarding (3.17d) and (3.17d), then the violating variables are set to the corresponding boundary values.

Finally, the case studies exemplify the application of the MS method to two benchmark cases. The SPE1 case has volatile oil and the SPE3 case has wet gas. We include constraints according to the original problem specification and to extrapolations on the PVT curves. The MS solution method in (Codas et al. 2015) allows the inclusion of constraints in a broader sense. Thus, the verification of these constraints on every simulated step is not an issue in these problems.

3.6 Conclusion

In this paper we extend the MS optimization formulation developed in (Codas et al. 2015) to black-oil reservoirs including miscible gas. The original formulation considered only water-flooding problems. The extension is not straightforward due to the requirement of extra variables to fully represent the miscibility of fluids. Therefore, we develop a transformation that allows a minimal fluid state representation. Finally, we show the potential of the MS algorithm with this state representation in two test cases where output constraints are critical, the first involving live-oil and the second wet gas.

3.A Simulation

The discretization of the eq. (3.1) is provided in (Lie et al. 2011; Krogstad et al. 2015) and implemented in MRST. In a nutshell, the equations are discretized in space with the Two Point Flux Approximation method (TPFA) (Lie et al. 2011), and the equations are discretized in time using the implicit backward Euler scheme, which are solved with Newton updates (Krogstad et al. 2015). The residuals and Jacobians required to solve the Newton updates are efficiently obtained with Automatic Differentiation (Griewank et al. 2008). Finally, well equations are included to the discretized system with standard Peaceman models. Examples on how to instantiate and solve these equations are available in (Lie 2014).

To solve the non-linear Newton updates resulting from the discretization of (3.1), a set of primary variables are required. The functions $\phi, B_\alpha, p_{cla}, p_{cvl}, \rho_\alpha, k_{r\alpha}, \mu_\alpha$ depend on 8 variables, namely, the phase pressures, saturations for each phase, in addition the gas solubility and the oil volatility. Nevertheless, only 6 equations are available which are (3.1d), (3.1e) and the components conservations for each grid-block. Two more equations are added according to the fluid saturation state as shown in Table 3.2.

The saturation state $s \in \mathcal{S} = \left\{\mathcal{S}^l, \mathcal{S}^v, \mathcal{S}^s, \mathcal{S}^a\right\}$ can be uniquely determined by the saturation variables, thus the fluid is called either under-saturated liquid ($\mathcal{S}^l$), under-saturated vapor ($\mathcal{S}^v$), saturated ($\mathcal{S}^s$) or water ($\mathcal{S}^a$). For simulation, the grid blocks are

Table 3.2: Fluid saturation state. The variable ζ is a primary variable for simulation and adopts the value of either R_l, R_v or S_v depending on the saturation state.

Label	Saturation state	Condition	Equations	ζ
$\mathcal{S}^l$	$S_l > 0$, $S_v = 0$	$0 \leq R_l \leq R_l^{\max}$	$S_v = 0$, $R_v = R_v^{\max}$	R_l
$\mathcal{S}^v$	$S_l = 0$, $S_v > 0$	$0 \leq R_v \leq R_v^{\max}$	$S_l = 0$, $R_l = R_l^{\max}$	R_v
$\mathcal{S}^s$	$S_l > 0$, $S_v > 0$	$S_l > 0$, $S_v > 0$	$R_v = R_v^{\max}$, $R_l = R_l^{\max}$	S_v
$\mathcal{S}^a$	$S_l = 0$, $S_v = 0$	$S_l = 0$, $S_v = 0$	$R_v = R_v^{\max}$, $R_l = R_l^{\max}$	S_v

labeled according to their saturation state at each iteration. The solver handles three primary variables for each grid block, p_l, S_a and ζ, being the latter dependent on the saturation state, see Table 3.2. The equations (3.1d), (3.1e) and the two additional equations depending on the saturation state are solved by variable substitution, thus remaining the mass balances to solve iteratively. The variables p_a, p_v and S_l are always eliminated due to the equations (3.1d) and (3.1e), therefore the solver keeps $\chi = (p_l, S_a, S_v, R_l, R_v)$ to describe the grid block state completely.

Each well includes four additional primary variables to the Newton iterations, $v^w = (q_{Ws}, q_{Os}, q_{Gs}, \ p_{\text{bh}})^w \ w \in \mathcal{W}$, which are the well flows of water, oil and gas at standard conditions, and the bottom hole pressure. Accordingly, 4 equations are included to the implicit system accounting for eq. (3.2). The fourth well equation is a closure equation, or well control. Typically, it is imposed a constant flow rate or bottom pressure of the well.

In summary, the solution to the simulation problem consists of finding the reservoir state $\chi_k = (p_l, S_a, S_v, R_l, R_v)_k$ and the well variables $\mathbf{v}_k = (q_{Ws}, q_{Os}, q_{Gs}, p_{\text{bh}})$ given an initial reservoir state χ_{k-1} and the boundary conditions $\mathbf{u}_k$ for each well and for all time step k. To this end, at the iteration r, it is first determined a saturation label s_k^r for each grid-block given the current guess χ_k^r for χ_k. Then, the variables $\mathbf{x}_k^r = (p_l, S_a, \zeta)_k^r$ are determined and a Newton step is solved:

$$-R^r = \begin{bmatrix} \frac{\partial R_{\text{c}}^r}{\partial \mathbf{x}^r} & \frac{\partial R_{\text{c}}^r}{\partial \mathbf{y}^r} \\ \frac{\partial Q_{\text{w}}^r}{\partial \mathbf{x}^r} & \frac{\partial Q_{\text{w}}^r}{\partial \mathbf{y}^r} \\ 0 & \frac{\partial B^r}{\partial \mathbf{v}^r} \end{bmatrix} \begin{bmatrix} \Delta^r \mathbf{x} \\ \Delta^r \mathbf{v} \end{bmatrix} \tag{3.19}$$

where R_c represents the residual of the mass balances related to eqs. (3.1a)-(3.1c) for the grid-blocks, Q_{w} is the residual of eq. (3.2), and B is the residual to the well closure equations.

Finally, compatibility measures are applied after the application of the correction steps $(\Delta^r \mathbf{x}, \ \Delta^r \mathbf{v})$ to keep the consistency of the variables. The compatibility measures make sure that the saturation variables are limited within 0 and 1, and the solubility variables must be bounded according to their saturation functions. Therefore, the Newton steps are chopped if these hard constraints are not fulfilled. Thus, the next state iterate χ_k^{r+1} is determined by a function $\mathbf{x}_k^{r+1} = U^{\text{x}}(\mathbf{x}_k^r, \Delta^r \mathbf{x}_k, s_k^r)$ and $\mathbf{s}_k^{r+1} = U^{\text{s}}(\mathbf{x}_k^r, \Delta^r \mathbf{x}_k, s_k^r)$.

The functions U^{x} and U^{s} ensure the consistency of the pair $\bar{\mathbf{x}}^r = \mathbf{x}^r + \Delta^r \mathbf{x}$ and s_k^r with respect to the conditions in Table 3.2. If the pair is consistent then $\bar{\mathbf{x}}^r$ induces $\mathbf{x}_k^{r+1}$ and χ_k^{r+1}, and $s_k^{r+1} = s_k^r$. Otherwise, if the saturation state conditions are violated, then the saturation status changes, *i.e.*, $s_k^{r+1} \neq s_k^r$ and therefore, the set of equations to be solved also changes according to Table 3.2.

Throughout the paper, the residual of the simulator equations is represented with $R\left(\chi_{k+1}, \chi_k, \mathbf{v}_k, \ \mathbf{u}\right)$. This system of equations includes eq. (3.19) and the equations in Table 3.2 according to the fluid saturation state.

This appendix gave a simplified overview of the black-oil reservoir simulator implemented in MRST. The intention was to provide the reader with insights on how the reservoir state is defined and simulated. Nevertheless, the solver embedded in the simulator possess more sophisticated heuristics to deal with oscillations and to enforce convergence which are beyond the scope of this document.

Chapter 4

Multiple Shooting applied to robust reservoir control optimization including output constraints on coherent risk measures.

This chapter is based on (Codas et al. 2016b):

Codas, A. et al. (2016b). 'Multiple Shooting applied to robust reservoir control optimization including output constraints on coherent risk measures.' To be submitted.

Abstract

The production life of oil reservoirs starts under significant uncertainty regarding the actual economical return of the recovery process due to the lack of oil field data. Consequently, investors and operators make management decisions based on a limited and uncertain description of the reservoir. In this work we propose a new formulation for robust optimization of reservoir well controls. This formulation exploits coherent risk measures, a concept traditionally used in finance, to deal with the uncertainty. It is inspired by the Multiple Shooting (MS) method which permits broad range of parallelization opportunities. A variable elimination procedure allows to solve this problem in a reduced space and an active-set method helps to handle a large set of inequality constraints. Finally, we demonstrate the application of constraints to limit the risk of water production peaks on a standard test case.

4.1 Introduction

Almost every decision making problem includes variables which remain unknown at the time to act. However, these variables are not completely unknown, and it is often possible to estimate their range of variation with historical data or knowledge from experts. Oil reservoirs are located far below the earth surface, therefore only indirect observations of the recovery process can be carried out from wells and from the surface. Thus, solving this decision problem deterministically is discouraged due to the inherent uncertainty prevailing in the reservoir production process. Besides calculating an initial estimate of this uncertainty, it is also necessary to assimilate measured data during production to periodically correct the estimates and review the production strategy. This problem has been solved using the closed-loop reservoir management strategy (Brouwer et al. 2004; Aitokhuehi et al. 2005; Jansen et al. 2005; Jansen et al. 2009). Figure 4.1 illustrates the principles of closed-loop reservoir management. This strategy consists of the sequential application of data-assimilation and production optimization. A robust approach to control optimization (Van Essen et al. 2009) for reservoir management suggests to use the uncertainty description generated during the data assimilation phase to instantiate a stochastic programming problem. Thus, the solution of this problem leads to robust operation with respect to the probable reservoir parameters.

The production phase of an oil reservoir starts while most reservoir parameters are very uncertain. In general, the available data is insufficient to generate an accurate reservoir description. For instance, the reservoir fluid flows through a porous medium with complex geometrical structure. Typically, reservoir models describe this medium with averaged quantities for porosity and permeability. These simplifications evade the need to model the geometry of the pore space. In the most general sense, these quantities may have different values at every single point of the reservoir domain, thus an infinite dimensional space is required for their parametrization. In practice, these properties are considered constant within a finite but usually high number of grid-blocks (Mattax et al. 1990). Therefore, the amount of measured data used for reservoir parameter estimation is insufficient to find an unique parametrization solution, *i.e.*, the data-assimilation problem is underdetermined. Thus, it is possible to find an infinite number of parametrizations that match the production history exactly, however the forecast capability of such solutions is not guaranteed and often inaccurate (Oliver et al. 2008). Nevertheless, the consistent application of data-assimilation leads to a description of the uncertainty which is critical for designing production strategies because it helps to identify how the outcome of these decisions are affected by the uncertainty.

The goal of robust reservoir management methods (Van Essen et al. 2009) is to find a control schedule that optimizes a performance indicator, such as the accumulated total field oil production, for any of the reservoir conceivable scenarios. Moreover, a safe operation is always a requirement albeit the uncertainty (Chen et al. 2012). The considered scenarios are usually taken from the posterior distribution of data-assimilation

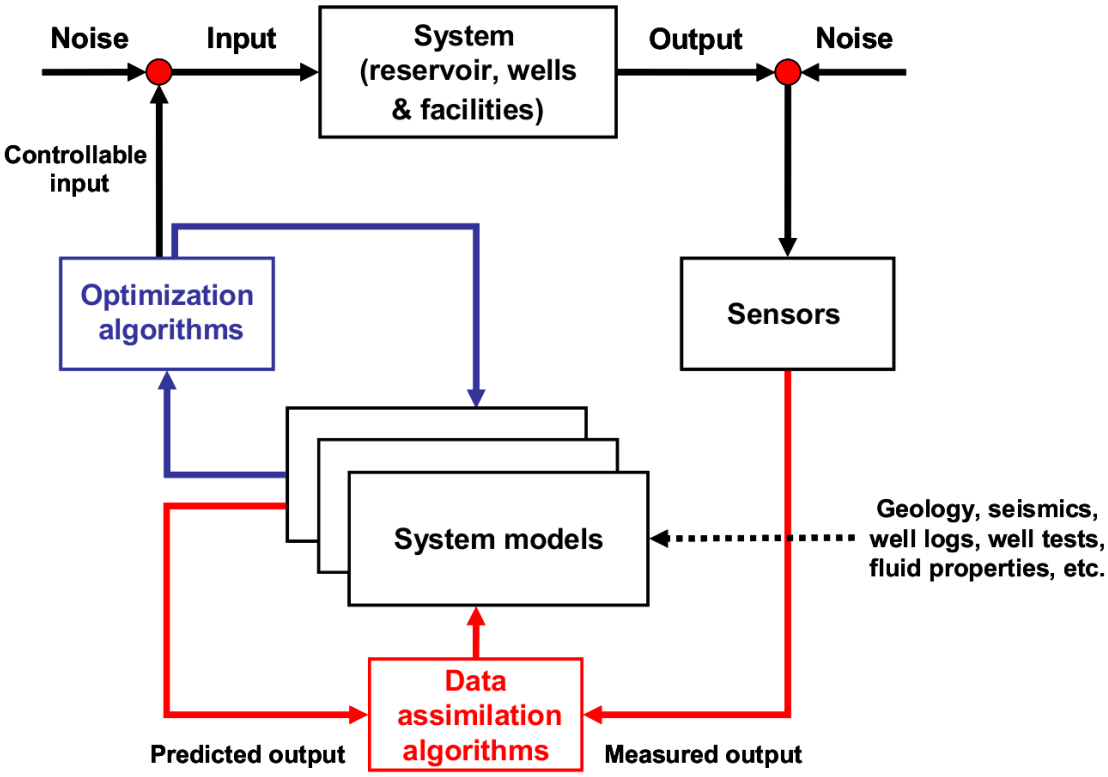

Figure 4.1: Reservoir management feedback loop (Jansen et al. 2009). Data assimilation algorithms generate scenarios that describe the reservoir uncertainty. Then, an optimization algorithm uses this description to compute a production strategy.

algorithms such as the Ensemble Kalman Filter (EnKF) (Evensen 1994; Naevdal et al. 2005). Typical robust reservoir optimization approaches consider the maximization of the expected Net Present Value (NPV) of the recovery process (Chen et al. 2009; Van Essen et al. 2009; Chen et al. 2012). In addition, it has been suggested to extend the expectancy functional with the standard deviation or the variance (Yeten et al. 2003; Bailey et al. 2005; Alhuthali et al. 2010; Capolei et al. 2015b; Yasari et al. 2015) aiming to reduce the variability and the risk due to uncertainty. However, it has been shown that the inclusion of this deviation measures is not coherent (Artzner et al. 1999; Rockafellar 2007). Therefore, we propose and demonstrate the application of the Average Value at Risk[1] (Rockafellar et al. 2000) to handle risk of constraint violation.

To date, it is not possible to find a computationally tractable, closed-form mathematical expression that solves such stochastic optimal control problems. Therefore, it has been suggested to parametrize the control schedule and to solve a stochastic optimal

[1]Also known as Conditional Value at Risk

control problem with direct methods (Jansen 2011; Hou et al. 2015). Direct methods for optimal control transform the optimal control problem into a nonlinear programming problem (Binder et al. 2001). The uncertainty is introduced to the optimization problem using the Sample Average Approximation (SAA) method (Shapiro et al. 2009a), where the samples are obtained from the EnKF after the assimilation stage. According to the SAA theory and the *Law of Large Numbers*, the solution of the optimization problem considering a sampled set of scenarios converges to the solution of the stochastic optimization problem as the sample size increases. Accordingly, a consistent approach for the construction of scenarios plays a central role for the application of this methodology.

This work seeks an efficient strategy to solve constrained robust reservoir control optimization problems. To this end, we propose the extension of the optimization algorithm based on the Direct Multiple Shooting Method (MS) (Codas et al. 2015). This method allows for an efficient evaluation of the reservoir simulation because the problem can be decomposed in the dimension of the uncertainty and in the dimension of time. Moreover, constraints are easily included as bounds on the decision variables.

In the following, Section 4.2 describes the formulation of the optimization problem based on MS and 4.3 describes the assumptions made by the reservoir simulator used in our test cases. In Section 4.4 we describe the implementation of the MS algorithm for robust optimization and Section 4.5 shows the risk measures considered in this work. A numerical study is conducted in Section 4.6 and a discussion of our approach is provided in Section 4.7. Finally, Section 4.8 provides a very brief summary of the contributions in this paper.

4.2 Multiple Shooting applied to Robust Optimization

Direct methods for optimal control have been in the focus of research due to the increasing availability of computational power and efficient numerical methods. The direct methods discretize the dynamical equations and the control parameters, and transform the Optimal Control Problem to a Nonlinear Programming Problem (NLP). Depending on the discretization, direct methods can be classified into Single Shooting, Multiple Shooting or Collocation. Single Shooting is the most popular method for reservoir control applications (Jansen 2011; Hou et al. 2015), whereas collocation has been suggested in (Heirung et al. 2011). Multiple Shooting (MS) was suggested for dynamical optimization of a deterministic reservoir water-flooding problem (Codas et al. 2015). Here, MS will be introduced for robust optimization.

4.2.1 Mathematical formulation for the robust optimal control problem.

Consider the robust reservoir control optimization problem which consists of finding well control schedules, which are parametrized by $\mathbf{u}$, for the remaining reservoir production life given the current uncertainty. The uncertainty is represented by a discrete

set $\mathcal{J} = \{1, \ldots, J\}$ of equally probable scenarios. Thus, the predicted reservoir state variables $\mathbf{x}$ and the algebraic state variables $\mathbf{v}$ are defined for each scenario $j \in \mathcal{J}$. In contrast, $\mathbf{u}$ is unique and must be suitable for all scenarios because the controls are applied assuming that no further feedback is received, thus the control trajectory cannot be changed at any later stage. The control schedules prescribe either the bottom hole pressure or the flow-rate for the active wells for a given production period. From the MS problem formulation perspective, this production period is known as a control interval, because the control set points are fixed within this period. Thus, there is a set of control periods $\mathcal{U} = \{1, \ldots, U\}$ and the control parameters for the i_{th} period are denoted by $\mathbf{u}_i$. For simulation and constraint evaluation purposes, the prediction horizon is also discretized in a set $\mathcal{K} = \{1, \ldots, K\}$ of simulation time steps, and each control period is divided in several simulation time steps. Therefore, the surjective function $\kappa : \mathcal{K} \to \mathcal{U}$ maps a time step to a control period and indicate which control is to be applied during each simulation step.

Observe that variables or functions such as $\mathbf{x}$ and $\mathbf{v}$ are indexed in the set $\mathcal{J}$ and $\mathcal{K}$. To keep the notation compact, when an index referring to one dimension is absent, we refer to all the variables. Thus, $\mathbf{v}$ is $\mathbf{v}_{k,j}$, $\forall k \in \mathcal{K}$, $\forall j \in \mathcal{J}$ and $\mathbf{x}$ is $\mathbf{x}_{k+1,j}$, $\forall k \in \mathcal{K}$, $\forall j \in \mathcal{J}$. The initial state variables $\mathbf{x}_{1,j}$, $\forall j \in \mathcal{J}$, which are obtained from a state estimation algorithm, are fixed parameters for the optimization procedure, thus they are excluded from the optimization variables.

Robust optimization is achieved with the help of a set $\mathcal{M} = \{1, \ldots, M\}$ of auxiliary variables $\mathbf{s}$. The variables $\mathbf{s}_m$, $\mathbf{s}_m \in \mathbb{R}$, $m \in \mathcal{M}$ are obtained by the application of a risk measure S_m, $m \in \mathcal{M}$ on the simulation outputs $\mathbf{o}_{m,j}$, $m \in \mathcal{M}$, $j \in \mathcal{J}$, $\mathbf{o}_{m,j} \in \mathbb{R}$, thus $\mathbf{s}_m = S_m(\mathbf{o}_m)$. Section 4.5 provides more details on this function.

The output variable $\mathbf{o}_{m,j}$ is obtained by the application of an output function $O_{m,j}$ on all the variables related to the simulation of the realization j. For efficiency, an explicit function $O_{m,j}\left(\mathbf{x}_j, \mathbf{v}_j, \mathbf{u}\right)$ is advantageous. Depending on the objective function and the constraints, these functions may instantiate the Net Present Value (NPV) or well flow-rates for each realization.

Summarizing, robust optimization of reservoir water-flooding can be stated as:

$$\min_{D} \psi(\mathbf{s}, \mathbf{u}) \tag{4.1a}$$

$$\text{s.t.}: \quad 0 = R^{\mathbf{x}}_{k,j}\left(\mathbf{x}_{k,j}, \mathbf{u}_{\kappa(k)}\right) - \mathbf{x}_{k+1,j}, \quad k \in \mathcal{K},\, j \in \mathcal{J} \tag{4.1b}$$

$$0 = R^{\mathbf{v}}_{k,j}\left(\mathbf{x}_{k,j}, \mathbf{u}_{\kappa(k)}\right) - \mathbf{v}_{k,j}, \quad k \in \mathcal{K},\, j \in \mathcal{J} \tag{4.1c}$$

$$\mathbf{o}_{m,j} = O_{m,j}\left(\mathbf{x}_j, \mathbf{v}_j, \mathbf{u}\right), \quad \in \mathcal{M},\, j \in \mathcal{J} \tag{4.1d}$$

$$\mathbf{s}_m = S_m\left(\mathbf{o}_m\right), \quad m \in \mathcal{M} \tag{4.1e}$$

$$\mathbf{b}^{\mathrm{x}}_l \leq \mathbf{x} \leq \mathbf{b}^{\mathrm{x}}_u \tag{4.1f}$$

$$\mathbf{b}^{\mathrm{v}}_l \leq \mathbf{v} \leq \mathbf{b}^{\mathrm{v}}_u \tag{4.1g}$$

$$\mathbf{b}^{\mathrm{s}}_l \leq \mathbf{s} \leq \mathbf{b}^{\mathrm{s}}_u \tag{4.1h}$$

$$\mathbf{b}^{\mathrm{u}}_l \leq \mathbf{u} \leq \mathbf{b}^{\mathrm{u}}_u. \tag{4.1i}$$

The set of decision variables is $D = (\mathbf{x}, \mathbf{v}, \mathbf{s}, \mathbf{u})$. The actual number of degrees of freedom of problem (4.1) is equal to the number of variables in $\mathbf{u}$ since the variables $\mathbf{x}$, $\mathbf{v}$, $\mathbf{o}$ and $\mathbf{s}$ can be obtained by solving the equations (4.1b), (4.1c), (4.1d) and (4.1e). The choice of D is related to the variable reduction procedure for solving problem (4.1), which is further developed in Section 4.4.

The reservoir simulator is represented by the functions $R^{\mathbf{x}}_{k,j}$ and $R^{\mathbf{v}}_{k,j}$, which are the state transition and the algebraic variables for each simulation time step $k \in \mathcal{K}_j$ and each realization $j \in \mathcal{J}$, respectively. Although the reservoir simulator is described as an explicit function for simplicity, the simulator may solve implicit functions, see (Lie et al. 2011; Codas et al. 2015). Further details on the actual reservoir simulator used in our numerical cases are presented in Section 4.3.

The objective function ψ depends on the risk measures $\mathbf{s}$ and the controls $\mathbf{u}$. Moreover, the constraints (4.1h) allow to limit the risk of a given event. These constraints may be thought of as soft constraints because a feasible solution may satisfy $\mathbf{s}_m \leq \mathbf{b}^{\mathrm{s},m}_u < \mathbf{o}_{m,j}$ for some particular pair (m, j). In contrast, worst-case output constraint bounds may be imposed with (4.1f) and (4.1g). Observe that all the inequality constraints are simple bounds in the Multiple Shooting formulation. Although the constraints on the states may be inactive at a solution, they are required by the optimization procedure to prevent evaluations of the simulator out of the physical bounds, for instance, on negative grid-block water saturations. Finally, control input bounds may be specified in (4.1i).

The dependency structure of variables is represented in Figure 4.2. This structure unveils parallelization opportunities during simulation and gradient computation. The parallelization of the evaluation of (4.1b) for each realization in $\mathcal{J}$ is straightforward provided a fixed $\mathbf{u}$. However, the parallelization of (4.1b) for each time step $\mathcal{K}$ requires an initial guess of $\mathbf{x}$ and a mechanism to reach feasibility which is further developed in Section 4.4.

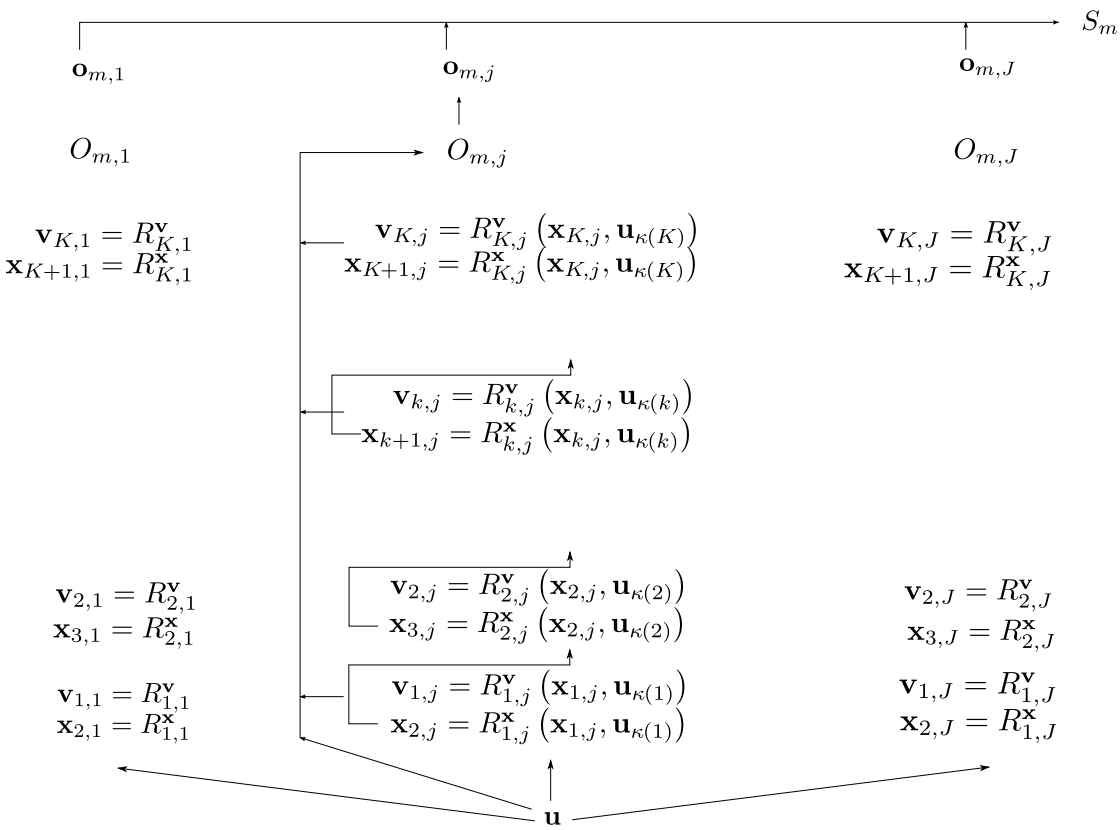

Figure 4.2: The variables dependency structure is represented.

4.3 Reservoir model

In the problem (4.1), a reservoir simulator is represented with the functions $R^{\mathbf{x}}$ and $R^{\mathbf{v}}$. These functions must conform to physical properties and assumptions made by the simulation model. In this work, we tailor the formulation (4.1) to solve reservoir models in the Matlab Reservoir Simulation Toolbox (MRST) (Lie et al. 2011; Krogstad et al. 2015). MRST can simulate isothermal two-phase oil-water reservoir models using either a fully-implicit solver or a sequential scheme. We use the sequential solver in this work. Although a more accurate solver could have been applied as in (Codas et al. 2015), the simpler solver was chosen to lower the computational burden.

We assume that the reservoir state is fully described by the water saturation field. Therefore, it is possible to predict the reservoir performance provided the initial saturations and the boundary conditions of the reservoir are known. We consider the wells as controllable boundary conditions and no flow across other geometrical reservoir boundaries. Due to the incompressible flow assumption, there is one additional constraint on the set of well controls to guarantee that the fluid volume within the reservoir is pre-

served. Therefore, it is not possible to prescribe independent flow-rate boundaries for all the wells. Moreover, the absolute pressure at any point of the reservoir can be determined only if at least one boundary condition is specified by pressure (Jansen 2013, p. 33). Therefore, to avoid singularity conditions, we require that the bottom hole pressure of one well is fixed to a prescribed value independently of the optimization procedure.

Summarizing, the variables $\mathbf{x}$ in problem (4.1) correspond to the predicted water saturation states. For the incompressible solver, no algebraic variables are required for hot-starting the simulator. However, the flow-rate through the wells is included in the algebraic variables $\mathbf{v}$. The reason is that we will require that the flow directions through all of the perforations of every well are always preserved. This condition is imposed as a hard constraint in (4.1g). In other words, a feasible control schedule must prevent cross-flow in any conceivable scenario. Moreover, the vector of algebraic variables may be extended with other constraints that are specific to the problem being solved.

4.4 A rSQP algorithm for robust control optimization

The MS formulation for robust reservoir control optimization in (4.1) possesses many more variables than other methods suggested in the literature. In particular, the state variables at the simulation time steps and the stochastic measure variables are explicitly available. Observe that the parametrization of the control variables is independent of the number of realizations, thus the number of degrees of freedom is much lower than the number of total variables. This fact motivates to devise an extension of the algorithm proposed in (Codas et al. 2015), *i.e.*, a Reduced Sequential Quadratic Programming (rSQP) algorithm that handles multiple realizations efficiently.

The main ingredients of the optimization method in (Codas et al. 2015) are:

- A MS simulator evaluating time steps in parallel.
- A condensing algorithm to calculate a range space solution and a matrix spanning the nullspace of the linearized equality constraints. The latter was referred as the reservoir state predictor matrix.
- An iterative Quadratic Programming (QP) solver to deal with a large number inequality constraints.
- A linesearch algorithm on a $l1$-merit function.

We propose an extension of these features to deal more efficiently with robust optimization and in particular with the set of independent constraints defined by different realizations.

- The evaluation of the constraints (4.1b) and (4.1c) is parallelizable for the different reservoir realizations and simulation time steps.

- The condensing procedure is modified to allow vector products of the reservoir state predictor matrix without explicitly building this matrix. In addition, the range space solution of the constraints (4.1b) and (4.1c) is computed without explicitly building the matrix spanning the range space. This procedure diminishes the memory size requirements to execute the algorithm. Thus, modern central processing units, with several cores, can process in parallel more reservoir realizations before the memory capacity limitation is reached.
- The QP solver is instantiated iteratively and at each iteration a working set of active constraints is estimated. The adjoint gradient calculation method (Ramirez 1987; Kraaijevanger et al. 2007) calculates the gradient of the current working set. The adjoint method keeps a low computational burden when few active constraints are expected. A new estimate of the working set is estimated checking the constraint violations with the incumbent solution to the QP problem. This iterative method to solve the QP problem may require more time to converge if many iterations are necessary to find the correct active set. In this case, it is preferably to build the state predictor matrix at once as in (Codas et al. 2015), to prevent extra computational incurred by assembling the Jacobian of (4.1b) and (4.1c) several times.

Problem (4.1) may be represented by:

$$\min_{D} \ \psi\left(D\right) \tag{4.2a}$$

$$\text{s.t.}: \quad 0 = c(D) \tag{4.2b}$$

$$\mathbf{b}_l \leq D \leq \mathbf{b}_u \tag{4.2c}$$

where $c = (c^x, c^v, c^s \circ c^o)$ represents, as a whole, the constraints (4.1b), (4.1c) and (4.1e) composed with (4.1d), respectively.

The choice of the variables in D and the function c is related to the inequality constraints (4.2c). It is attractive to assemble variables in D for three reasons:

- It enables the application of decomposition techniques and the parallelization of heavy computations.
- Implicit equations, such as the reservoir equations, can use D as an initial guess to expedite iterative solvers for simulation.
- Inequality constraints are easily applied on these variables because they appear as simple bounds in (4.2c).

The variables $\mathbf{o}$ were not included in D because it is not desired to impose inequality constraints on them, moreover the function O is assumed to be explicit (linear by design), and therefore easy to calculate.

Sequential Quadratic Programming (SQP) algorithms solve problem (4.2) iteratively, by improving the current iterate l of the decision variables D and the dual variables λ. An update to this variables is calculated making a linear approximation of the constraints

and a quadratic approximation of the gradient of the Lagrangian (Nocedal et al. 2006). These approximations lead to a QP problem:

$$\min_{d} \; g^{\top} d + \frac{1}{2} d^{\top} W d \tag{4.3a}$$

$$\text{s.t.:} \quad 0 = c + A^{\top} d \tag{4.3b}$$

$$\mathbf{b}_l \leq D + d \leq \mathbf{b}_u \tag{4.3c}$$

where g is the gradient of the objective function, W is the Hessian of the Lagrangian function, and $A^{\top}$ the Jacobian of eq. (4.2b). The decision variables d have same dimensions as D. The next iterate $l+1$ of the decision variables is given by $D_{l+1} = D_l + d_l$. Likewise, the dual variables on the next SQP iterate are the optimal dual variables of the QP (4.3). The iteration index l will be included only to avoid ambiguity.

Reduced SQP methods (Biegler et al. 1997; Nocedal et al. 2006) decompose the decision variables d in a range space solution p_y and a nullspace solution p_z with respect to the equality constraints (4.3b):

$$d = Y p_y + Z p_z \tag{4.4}$$

where Z satisfies $A^{\top} Z = 0$. In this work, we suggest a particular choice for these matrices:

$$Y = \begin{bmatrix} I_{\mathbf{x}} & 0 & 0 \\ 0 & I_{\mathbf{v}} & 0 \\ 0 & 0 & I_{\mathbf{s}} \\ 0 & 0 & 0 \end{bmatrix}, \quad Z = \begin{bmatrix} -C^{-1}N \\ I_{\mathbf{u}} \end{bmatrix}, \quad C = \begin{bmatrix} \frac{\partial c}{\partial \mathbf{x}} & \frac{\partial c}{\partial \mathbf{v}} & \frac{\partial c}{\partial \mathbf{s}} \end{bmatrix}, \quad N = \frac{\partial c}{\partial \mathbf{u}} \tag{4.5}$$

If the problem is deterministic, *i.e.*, if M is 1 and only one realization is considered, then $-C^{-1}N$ is essentially the reservoir state predictor matrix as in (Codas et al. 2015). For problem (4.1), the matrices $A^{\top}$ and Z are rich in structure:

$$A^{\top} = \begin{bmatrix} \left(\frac{\partial c^x}{\partial x} - I_x\right) & 0 & 0 & \frac{\partial c^x}{\partial u} \\ \frac{\partial c^v}{\partial x} & -I_v & 0 & \frac{\partial c^v}{\partial u} \\ \frac{\partial c^s}{\partial x} & \frac{\partial c^s}{\partial v} & -I_s & \frac{\partial c^s}{\partial u} \end{bmatrix}, \tag{4.6a}$$

$$Z = \begin{bmatrix} -\begin{bmatrix} \left(\frac{\partial c^x}{\partial x} - I_x\right)^{-1} & 0 & 0 \\ \frac{\partial c^v}{\partial x}\left(\frac{\partial c^x}{\partial x} - I_x\right)^{-1} & -I_v & 0 \\ \left(\frac{\partial c^s}{\partial v}\frac{\partial c^v}{\partial x} + \frac{\partial c^s}{\partial x}\right)\left(\frac{\partial c^x}{\partial x} - I_x\right)^{-1} & \frac{\partial c^s}{\partial v} & -I_s \end{bmatrix} \begin{bmatrix} \frac{\partial c^x}{\partial u} \\ \frac{\partial c^v}{\partial u} \\ \frac{\partial c^s}{\partial u} \end{bmatrix} \\ I_u \end{bmatrix} \tag{4.6b}$$

Moreover, the matrices $\left(\frac{\partial c^x}{\partial x} - I_x\right)^{-1}$ and $\frac{\partial c^v}{\partial x}$ can be arranged in J diagonal blocks due to the independence of state variables for different realizations. Therefore, the Lift-Opt

trick as presented in (Codas et al. 2015) is still applicable and it is a theoretically possible procedure to build Z. To this end, the condensing procedure can be applied independently to each realization to assemble $\left(\frac{\partial c^x}{\partial x} - I_x\right)^{-1}$. Observe that given the particular selection of Y and Z in (4.5), the range space solution for (4.3b) is determined by:

$$p_y = -\left(A^\top Y\right)^{-1} c \tag{4.7}$$

which is rich in structure. Similarly to the computation of the nullspace, the block structure of $\left(\frac{\partial c^x}{\partial x} - I_x\right)^{-1}$ and $\frac{\partial c^v}{\partial x}$ are suitable for the application of the condensing procedure in (Codas et al. 2015) to obtain the range space of eq. (4.3b) independently, for each realization of the reservoir, in parallel. This requires a forward gradient propagation on each realization. Finally, the block lower triangular structure of $A^\top Y$ makes it possible to calculate the range space solution for the risk variables $\mathbf{s}$ after the others are obtained.

Building Z may be impractical due to its high storage requirements, in particular, for robust optimization. This procedure is recommendable for dynamic optimization problems with few controls and/or large number of possible active constraints. Hence, we propose an algorithm which requires adjoint simulations to obtain the nullspace with respect to a working set of active constraints only. Deriving the gradient equations, either by forward sensitivity analysis or by the adjoint method, is a tedious process. Fortunately, this subject is extensively discussed in the literature, see (Kraaijevanger et al. 2007; Oliver et al. 2008; Kourounis et al. 2014; Codas et al. 2015). In (Codas et al. 2015), Z and p_y are obtained using the Lift-Opt Z trick. In addition to these procedures, it is not difficult to show how to efficiently obtain products of Z by a nullspace solution vector p_z, and an estimate of the Lagrange multipliers.

The reduced-space parametrization in (4.4) applied to problem (4.3) leads to:

$$\min_{p_z} \; g^\top Z p_z + \frac{1}{2} p_z^\top Z^\top W Z p_z \tag{4.8a}$$

$$\text{s.t.:} \quad \mathbf{b}_l \leq D + Y p_y + Z p_z \leq \mathbf{b}_u \tag{4.8b}$$

The problems (4.3) and (4.8) are not equivalent due to approximations introduced in the objective function. The objective function in problem (4.8) ignores the terms $\frac{1}{2} p_y^\top Y^\top W Y p_y$ and the cross-product term $p_y^\top Y^\top W Z p_z$. The former is constant since p_y is fixed by (4.7). However, the cross-product term is not constant and its omission is motivated by the costly computation of $p_y^\top Y^\top W Z$. It is reasonable to neglect the cross-product term because the range space steps p_y typically converge faster to zero than the nullspace steps p_z (Nocedal et al. 2006, p. 539). Detailed SQP algorithms including the cross-product term are available in (Biegler et al. 1995; Biegler et al. 1997; Ternet et al. 1998; Biegler et al. 2000). Further, the calculation of $Z^\top W Z$ incurs a substantial computational burden and can lead to a non-convex problem (4.8). Therefore, $Z^\top W Z$ is approximated with damped BFGS updates as in (Codas et al. 2015).

Problem (4.4) might be infeasible to solve if $D + Yp_y \notin [\mathbf{b}_l, \mathbf{b}_u]$. This motivates the introduction of the minimum $\xi \in [0, 1]$ so that if $D \in [\mathbf{b}_l, \mathbf{b}_u]$, then there is a p_z such that $D + (1 - \xi) Yp_y + Zp_z \in [\mathbf{b}_l, \mathbf{b}_u]$. Thus, a non-zero value of ξ is required to deal with a provisional infeasibility of problem (4.8).

Hence, problem (4.8) is approximated by:

$$\min_{p_z} g^\top Z p_z + \frac{1}{2} p_z^\top Z^\top W Z p_z \tag{4.9a}$$

$$\text{s.t.:} \quad \mathbf{b}_l \leq D + (1 - \xi) Yp_y + Zp_z \leq \mathbf{b}_u, \quad (\lambda_l, \lambda_u) \tag{4.9b}$$

where $\lambda_l, \lambda_u \geq 0$ are the Lagrange multipliers for the constraint (4.9b) and:

$$\xi = \min_{\hat{\xi}, p_z} \hat{\xi} \tag{4.10a}$$

$$\mathbf{b}_l \leq D + \left(1 - \hat{\xi}\right) Yp_y + Zp_z \leq \mathbf{b}_u \tag{4.10b}$$

$$0 \leq \hat{\xi} \leq 1 \tag{4.10c}$$

Thus, to maintain $D \in [\mathbf{b}_l, \mathbf{b}_u]$, the SQP step is redefined as:

$$d^\xi = (1 - \xi) Yp_y + Zp_z \tag{4.11}$$

The introduction of ξ is particularly important in reservoir applications because the evaluation of the simulator outside of variable bounds may not be defined, for instance, physical volume values must be positive. Thus, following problem (4.9) and choosing the initial guess D_1 such that $D_1 \in [\mathbf{b}_l, \mathbf{b}_u]$, the inequality constraints (4.2c) are never violated. However, if $\xi = 1$ and $p_z = 0$ then the NLP solver fails due to convergence to a point of local infeasibility. If problem (4.2) is infeasible this type of failure is inevitable.

The Linear Programming (LP) problem (4.10) and QP problem (4.9) are not solved at once, but iteratively for a subset of constraints. Given a guess of the active constraints of problem (4.9), problem (4.10) and problem (4.9) are solved. Then, the feasibility of the incumbent solution of problem (4.9) is tested against all the constraints in (4.9b). If the solution is feasible, then it is a solution for problem (4.9), if it is infeasible, a subset of the infeasible constraints is appended to the working set of constraints. This process is repeated until all the constraints are feasible. This procedure requires an adjoint gradient computation for each constraint included in the active set and a forward gradient propagation for each feasibility test.

The update d^ξ calculated by problem (4.9) is assessed by a globalization strategy. This strategy enforces convergence to a local optimum regardless of the quality of the initial solution guess. To this end, progress of the objective function and the equality constraints after the application of d^ξ is required. Thus, a line-search over $\left[D, D + d^\xi\right]$ is performed to find a new iterate which provides a sufficient decrease of the l_1 merit function:

$$\phi_\mu = \psi(D) + \mu \left\| c(D) \right\|_1 \tag{4.12}$$

where μ is chosen large enough to ensure that d^{ξ} is a descent direction for ϕ_{μ}. This is achieved by selecting (Biegler et al. 1997, p. 115, eq. (2.65)):

$$\mu^{l} = \begin{cases} \mu^{l-1}, & \text{if} \quad \mu^{l-1} \left\| c^{l} \right\|_{1} \geq \left| \bar{g}^{\top} Y p_{y} \right| + 2\rho \left\| c^{l} \right\|_{1} \\ \frac{\left| \bar{g} Y p_{y} \right|}{\left\| c^{l} \right\|_{1}} + 3\rho, & \text{otherwise.} \end{cases} \tag{4.13}$$

where ρ is a fixed positive parameter and

$$\bar{g} = (g + \lambda_{u} - \lambda_{l}) \tag{4.14}$$

Like in (Codas et al. 2015), line-search is implemented with a watchdog strategy to promote acceptance of unitary steps and avoid the Marato's effect (Chamberlain et al. 1982). If backtracking is required, a piecewise 3^{rd} order polynomial is used to determine the step length.

4.5 Risk measures for robust dynamic optimization

Optimization of uncertain processes involves random variables which can be described by probability density distributions. The aim is to optimize the shape of the probability distributions rather than particular outcomes of the process. Popular measures for the probability distributions are the mean, variance, standard deviation, mode and median. Previous work proposed the use of some of these measures for robust optimization of water-flooding, for instance Alhuthali et al. (2010) and Capolei et al. (2015b) used a combination of mean and standard deviation. Recently, Capolei et al. (2015a) provided a review and discussion of profit and risk measures used in oil production optimization. According to previous publications in the field, a reasonable way to optimize uncertain processes is to maximize the expected profit and penalize its dispersion. Moreover, constraints were satisfied for every possible scenario (Chen et al. 2012). This approach to constraint handling may lead to overly restrictive optimization problems. Furthermore, the inclusion of a penalty to the dispersion of the objective is not a coherent measure (Artzner et al. 1999).

The concept of coherent measures was first introduced by Artzner et al. (1999) in the mathematical finance community. Their motivation was to develop coherent risk measures to assess investment decisions under uncertainty. In addition, this can be applied for constraint handling in production optimization. To this end, consider a random variable Z_x representing water production which depends on the decision variables x. Furthermore, consider the functional $R(Z_x)$ to be a measure of risk of water production. This measure of risk is coherent according to Artzner et al. (1999) if it agrees with the following axioms:

1. Translation invariance. $R(Z_x + c) = R(Z_x) + c$.

If a constant water production c, *i.e.*, water production independent of our decisions, is added to the production operation, then the water production risk is increased exactly by this constant. This axiom also indicates that Z_x, c and $R(Z_x)$ are all measured in the same units.

2. Sub-additivity. $R\left(Z_x^1 + Z_x^2\right) \leq R\left(Z_x^1\right) + R\left(Z_x^2\right)$.

   Let Z_x^1 and Z_x^2 be the water production from two different wells, further, assume there is an uncertain channelized permeability structure and fixed water injection. Observe that the risk of water production considering the two wells is at most equal to the total water injection, while the sum of risks applied independently on each well is twice the total water injection.

3. Positive Homogeneity. If $\lambda > 0$, then $R(\lambda Z_x) = \lambda R(Z_x)$.

   If the water production value is multiplied by a positive constant so is the risk. This scaling invariance property is very important for optimization because the risk must be scalable to any unit.

4. Monotonicity. If $Y_x \leq Z_x \, \forall x$, then $R(Y_x) \leq R(Z_x)$.

   If for every fixed decision x, $Y_x \leq Z_x$ then Y is less risky than Z. This axiom seems to state an obvious desired property, however, the mean-variance measure fails to fulfill this requirement (Rockafellar 2007). Thus, despite the simplicity of the mean-variance, it must be avoided in the formulation of optimization problems.

The careful reader may realize that some of the aforementioned axioms have changes in signs, when compared to its presentation in (Artzner et al. 1999), however, its current form was previously suggested by Rockafellar (2007). The intention of the adjustments is to introduce risk measures for cost rather than profit, so that risk can be easily applied to minimization problems. Furthermore, this formulation is more intuitive for constraints.

The mean value and the worst case functionals are examples of coherent risk measures. Assessing the outcome on a single scenario, or in other words, assessment of performance on a nominal model, is also a coherent risk measure. However, this measure is subject to criticism since a single instance of the reservoir parameters does not span the uncertainty.

As seen above, the risk may assess the uncertainty of an undesired event in a given process. For constraint handling, the mean-variance measure has been proposed to include a large penalty on the variance term so as to mimic a safety margin (Rockafellar 2007) . However, mean-variance is not coherent in the sense of (Artzner et al. 1999). Furthermore, there is no axiom indicating that higher dispersion or uncertainty is undesired. Motivated by this shortcoming, Rockafellar et al. (2002) and Rockafellar (2007) further request an averseness axiom:

5. Averseness. $R(Z_x) > \mathbb{E}(Z_x)$ for all non-constant Z_x.

With this extra requirement, it is clear that non-constant distributions are more risky than constant distributions. Moreover, observe that an important risk measure, the mean, does not fulfill the averseness requirement.

Another way to deal with risk in constraints is to introduce chance constraints:

$$\Pr\{Z_x \leq \tau\} \leq \alpha \tag{4.15}$$

where τ is a threshold and α a bound on probability, adopting a value like 95%. The condition $Z_x > \tau$ is undesired and (4.15) constrain the decision x to limit the probability of this event.

The chance constraint (4.15) may be written by means of the Value-at-Risk functional:

$$\text{V@R}_\alpha[Z_x] \leq \tau \tag{4.16}$$

where

$$\text{V@R}_\alpha[Z] = \inf\{t : \Pr(Z \leq t) \geq \alpha\} \tag{4.17}$$

In words, larger values than t in (4.17) occurs with probability not exceeding $(1-\alpha)$. Although chance constraints are the conceptual feature desired in stochastic optimization, chance constraints may have non-convex feasible regions and even if convex, they may be difficult to compute (Shapiro et al. 2007; Shapiro et al. 2009a, p. 257). Therefore, Rockafellar et al. (2000) proposes a convex over-estimate of $\text{V@R}_\alpha[Z]$:

$$\text{AV@R}_\alpha[Z] = \inf_{t\in\mathbb{R}} \left\{ t + (1-\alpha)^{-1}\,\mathbb{E}\left[Z-t\right]_+ \right\} = \frac{1}{1-\alpha}\int_\alpha^1 \text{V@R}_s(Z)ds \tag{4.18}$$

where $[t]_+ = \max(0,t)$ and $\alpha \in (0,1)$. From the second relation in (4.18) it is easy to derive that $\text{V@R}_\alpha[Z] \leq \text{AV@R}_\alpha[Z]$. Therefore,

$$\text{AV@R}_\alpha[Z_x] \leq \tau \tag{4.19}$$

is a conservative approximation of (4.16). However, AV@R is a coherent risk averse measure in contrast to V@R. Observe that AV@R is the center of mass of the tail of the associated distribution. This tail starts at the value of V@R. Thus, (4.19) implies that Z_x is less than τ with α probability, furthermore it implies that the mean of the worst-cases that happen with probability $1-\alpha$ is less than τ. Therefore, AV@R provides the safety margin that was desired with the introduction of the penalty on the variance. In addition, AV@R is sensitive to the shape of the tail of the distribution in contrast to V@R. As a final remark, observe that $\lim_{\alpha\to 0^+} \text{AV@R}_\alpha[Z] = \mathbb{E}[Z]$ and $\lim_{\alpha\to 1^-} \text{AV@R}_\alpha[Z] = \max[Z]$ (worst-case).

Due to the aforementioned reasons AV@R will be used hereafter as our risk indicator in addition to the mean and the worst-case functionals. The use of AV@R for stochastic

optimization of oil production was also proposed in (Capolei et al. 2015a; Hanssen et al. 2015).

The risk measures S in problem (4.1) are instantiated with AV@R with an appropriate value of α for each constraint:

$$S_m(\mathbf{o}_m) = \inf \left\{ t_m + \frac{1}{J\,(1-\alpha_m)} \sum_{j=1}^{J} [\mathbf{o}_{j,m} - t_m]_+ \right\} \tag{4.20}$$

However, the introduction of this function is not straightforward due to the $\max$ function and the $\inf$ operator appearing in (4.20). Fortunately, it is possible to reformulate a problem including expressions with AV@R with the help of additional variables and constraints as shown in (Rockafellar et al. 2000; Hanssen et al. 2015):

$$S_m(\mathbf{o}_m) = \min_{t_m, z_{j,m}} \quad t_m + \frac{1}{J\,(1-\alpha_m)} \sum_{j=1}^{J} z_{j,m} \tag{4.21a}$$

$$\text{subject to:} \quad \mathbf{o}_{j,m} - t_m \leq z_{j,m}, \quad z_{j,m} \geq 0 \tag{4.21b}$$

Although this reformulation is suitable for problem (4.1), it requires $2MJ$ additional inequality constraints. Moreover, if $M > 1$, then additional artifacts are needed to calculate the optimal value of $\mathbf{s}$ rather than a feasible one as in (Hanssen et al. 2015). Hence, instead of including the additional variables and constraints from problem (4.21) in (4.1), we propose to solve problem (4.21) as a subproblem when evaluating the constraints and its Jacobian. This approach has the advantage of simplicity, however, $S_m(\mathbf{o}_m)$ is only piecewise differentiable.

For fixed $\mathbf{o}_m$, solving the LP problem (4.21) requires sorting the vector $\mathbf{o}_m$ in descending order. Say $\hat{\mathbf{o}}_m$ is the sorted vector, then:

$$S_m(\mathbf{o}_m) = \frac{1}{J(1-\alpha_m)} \sum_{j=1}^{\lfloor J(1-\alpha_m) \rfloor} \hat{\mathbf{o}}_{j,m} + \left(1 - \frac{\lfloor J(1-\alpha_m) \rfloor}{J(1-\alpha_m)}\right) \hat{\mathbf{o}}_{\lceil J(1-\alpha_m) \rceil, m} \tag{4.22}$$

Some notes are in order:

- The solution of $S_m(\mathbf{o}_m)$ is the average of the highest $J(1-\alpha_m)$ values of $\mathbf{o}_m$.
- Although the value of $S_m(\mathbf{o}_m)$ always has a unique solution, the partial derivatives $\frac{\partial S_m}{\partial \mathbf{o}_m}$ can have several solutions if $\mathbf{o}_m$ can be sorted in several ways, *i.e.*, if some particular values in the vector $\mathbf{o}_m$ are the same.
- The discontinuity in the Jacobian occurs when there are several samples on the tail boundary. Considering the optimization procedure developed in Section 4.4, the discontinuity in the Jacobians may cause backtracking during line-search due to a wrong prediction of the mean of the tail.

Besides the eventual difficulties, this approach is attractive because it circumvents further complications related to the resolution of LP problems in (4.21). The complexity of this problem is reduced to sort a vector. Moreover, the possible difficulties related to the multiplicity of $\frac{\partial S_m}{\partial \mathbf{o}_m}$ also appear with the reformulation in (4.21), as multiple solutions of the dual variables and as changes in the constraints active sets.

4.6 Test case of robust reservoir control optimization.

This section demonstrates the application of the MS formulation and the risk measures on the Egg-Model (Jansen et al. 2013). The Egg-Model is a channelized two-phase (oil-water) synthetic reservoir model with 18553 active cells. It has 12 wells, 8 water injectors and 4 producers. It considers uncertainty in the channel structure and provides 100 permeability fields representing plausible scenarios. It inspired and enabled the exploration of robust optimization in several research activities (Van Essen et al. 2009; Fonseca et al. 2014; Fonseca et al. 2015; Siraj et al. 2015). More details about this model can be obtained either in its research note or in the actual data available in (Jansen et al. 2013).

We propose five test cases to assess output constraint handling capabilities. The five cases are related to a Base case (B). The B case considers constraints on flow-rates on each well perforation. These constraints ensure that all the perforations associated to a well injector are actually injecting and that all the perforations related to a well producer are producing. In technical terms, these constraints prevent flow reversion or cross-flow between perforations of the same well. The Egg-Model has 7 perforations for each well, one for each vertical layer of the discretized reservoir model. Thus, 84 constraints are imposed for each predicted time step. Observe that these constraints are required even if the well control is specified by flow-rate because this type of control prescribes the flow-rate for the sum of all the perforations rather than for the individual perforations. In addition to the cross-flow constraint, constraints are included on the saturation states to honor the residual saturations and the initial conditions. Furthermore, the constraints on the states must limit the saturations to remain in $[0, 1]$ to avoid invalid inputs to the reservoir simulator during optimization.

The B case considers the same well schedule for the 100 realizations $(J = 100)$. The well schedules span for 3600 days (~ 10 years). The simulation time steps are fixed and each year of production is divided in 3 steps equal to 30 days, 150 days and 180 days, respectively. Thus, $K = 30$. We require shorter steps at the beginning of each year in order to improve the simulator approximations after a well control change. The well controls are discretized in 10 equal periods of 360 days (~ 1 year), hence, $U = 10$. During these periods, the well injectors inject at a fixed flow-rate and the well producers maintain a fixed bottom hole pressure. Therefore, the control schedule is fully parametrized with 120 variables which are the degrees of freedom of the optimization algorithm. However,

since the reservoir model is incompressible, all the solutions with the same bottom hole pressure difference between the boundary conditions provide the same flow pattern. Therefore, the bottom hole pressure of the producer labeled as "PROD1" is fixed during all the control periods, and then the problem remains with 110 degrees of freedom.

The objective function models the Net Present Value (NPV) of the recovery. The NPV function of one reservoir realization is given by:

$$\text{NPV} = \sum_{k=1}^{K} \left(\frac{q_{o,k} r_o - q_{wp,k} r_{wp} - q_{wi,k} r_{wi}}{(1+d)^{t_k/t_K}} \right) \Delta t_k \tag{4.23}$$

where $q_{o,k}$, $q_{wp,k}$ and $q_{wi,k}$ represent the sum of oil produced, water produced and water injected in all wells, respectively, and r_o, r_{wp} and r_{wi} are their corresponding prices. Moreover, d is the discount factor and t_k is the time at the end of the step time k. In our experiments $(r_o, r_{wq}, r_{wi}) = (100, 10, 10)\, STB/Sm^3$ and $d = 0$. The objective ψ of problem (4.1) is the expected NPV value over all the realizations.

Constraints on the wells may be imposed as bounds on the well schedule parameters. Thus, well injection flow-rates are limited between 0 and $500\ Sm^3/day$ and the well producers bottom hole pressure are limited between 100 and $450\ bar$. Moreover, the bottom hole pressure of PROD1 is fixed to $300\ bar$ during the entire production horizon.

In the B case the vector of algebraic variables $\mathbf{v}$ contains the fluid flow-rate through all the well perforations, for all realizations and all time steps. Moreover, variables representing cash-flow accumulation (NPV) at each time step are appended to $\mathbf{v}$. With this choice of the algebraic state variables, the function O is linear on the decision variables, *i.e.*, the sum of the contributions to the NPV at every step. Furthermore, the function S is the simple mean of the accumulated NPV values of each realization calculated in the variables $\mathbf{o}$.

Scaling plays an important role in non-linear optimization methods. In our experiments the pressure variables are scaled by $5\ bar$, the saturations by 1%, the flow-rates by $10\ Sm^3/day$ and the NPV by $10^7\ USD$. Moreover, the infinity norm tolerance for the constraints $c(D)$ is set to 0.01. This implies that the reduced SQP algorithm stops when the solution is within an accuracy of $0.05\ bar$, $0.1\ Sm^3/day$ and $10^5\ USD$.

Figures 4.3, 4.4 and 4.5 provide optimized well schedules and production forecasts. The flow-rates of oil and water are uncertain in the producers, and the bottom hole pressure is uncertain in the injectors. Therefore, for these variables we plot the mean, the maximum and minimum limits and the mean of the tail of the distribution on both sides. In the optimized solution we observe that the oil production during the last years is close to 0 Sm^3/day, suggesting that the well is drained of oil disregarding the uncertainty. However, there is a large uncertainty on the water being produced. Figure 4.6 illustrates the NPV accumulation in time for the B case. Here we observe that the uncertainty in the recovery starts to be significant from the third year on. The expected NPV is $2.255\text{E}8\ USD$ being the worst case 7.3% lower and the best case 4.4% higher than the

mean. Figure 4.7 shows the predictions for the total oil production (FOPT) and total water production (FWPT) together with the total scheduled water injection (FWIT).

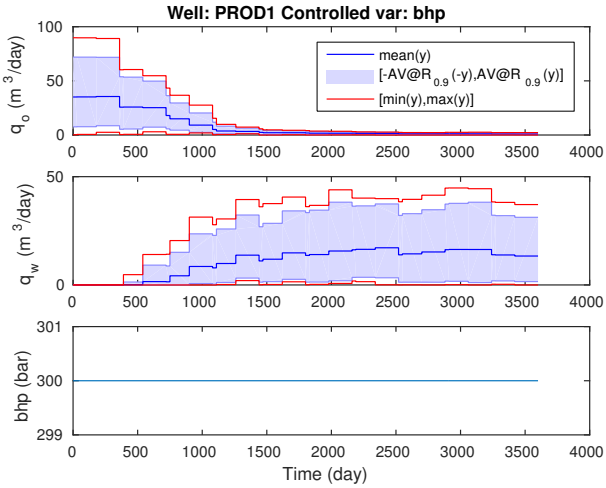

Figure 4.3: Optimized solution for the B case. q_o Oil Production. q_w Water Production. bhp Bottom hole pressure.

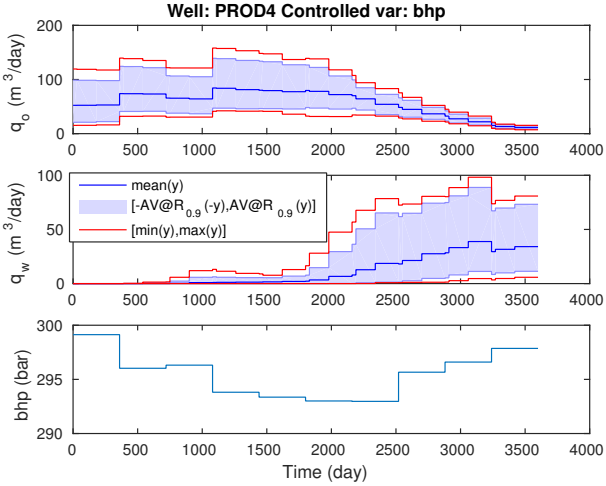

Figure 4.4: Optimized solution for the B case. q_o Oil Production. q_w Water Production. bhp Bottom hole pressure.

Two sets of cases are created by imposing additional constraints to the B case. These cases are motivated by the high water injection and production observed dur-

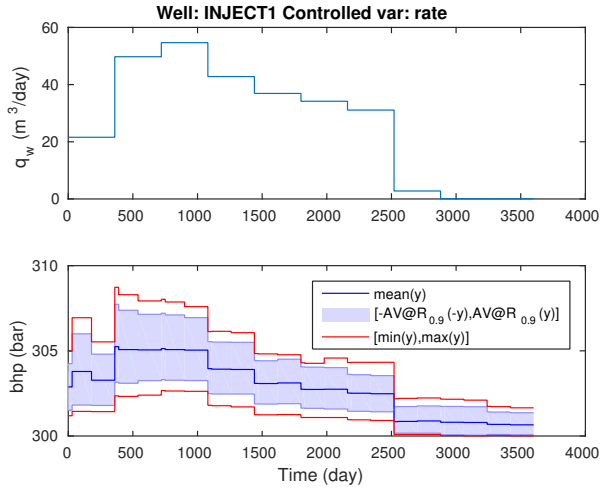

Figure 4.5: Optimized solution for the B case. q_o Oil Production. q_w Water Production. bhp Bottom hole pressure.

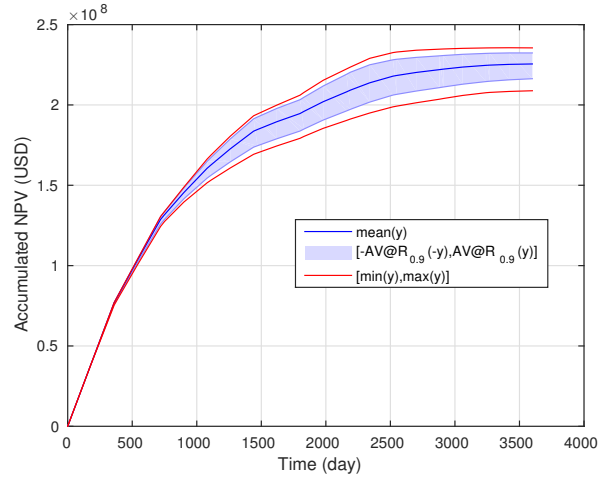

Figure 4.6: Optimized solution for the B case. The expected NPV is $2.255\text{E}8\ USD$, and the worst case (best case) is 7.3% lower (4.4% higher) than the expected value.

ing the last years in Figure 4.7. The constrained cases consider different approaches to limit the FWPT. To this end, variables representing the FWPT for all predicted time steps are included in $\mathbf{v}$. The case "H30" requires FWPT $\leq 30\ Sm^3/day$ for all scenarios for all time steps and similarly, the case "H20" requires FWPT $\leq 20\ Sm^3/day$. To this end, the corresponding $\mathbf{v}$ variables are constrained in eq. (4.1g). Since the cases "H30" and "H20" may be overly restrictive due to a particular scenario, their counter-

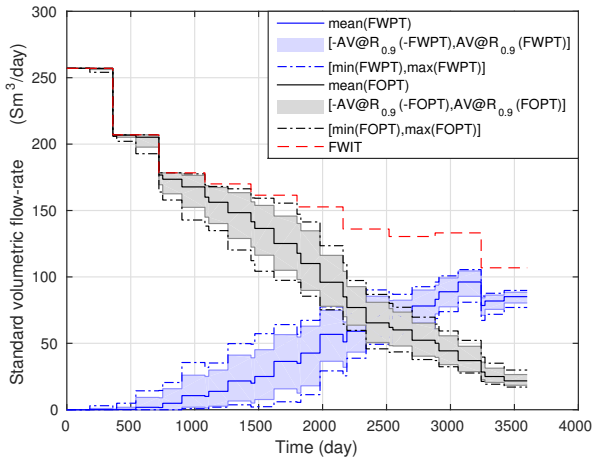

Figure 4.7: B case. Total production and injection considering all wells.

part "C30" and "C20" require AV@R$_{0.9}$ (FWPT) $\leq 30\ Sm^3/day$ and AV@R$_{0.8}$ (FWPT) $\leq 20\ Sm^3/day$, respectively. Since there are a 100 scenarios, all of them with equal probability, AV@R$_{0.9}$ (FWPT) $\leq 30\ Sm^3/day$ implies that the mean of the worst 10 water production scenarios must be lower than $30\ Sm^3/day$ and AV@R$_{0.8}$ (FWPT) $\leq 20\ Sm^3/day$ requires the mean of the 20 worst FWPT scenarios to be lower than $20\ Sm^3/day$.

Figure 4.8 shows the FOPT, FWPT and FWIT for the optimized constrained cases. In comparison to the results of the B case, the constrained cases produce less oil and the FWPT constraints are active at several time steps. However, the water injection is seized better because there is less water recirculation and the difference between FOPT and FWIT is smaller. Moreover, the dispersion of the uncertainty on FOPT and FWPT is reduced, therefore a better planning of the capacity utilization may be achieved with the constrained cases. Figure 4.9 show the predicted accumulation of NPV in time for the constrained cases. In contrast to the B case that reaches $10^8\ USD$ in around 500 days, the constrained cases require twice the time to reach this value. Therefore, the B case is preferable for fast recovery of investments. However, observe that $d = 0$ and short-term recovery is not set as an objective, thus, the optimization procedure is not intended to maximize short-term recovery. Table 4.1 shows the predicted recovery for all strategies. Although the best expected value is achieved with the B case, this case also has the highest uncertainty span. Moreover, although the economical return of the strategies using AV@R constraints (C) is better compared to the robust counterpart (H), the strategies with AV@R constraints may violate constraints with a marginal probability.

The progress of the scaled objective function and the constraints for the cases B and C30 are illustrated in Figure 4.10. The convergences of the omitted cases are similar to the convergence of C30. All the cases were aborted before the predefined tolerance was

	B	C30	H30	C20	H20
Best case	2.36	2.29	2.25	2.20	2.18
Expected value	2.26	2.19	2.17	2.12	2.08
Worst case	2.01	2.05	2.04	1.98	1.96

Table 4.1: Predicted NPV ($10^8 USD$)

reached. The B case was halted after reaching 7 days of execution, and the constrained cases were halted after reaching 1000 iterations. As in (Codas et al. 2015), the main SQP iterations make significant progress in the first 200 steps, then the convergence error remains at the same level and the objective progresses logarithmically, see Figure 4.11. The algorithm performed backtracking less than 100 times for the constrained cases and never for the B case, *i.e.*, it performed only unitary steps. We attribute the convergence rate behavior to the typical ill-conditioning characteristic of reservoir water-flooding control problems. Although by the last iteration there is a large error norm, the control schedule of this iteration is simulated and the maximum error reported is feasible within a tolerance of 0.01 in infinity norm. The reason for the larger error norm in Figure 4.10 is related to the convergence error of the implicit functions within the reservoir simulator. The simulation convergence error affects the convergence error of the multiple shooting algorithm. Although, this convergence error may be reduced by imposing tighter convergence conditions in the simulator and stricter acceptance of steps in the line-search procedure, we preferred to relax these conditions to favor faster steps.

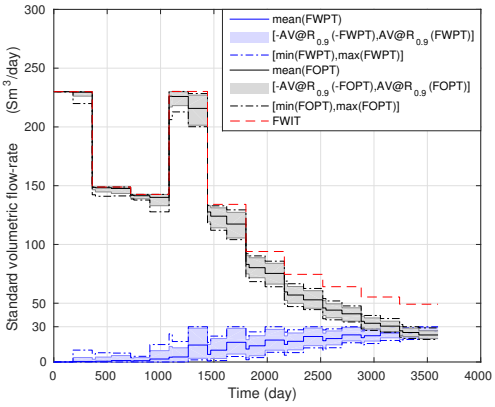

((a)) H30.

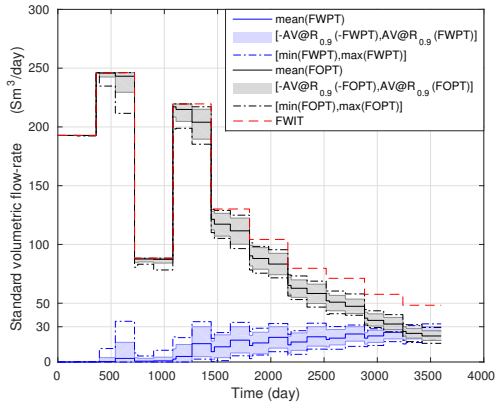

((b)) C30.

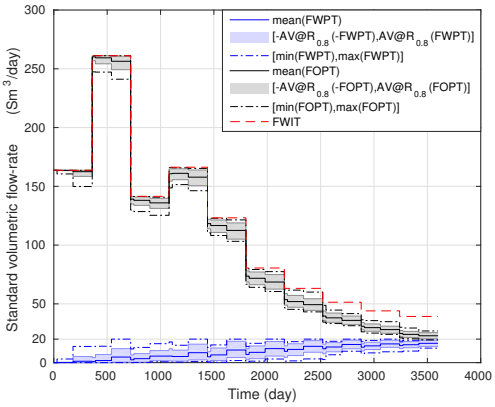

((c)) H20.

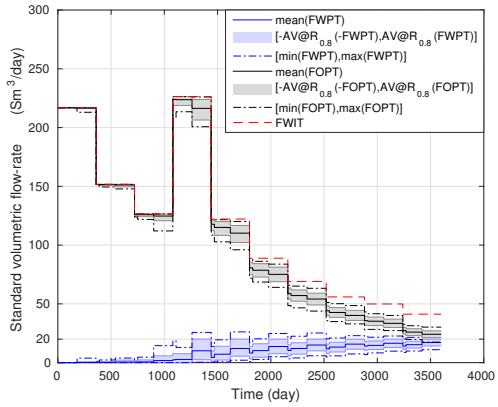

((d)) C20.

Figure 4.8: Optimized field total flow-rates for the constrained cases.

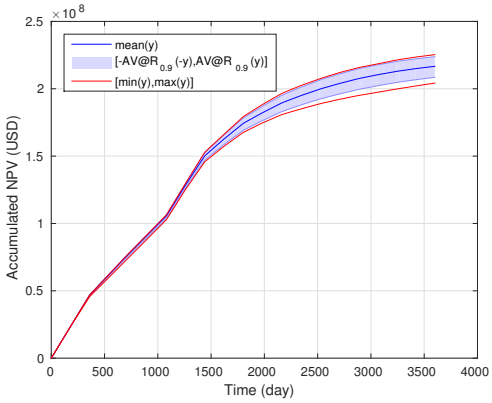

((a)) H30.

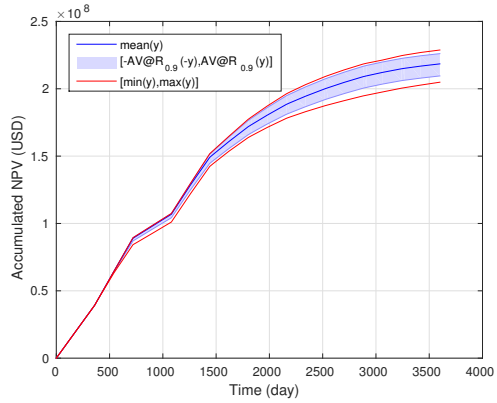

((b)) C30.

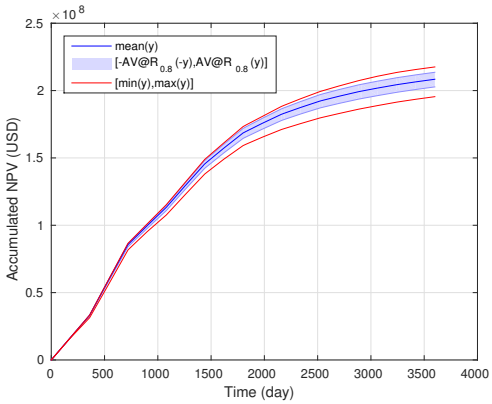

((c)) H20.

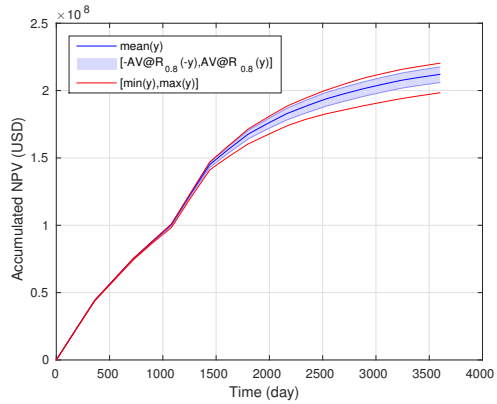

((d)) C20.

Figure 4.9: Optimized accumulated NPV for the constrained cases.

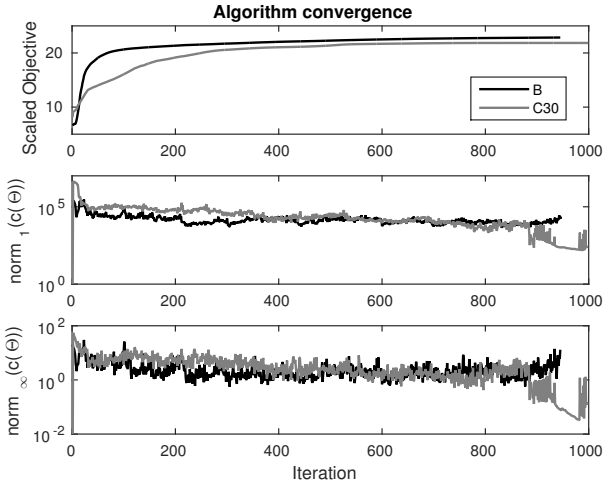

Figure 4.10: Algorithmic convergence for the B and C30 cases.

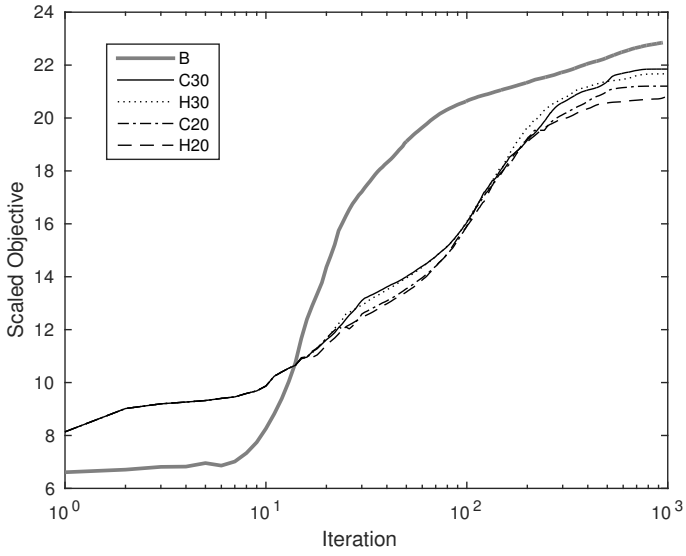

Figure 4.11: Convergence of the objective function for all the cases.

4.7 Discussion

In this work, we propose an extension to the Multiple Shooting (MS) algorithm developed in Codas et al. (2015) for robust reservoir control optimization. Due to the uncertainty in the process, there is a risk concerning the expected recovery and an operation within constraint limits. Thus, an efficient procedure to deal with output constraints is fundamental.

As mentioned earlier, MS allows for parallelization. Besides the parallelization of the simulation computation for each ensemble member, MS allows for parallelization of the simulation time steps. This may lead to a computational speed up for costly simulations. For instance, the computational experiments in this work were carried out on the supercomputer at NTNU named "Vilje". This computer has 1404 nodes, each node having 32GB of RAM and 16 cores. The 100 realizations of the Egg-Model were allocated to 10 computer nodes, 10 for each node, not more due to RAM memory limits. Thus, the 6 remaining cores could be used for running simulation time steps in parallel. Observe that the allocation of computational power (and its related cost) on such supercomputers is charged by indivisible node units, therefore it is always desired to consume all the computational power within a node. As opposed to the traditional Single Shooting formulation, MS has an extra flexibility to take advantage of this remaining computational power.

The MS formulation and the proposed solution algorithm deal with all the state variables as independent decision variables. Therefore, it is easy to impose output inequality constraints as bounds. However, the solver must take care of a large number of equality constraints. A correction to these equality constraints mismatch is obtained with a single forward gradient propagation. For the inequality constraints handling, we devise a reduced space method which leads to a QP problem with the same number of decision variables as the degrees of freedom of the optimization problem. The reduced space approach exploits an active-set method to selectively compute adjoint simulation of the active constraints.

The proposed formulation and algorithm deals with risk coherently (Artzner et al. 1999). For profitability reasons, the Average Value at Risk approach is more attractive than imposing constraints on every single realization because the latter leads to the worst case scenario optimization. However, it requires the inclusion of multiple new variables and inequality constraints as suggested by Rockafellar et al. (2000) and Hanssen et al. (2015). To prevent this complication we tailor our optimization solver and suggest alternative approach which computes the risk measure without additional variables and constraints. A weakness of this approach appears in some particular cases because the solution is only piecewise differentiable. However, on these particular points the original approach possesses multiple Lagrange multiplier solutions which lead to the same algorithm difficulty. Besides these potential difficulties, the line-search process performed well in our experiments. Further, Rockafellar et al. (2010) and Basova et al. (2011)

compare alternative approaches to deal with the constraints arising from the risk measures. Basova et al. (2011) show that the efficiency of optimization methods is deteriorated when considering all the additional constraints and variables. Thus, they suggest smoothing approximations to the $\max$ operator in (4.20) or active-set methods for the additional constrains in (4.21b). Our approach relies on the inclusion of a single additional variable and constraint as the approach is based on the smoothing approximation, however, a smoothing function is not required.

The numerical examples are difficult to solve due to ill-conditioning. We arrive at this conclusion because the BFGS updates are damped very frequently close to the solution in the three explored cases. Therefore the expected super-linear convergence of the Quasi-Newton algorithms is not achieved. This is a common behavior in reservoir control optimization problems and in economical MPC problems since there is no regularization in the objective function. The execution of our test cases was halted due to a slow progress of the objective function.

Although the norm one of the convergence error is around 20E4 for the B case, the forward simulations of the resulting controls yield a satisfactory solution which satisfies the bounds within the predefined tolerance of 0.01. Thus, we conclude that this convergence error is associated with the underlying convergence error of the simulator. Observe that the problems have 18553 state variables, 100 realizations and 30 steps. Therefore, the average error is $20000/(18553 \times 100 \times 30) = 0.00036$ which is considerably low. Nevertheless a way to mitigate this undesired effect is tightening the simulator convergence tolerances, however, this may increase the overall computational burden.

Despite the premature interruption of the algorithm and the possibility of multiple local optima, a comparison of the achieved objective values deserves a discussion. The calculated objective values, after a forward simulation of the last computed controls, are shown in Table 4.1. The results are reasonable because the best profit is attained in the B case. Moreover, the cases using AV@R provides better profit than the counterparts were satisfaction of the constraints in all cases is required. However, according to the evolution of the incumbent solutions shown in Figure 4.11, the difference between these solutions is not substantial and requires around 600 iterations to be reached. Nevertheless, observe that this high number of iterations depends on the initial solution guess and the fact that our test cases do not apply any particular procedure to provide a good initial guess. Considering real-time close-loop applications, the algorithm may be hot-started with the previous optimal solution according to a receding horizon scheme.

The proposed formulation and algorithm contributes to constraint handling for robust optimization compared to previous publications. Compared to the ensemble methods (Chen et al. 2009), our algorithm use exact gradients, therefore it is usually faster but the implementation effort is higher. Recently, Leeuwenburgh et al. (2015) showed the application of ensemble methods on robust optimization considering output constrained problems. It shows that the gradients approximated with an ensemble are suitable for constrained optimization, but they suggest lumping constraints to deal with high

number of output constraints. In contrast, robust optimization using the Augmented Lagrangian method (Chen et al. 2012) requires a single adjoint simulation independently of the number of output constraints. However, it requires a two-layered iterative process to estimate Lagrange multipliers and optimize the problem. Therefore, compared to our single-layered active-set algorithm, faster convergence is not guaranteed. Moreover, our algorithm promotes further parallelization opportunities. Recently, Liu et al. (2015a) and Liu et al. (2015b) proposed the Augmented Lagrangian algorithm to maximize NPV and minimize return risk. Their formulation is a special case of the one in this paper because they consider the risk as the worst-case and here the risk is modeled with the tail of the probabilistic distribution of the nonlinear output functions. Moreover, here we apply risk measures to multiple output variables, so constraints may be included to the problem considering a trade-off between the risk of constraint violation and economical return.

4.8 Conclusion

In this work develop a novel method for robust optimization in reservoir control. The method exploits the Multiple Shooting formulation which allows broader parallelization opportunities and an efficient handling of constraints. Further, the formulation incorporates coherent measures of risk to control the probability of constraint violation. Tests on a medium-sized benchmark problem clearly demonstrated the ability to handle output constraints of the proposed approach.

Chapter 5

Integrated Production Optimization of Oil Fields with Pressure and Routing Constraints: The Urucu Field

This chapter is based on (Codas et al. 2012b):

Codas, A. et al. (2012b). 'Integrated Production Optimization of Oil Fields with Pressure and Routing Constraints: The Urucu Field'. In: *Computers & Chemical Engineering* 46, pp. 178–189. ISSN: 00981354. DOI: 10.1016/j.compchemeng.2012.06.016.

Abstract

This paper develops a framework for integrated production optimization of complex oil fields such as Urucu, which has a gathering system with complex routing degree of freedom, limited processing capacity, pressure constraints, and wells with gas-coning behavior. The optimization model integrates simplified well deliverability models, vertical lift performance relations, and the flowing pressure behavior of the surface gathering system. The framework relies on analytical models history matched to field data and simulators tuned to reflect operating conditions. A mixed-integer linear programming (MILP) problem is obtained by approximating these models with piecewise-linear functions. Procedures were developed to obtain simplified piecewise-linear approximations that ensure a given accuracy with respect to complex and precise models. Computational experiments showed that the integrated production optimization problem can be solved sufficiently fast for real-time applications. Further, the operational conditions calculated with the simplified models during the optimization process match the precise models.

5.1 Introduction

Fast development of new technologies is being witnessed in several disciplines related to oil production, a result of the intensive work of experts from different research fields. Although innovations lead to more accurate models and operating strategies, integration and optimization modeling is still a challenge. The industry response has been the concept of integrated operations developed in the past decade, emphasizing the collaboration across disciplines. Such initiatives have led to improvements in operations, field management, and production through mathematical optimization of integrated models.

Several works addressed oil field production optimization subject to rate capacity constraints and lift-gas availability (Buitrago et al. 1996; Fang et al. 1996; Alarcón et al. 2002; Camponogara et al. 2009; Misener et al. 2009; Codas et al. 2012a). These works do not treat pressure constraints which increase problem complexity significantly because nonconvex multivariable pressure-drop functions must be modeled across the network. Pressure modeling is required when dealing with production networks that contain wells sharing flowlines, in which case the variation in the operation of any well affects the others (Dutta-Roy et al. 1997). Further, the representation of back-pressure from separation facilities and flowline pressure drop is critical to define the operating range for mature fields, which experience pressure depletion.

Grothey et al. (2000) present an optimization model which consists of several subnetworks of compressor, wells, manifolds, and separators linked by a common gas vessel. They focus on the analysis of decomposition methods to accelerate problem solving. However, simplistic pressure-drop models are used without an analysis of their accuracy and suitability.

Litvak et al. (1995), Litvak et al. (1997) and Litvak et al. (2002) describe procedures for determining well production rates and surface pipeline interconnections honoring network rate and pressure constraints. They use integrated reservoir and surface facility models, develop an automatic tuning procedure to validate simulation models, and identify problems in simulations and field measurements. The procedures were successfully implemented in a commercial simulator-optimizer and applied to the Prudhoe Bay oil field.

Wang et al. (2002a) and Wang et al. (2002b) solve an oil production optimization problem with decision variables being well production rates, lift-gas rates, and routing to separation facilities subject to rate and pressure constraints. Optimization procedures are proposed based on linear programing, separable programming, sequential quadratic programming, and genetic algorithms. The gradient based techniques utilize automatic differentiation methods of coupled simulator functions. The effectiveness and business value of the optimization approach was demonstrated with applications in the Gulf of Mexico and the Prudhoe Bay oil field.

Kosmidis et al. (2004) and Kosmidis et al. (2005) formalize the previous works and present a mixed-integer nonlinear programming (MINLP) model for the daily well

scheduling problem of a production network with naturally producing and gas-lifted wells. The surface facilities allow well-separator and well-manifold-separator connections. The solution process uses piecewise linearization to represent well-bore models and nonlinear functions to represent pressure drops. The MINLP problem is solved by a sequence of mixed-integer linear programming (MILP) problems following a sequential linear programming (SLP) method.

Gunnerud et al. (2010a) and Gunnerud et al. (2010b) present a global optimization procedure for oil fields with decentralized structure such as Troll West. This kind of field is structured in clusters of independent wells, manifolds, and pipelines while the separation facilities are centralized in a platform. Piecewise linearization techniques based on special ordered sets of type 2 (SOS2) constraints are used to approximate nonlinear curves. The production gathering system is suitable for decomposition strategies. A comparison between strategies showed that the Dantzig-Wolfe technique outperforms the others in this application.

Although Litvak et al. (1995), Litvak et al. (1997), Litvak et al. (2002), Wang et al. (2002a) and Wang et al. (2002b) implemented and applied local optimization methods in complex oil fields, the mathematical formulations and solution procedures were not explicitly shown. On the other hand, Kosmidis et al. (2004), Kosmidis et al. (2005), Gunnerud et al. (2010a) and Gunnerud et al. (2010b) explicitly show the problem formulation and solution procedure, but the production gathering networks considered in these works are more simplistic than the Urucu field. To this end, this work advanced the state of the art by developing an integrated mathematical formulation for production optimization reflecting the complexity of the Urucu field.

Section 5.2 discusses briefly how production optimization is being carried out in the Urucu field. Section 5.3 presents an MINLP formulation for the production optimization problem accounting for the well bore model, the production network structure consisting of wells, manifolds, separators, and pipelines, complex interconnections such as manifold to manifold, multiphase flow, and pressure representation in pipelines. Section 5.4 develops an MILP reformulation of the production optimization problem by piecewise linearizing the nonlinear curves related to the well-inflow equations and pressure drops in pipelines. Section 5.5 presents procedures for setting up the daily instance of the production optimization problem based on data gathered from simulators tuned to the field. Before optimization, the instances are preprocessed to reduce the complexity of the piecewise-linear models while ensuring a given accuracy between the optimization proxy model and the simulator. Section 5.6 reports the performance of the developed models and procedures for production optimization. Section 5.7 gives a summary and suggests directions for future research.

5.2 The Production Optimization Problem

The Urucu field is located in a remote region of primary rainforest, 650 km southwest of Manaus in the heartland of the Brazilian Amazon (Campos et al. 2010). Petrobras started the production activities in Urucu after the discovery of a significant reserve of oil and natural gas in 1986. The field consists of three reservoirs called "River Urucu" (RUC), "Eastern Urucu" (LUC), and "Southeastern Urucu" (SUC). The field has more than 20 injection wells and more than 70 production wells flowing to several manifolds, with gas expansion being the primary recovery mechanism. The crude oil produced in Urucu has average oil gravity of 45 ^{o}API and gas-oil ratio (GOR) ranging from 500 to 5000 sm^3/sm^3 due to coning behavior. Typical field flow rates are 50,000 bpd and 10.5 million Nm^3/d of natural gas, with re-injection of 8 million Nm^3/day of processed gas as secondary recovery mechanism. LUC field is the main oil producer and has a gas rate constraint in the flowline to the liquefied petroleum gas (LPG) plant "Polo Arara". Therefore, high GOR is an issue in production operations.

Reservoir and production management is carried out in different timescales. In the short-term timescale, regulatory and supervisory control are responsible to maintain process stability and surveillance, honoring the set points defined by the upper layers. The processes are monitored by operators in the control room and supervised by production engineers. The daily production is planned by engineers at the headquarters in Manaus city, 600 km away from the field. These engineers perform middle-term timescale analysis to decide well status such as open, closed, routed to production separators, or on test procedure. To deal with gas coning effects, reservoir engineers perform analyses and define flowrate limits for the wells in order to maximize the recovery factor.

The gathering system is composed of a pipeline network that distributes the production to nine first-stage separators through twelve manifolds and twelve multivia valves. Three separators are for well testing and six others for production with the same design and capacity. Gas and oil pipelines, with total length of 35 km, work as a backbone collecting production from the first-stage separators and delivering the fluids to subsequent separation facilities and finally the LPG process plant.

The diverse routing possibilities in the LUC field are achieved by the following configurations:

1. Well routing through the test header at manifolds.
2. Well routing through the production header at manifolds.
3. Well routing through the multivia valve.
4. Bidirectional flow between manifolds through the test pipelines interconnections.
5. Flow production routed to test separator.
6. Flow production routed to production separator.

7. Equalization, which is the capability of sending production of a well to more than one separator at the same time.
8. Multiple pipeline connections between manifolds.

The routing strategy should be developed to maximize production efficiency through the correct allocation of the capacity available in the field. Currently, the operations follow a routing strategy depending on the status of the wells. The strategy is compiled in a document called "Technical Instructions" describing how the wells should be routed depending on the availability of test separators to run on production status. The operational configurations defined by the Technical Instructions are constructed from known past operational configurations and field simulations, however the current field integrated model optimize production based on fix routing. This work proposes an optimization strategy to support middle-term decisions including routing options to improve the strategies suggested by the Technical Instructions.

5.3 Model Formulation

This section begins by presenting models for the inflow performance relation (IPR) and the vertical lift performance (VLP). The IPR represents the oil, gas, and water production as a function of bottom hole pressure. In Urucu, the IPR consists of an analytical well model that was fit to data from a detailed 3D finite-difference numerical model. The VLP relates the drawdown to the wellhead pressure by using production string models. Network flow equations are used to relate the well flows to separation facilities assuming a feasible routing for the gathering system. Then, pressure in manifolds and separators are expressed in terms of the flow rates in the network. All of these models allow us to express constraints on choke openings, flow rates, and pressures in field equipment. Finally, we formalize the problem of optimizing production of oil fields with routing and pressure drop constraints.

5.3.1 Well Bore Modeling

A well deliverability model or inflow performance relationship is essential in matching and predicting the well inflow performance under varying drawdown conditions, liquid and gas ratio, and reservoir depletion. With the IPR curves and the production string models, it is possible to correlate wellhead pressure to drawdown, a correlation known as vertical lift performance curve.

Gunnerud et al. (2010a) combine IPR and VLP curves to obtain the well production curve (WPC) which relates the wellhead pressure to the multiphase flow rate. This model does not consider the drawdown of the well.

Kosmidis et al. (2005) use the IPR equation with the oil flow rate as the independent variable to determine the gas flow and water flow rates. Assuming a fully open choke

and fixed manifold pressure, the maximum oil flow rate is determined through the VLP equation. This model describes the feasible flows given the manifold pressure.

The model suggested by Gunnerud et al. (2010a) is not suitable for this work because different flow regimes can be achieved for the same wellhead pressure in some wells. Here, the well flow and wellhead pressure are directly related to the bottom hole pressure rather than the oil rate as suggested by Kosmidis et al. (2005), which provides more integrability since the data given by reservoir engineers is used without any modification.

The integrated optimization framework in place at the Urucu field (Campos et al. 2010) considers detailed 3D finite-difference models, history matched to the entire production data of each well. The detailed model is then used to forecast well production for drawdown ranges under gas and/or water coning regime. Because the complexity and computation time of this model are not suitable for short-term field optimization, simplified proxy models were developed. Several analytical models were tested against the detailed model until the adequate IPR was found. The chosen analytical proxy well model is based on the fundamental flow theory by Fetkovich (1973).

In this work, the analytical IPR curves $\mathbf{q}(u)$ are expressed in terms of the normalized bottom hole pressure u and subsequently piecewise-linearized for optimization purposes.

Finally, VLP curves are generated to model the performance of the production tubing. The existing integrated model for the Urucu field maintains VLP curves as look-up tables that give wellhead pressure as a function of bottom-hole pressure, liquid rate, gas-oil ratio, and water cut. VLP and IPR curves combined define the total well performance. For the purpose of this work, the analytical curves representing the IPR curves and the VLP lookup tables are combined to generate wellhead curves as a function of the drawdown ($p^{\mathrm{wh}} = VLP(u)$).

Typical wells of the Urucu field exhibit dynamic gas and water coning behavior, meaning that the oil-gas ratio varies in time. However, an empirical steady-state coning model, which relates gas-oil ratio and water cut to oil flow, is representative for short-term applications (Campos et al. 2010) and can be modeled with piecewise-linear functions.

5.3.2 Network Flow Modeling

The oil field can be seen as a directed graph as illustrated in Figure 5.1. The node set $\mathcal{N}$ is the union of a set of wells $\mathcal{W} = \{1, \ldots, W\}$, a set of manifolds $\mathcal{M} = \{1, \ldots, M\}$, a set of separators $\mathcal{S} = \{1, \ldots, S\}$, a set of connections to gas pipelines $\mathcal{C} = \{1, \ldots, C\}$, and a set of gas-pipeline terminal points $\mathcal{T} = \{1, \ldots, T\}$. Ordered pairs of nodes define pipelines $\mathcal{P} \subseteq \mathcal{N} \times \mathcal{N}$. The set of pipelines $\mathcal{P} = \mathcal{W}_{\mathcal{M}} \cup \mathcal{M}_{\mathcal{M}} \cup \mathcal{M}_{\mathcal{S}} \cup \mathcal{S}_{\mathcal{C}} \cup \mathcal{C}_{\mathcal{C}} \cup \mathcal{C}_{\mathcal{T}}$ where $\mathcal{A}_{\mathcal{B}} \subseteq \mathcal{A} \times \mathcal{B}$ for all node sets $\mathcal{A}$ and $\mathcal{B}$.

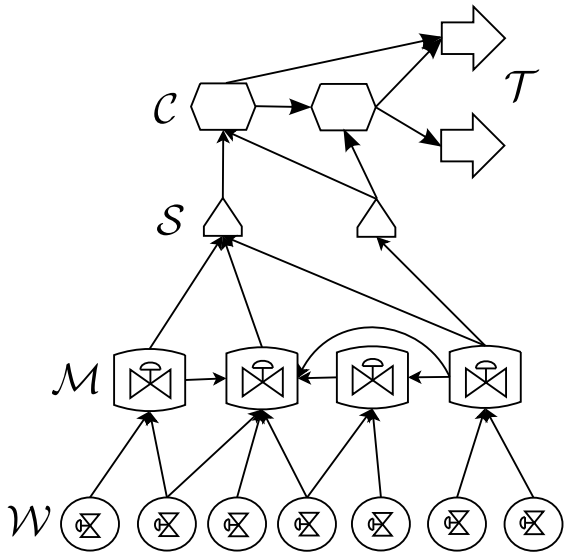

Figure 5.1: Sample production network.

The multiphase fluid flow rates through the network nodes and pipelines are modeled by the following formulation:

$$\mathbf{q}_w = \mathbf{q}_w(u_w),\ w \in \mathcal{W} \tag{5.1a}$$

$$\mathbf{q}_i = \sum_{j:(i,j)\in\mathcal{P}} \mathbf{q}_{i,j},\ i \in (\mathcal{N} \setminus (\mathcal{T} \cup \mathcal{S})) \tag{5.1b}$$

$$\mathcal{E}^s \mathbf{q}_s = \sum_{j:(s,j)\in\mathcal{P}} \mathbf{q}_{s,j},\ s \in \mathcal{S} \tag{5.1c}$$

$$\sum_{i:(i,j)\in\mathcal{P}} \mathbf{q}_{i,j} = \mathbf{q}_j,\ j \in (\mathcal{N} \setminus \mathcal{W}) \tag{5.1d}$$

$$\sum_{j:(i,j)\in\mathcal{P}} z_{i,j} \leq 1,\ i \in \mathcal{N} \tag{5.1e}$$

$$0 \leq \mathbf{q}_{i,j} \leq \mathbf{q}_{i,j}^{\max} z_{i,j},\ (i,j) \in \mathcal{P} \tag{5.1f}$$

where:

- $u_w \in \mathbb{R}_+$, $w \in \mathcal{W}$ is the squared normalized bottom hole pressure p^w_{wf} of well w with respect to the reservoir pressure p^w_{r}, *i.e.*, $u_w = \left(p^w_{\text{wf}}/p^w_{\text{r}}\right)^2$;
- $\mathbf{q}_w \in \mathbb{R}^3_+$, $w \in \mathcal{W}$ defines the flow input to the network from well w, with $\mathbf{q}_w(u_w)$ being a nonlinear function relating u_w to the production of each phase;
- $\mathbf{q}_i \in \mathbb{R}^3_+$, $i \in \mathcal{N}$ is the three-phase flow rate flowing through node i;
- $\mathbf{q}_{i,j} \in \mathbb{R}^3_+$, $(i,j) \in \mathcal{P}$ is the three-phase flow rate from node i to j;

- $z_{i,j} \in \{0,1\}$, $(i,j) \in \mathcal{P}$ is a binary variable taking on value 1 if the fluid from node i is directed to j, and 0 otherwise;
- $\mathbf{q}_{i,j}^{\max} = (q_{i,j}^{\mathrm{g,max}}, q_{i,j}^{\mathrm{o,max}}, q_{i,j}^{\mathrm{w,max}})$ is the maximum flow capacity of the pipeline (i,j) for the gas, oil, and water phases; this parameter is used to enforce the flow routing and should be chosen large enough so as not to constrain any feasible flow;
- $\mathcal{E}^s$ is a $\mathbb{R}^{3\times3}$ matrix modeling the efficiency of separator $s \in \mathcal{S}$; the efficiency is associated to oil properties, system temperature, and the separator operating pressure; zero oil flow is assumed in the gas pipeline, while the gas present in the oil output is a consequence of the gas dissolved in the oil under the separator condition (Standing 1952).

Equation (5.1a) models the fluid input to the network. Equations (5.1b)–(5.1d) ensure mass conservation across the network. Together, inequalities (5.1e) and (5.1f) establish that every node in the graph is allowed to have one output only.

Some remarks on the formulation are in order:

- All flow rates are expressed in stock tank conditions.
- For the sake of simplicity and compactness of the formulation, the separators are modeled with at most one output and the flows are considered three-phased. In the Urucu field, the water is re-injected at the separation facility site and does not flow through the gathering system after separation. There is no flow or pressure constraint in the oil pipeline. Therefore, the variables and constraints associated with these two phases can be dispensed with. The active constraints downstream separators are related to gas flow.
- The flow of fluids from one node to multiple nodes needs nonlinear models to represent the split of rates, since the flow in pipelines depends on the downstream pressure, fluid flow regime, and the equipment geometry. A fair assumption is to consider that the fluid has the same composition in all the outputs, which allows to represent this phenomenon with simple models. However, such models consist of nonlinear relations which would require new piecewise linear approximations. To avoid these nonlinear models, nodes are allowed to have one output only as imposed by inequality (5.1e) which is a simplifying assumption also applied in other works (Kosmidis et al. 2005; Gunnerud et al. 2010a; Codas et al. 2012a).

The gathering system constraints on fluid rates are:

$$\sum_{w \in \mathcal{W}} \mathbf{q}_w \leq \mathbf{q}^{\max} \tag{5.2a}$$

$$\mathbf{q}_i \leq \mathbf{q}^{i,\max},\ i \in \mathcal{N} \tag{5.2b}$$

$$u_w^{\min} \leq u_w \leq u_w^{\max},\ w \in \mathcal{W} \tag{5.2c}$$

where:

- $\mathbf{q}^{\max}$ is the maximum production allowed for each phase taking into account all the wells in the production network. If wells produce under gas (water) coning, the maximum gas (water) production constraint is typically active.
- $\mathbf{q}^{i,\max} = (q_{\mathrm{g}}^{i,\max}, q_{\mathrm{o}}^{i,\max}, q_{\mathrm{w}}^{i,\max})$ is the maximum handling capacity of node i for the three-phase flow.
- The bottom hole pressure is related to the liquid rate being produced. $u_w^{\min}$ is the minimum bottom pressure recommended by the reservoir engineer. A minimum bottom hole pressure is established to avoid erosional effects due to high fluid velocity. By limiting the bottom hole pressure ($u_w^{\max}$) below the reservoir pressure, the well is not allowed to shut-in. Although producing by natural flow, some wells need artificial lifting to start up, normally done with nitrogen injection. Therefore such wells should neither be closed frequently, nor become a swing well (Campos et al. 2010).

5.3.3 Network Pressure Modeling

Pressure drop through the pipelines should be modeled to guarantee the fluid flow direction and to honor maximum pressure constraints in the facilities. Dutta-Roy et al. (1997) studied the interaction of wells operated under a common gathering network. They concluded that the impact of the wells sharing a common flowline is the increase of back-pressure which reduces the production of the wells, thereby justifying the need of modeling pressure drops through the system.

To model pressure constraints, absolute pressure variables are associated to each node in the production network. Pressure drop variables through the pipelines are also defined. Since the pressure in the terminal points of the gas pipelines are controlled, they are assumed known parameters of the model.

Given a source node i and a sink node j, p_i and p_j are variables which represent the absolute pressure in the nodes while $p_{i,j}$ is the variable representing the pressure drop from i to j. In general, the pressure drop in a pipeline (i,j) is a nonlinear function $\Delta p_{i,j}\left(\mathbf{q}_{i,j}, p_j\right)$ of the pipeline geometry and properties of the flowing fluid, such as phase flow rates $\mathbf{q}_{i,j}$, temperature and boundary pressure p_j. It is assumed in this work that the temperature in the pipelines remains constant independently of the fluid flow rate, pressure and time. Regarding the boundary pressure p_j, a fixed nominal pressure $\hat{p_j}$ is adopted as an approximation to simplify one more variable in the function description, a simplification which is assessed in Section 5.5.2. For notation simplicity, pressure drop functions will be written just in terms of the fluid rates $\Delta p_{i,j}\left(\mathbf{q}_{i,j}\right)$ or more briefly $\Delta p_{i,j}$. Let $z_{i,j}$ be a binary variable indicating whether or not the pipeline is active, then the pressure drop and absolute pressure are linked by:

$$-L_{\mathrm{p}}\left(1-z_{i,j}\right) \leq p_i - p_j - \Delta p_{i,j} \leq U_{\mathrm{p}}\left(1-z_{i,j}\right),\ i \neq \mathcal{W} \tag{5.3}$$

where L_p and U_p are sufficiently large parameters following big M formulation. Conform this equation, $p_i - p_j = \Delta p_{i,j}$ if $z_{i,j} = 1$, otherwise the pressures p_j and p_i can assume any value when $z_{i,j} = 0$.

Equation (5.3) does not apply to well nodes because the pressure drop through the well choke is not being considered. The choke has a decoupling role between surface and wellbore elements. Regarding well w and manifold m, the pressure drop $p^c_{w,m}$ in the choke connecting them can be inferred by $p^c_{w,m} = p_w(u_w) - p_m - \Delta p_{i,j}$. Given any flow rate $\mathbf{q}_{w,m} \geq 0$ and pressure drop $p^c_{w,m} \geq 0$, it is assumed that there exists a choke valve opening satisfying the system.

Considering well i and manifold j, the inequality $-L_\text{p}\,(1 - z_{i,j}) \leq p_i - p_j - \Delta p_{i,j}$ holds since the pressure drop in the choke must be always positive. On the other hand, the right-hand side of equation (5.3) should not be enforced for the well nodes because otherwise the pressure drop through the choke would not be taken into account.

Absolute pressures can be established for all but the well nodes of the network using backward calculation, which consists of starting from the terminal nodes and calculating backwards the absolute pressures of the neighbor nodes using the pressure drop functions through the pipelines. On the other hand, the wellhead pressure is calculated as a function of the bottom hole pressure. Given the variable u_w, the bottom hole pressure and multiphase flows of well w are calculated, making it possible to obtain the wellhead pressure p_w by means of the pressure drop along the well production tube (VLP equations). Finally, the choke pressure drop is obtained by the difference between the wellhead pressure and the pressure downstream choke.

According to the discussion above, the absolute node pressures and pressure drops of the network are modeled using the following formulation:

$$p_{i,j} = \Delta p_{i,j},\ (i,j) \in \mathcal{P} \tag{5.4a}$$
$$p_w = p_w(u_w),\ w \in \mathcal{W} \tag{5.4b}$$
$$-L_\text{p}\,(1 - z_{i,j}) \leq p_i - p_j - p_{i,j},\ (i,j) \in \mathcal{P} \tag{5.4c}$$
$$p_i - p_j - p_{i,j} \leq U_\text{p}\,(1 - z_{i,j}),\ (i,j) \in (\mathcal{P} \setminus \mathcal{W}_\mathcal{M}) \tag{5.4d}$$

The pressure constraints are then added to the system as follows:

$$p_i \leq p_i^{\max},\ i \in (\mathcal{S} \cup \mathcal{M}) \tag{5.5a}$$
$$p_s^{\min} \leq p_s,\ s \in \mathcal{S} \tag{5.5b}$$
$$p_m + p_{w,m} - L_\text{p}(1 - z_{w,m}) \leq p_w^{\max},\ (w,m) \in \mathcal{W}_\mathcal{M} \tag{5.5c}$$
$$p_m + p_{w,m} - L_\text{p}(1 - z_{w,m}) \leq p_w,\ (w,m) \in \mathcal{W}_\mathcal{M} \tag{5.5d}$$

The new variables and parameters are:

- $p_i \in \mathbb{R}_+,\ i \in (\mathcal{N} \setminus \mathcal{T})$ is a variable representing the absolute pressure in node i;
- $p_{i,j} \in \mathbb{R},\ (i,j) \in \mathcal{P}$ is a variable representing the pressure drop in the pipeline from i to j;

- $p_t \in \mathbb{R}_+$, $t \in \mathcal{T}$ is a parameter defining the controlled absolute pressure in pipeline terminal point t;
- $p_i^{\max} \in \mathbb{R}_+$, $i \in (\mathcal{S} \cup \mathcal{M})$ is the maximum absolute pressure allowed for node i;
- $p_s^{\min} \in \mathbb{R}_+$, $s \in \mathcal{S}$ is the minimum absolute pressure allowed for separator s;
- $p_w^{\max} \in \mathbb{R}_+$, $w \in \mathcal{W}$ is the maximum absolute pressure allowed downstream the choke of well w.

The constraints (5.5a), (5.5b) and (5.5c) state pressure limits in network elements, while (5.5d) guarantees the flow direction through the chokes.

5.3.4 Problem Statement

The production optimization problem subject to facility constraints on fluid rates, pressures, and routings is defined as follows:

$$
\begin{aligned}
P: \quad \max \quad & \sum_{w \in \mathcal{W}} q_w^{\text{o}} && \text{(5.6a)}\\
\text{s.t.}: \quad & \mathbf{q} \leftarrow F_{\text{M}}(\mathbf{u}, \mathbf{z}) && \text{(5.6b)}\\
& F_{\text{C}}(\mathbf{q}, \mathbf{u}) \leq \mathbf{0} && \text{(5.6c)}\\
& \mathbf{p} \leftarrow P_{\text{M}}(\mathbf{q}, \mathbf{z}) && \text{(5.6d)}\\
& P_{\text{C}}(\mathbf{p}, \mathbf{z}) \leq \mathbf{0} && \text{(5.6e)}
\end{aligned}
$$

where: $\mathbf{u}, \mathbf{z}, \mathbf{q}$, and $\mathbf{p}$ are vectors grouping the normalized bottom hole pressures, routing decisions, phase rates, and pressure variables; F_{M} is a compact form representing the flow model equations (5.1), with the subscript M indicating model; F_{C} is a compact form representing the flow constraints (5.2), with the subscript C indicating constraints; P_{M} represents the pressure modeling for the nodes as given by equations (5.4); and P_{C} represents the pressure constraints defined by equations (5.5).

Notice that a solution is completely defined by $\mathbf{u}$ and $\mathbf{z}$.

5.3.5 Summary of Modeling Assumptions

The problem formulation (5.6) is valid under the following modeling assumptions:

- Steady state pressure drop functions can be satisfactorily modeled in terms of phases flow rates through the network elements in stock tank conditions, assuming fixed boundary pressure and temperature.
- The fluid flows in each node of the network are directed to at most one output node, with the exception of separator nodes for which at most one gas output node is allowed.
- Sufficiently slow reservoir dynamics allowing inflow performance relations as a function of static bottom hole pressure.

- There is a choke opening position matching any pressure drop and flow rates across the choke.
- Fixed controlled pressure at the gas pipeline terminal points, which establish the pressure boundary condition for the gathering system.
- The gas-oil-ratio (GOR) in the oil pipeline downstream separator is constant, a consequence of the fluid composition and nominal operating pressure and temperature of the separator.

The experimental results presented in this paper are obtained using nonlinear pressure drop functions in terms of the black-oil model with the parameters shown in Table 5.2. Piecewise-linear representations are generated after the nonlinear pressure-drop functions using the sampling parameters in Table 5.3. A fixed nominal outlet pressure is assumed during the pressure drop function sampling.

5.4 Piecewise Linearization

The functions $\mathbf{q}_w(u_w)$, $p_w(u_w)$, and $\Delta p_{i,j}\left(\mathbf{q}_{i,j}\right)$ modeling field flows and pressures are only assumed to be continuous. This assumption and the presence of binary variables $z_{i,j}$ render the production optimization problem a mixed integer nonlinear program (MINLP). Owing to the hardness of solving MINLPs directly, for which global optimality certificates may be impossible to obtain, an alternative is to solve mixed integer linear programs (MILP) obtained by piecewise linearizing the nonlinear functions, as it was previously done in (Camponogara et al. 2006; Gunnerud et al. 2010a; Codas et al. 2012a). Another solution approach consists of sequentially solving several MILPs that locally approximate the MINLP until a local optimum is achieved (Kosmidis et al. 2005).

Instead of solving a sequence of MILPs, this work tackles the problem by approximating the nonlinear functions with piecewise-linear forms of desired accuracy. The process models have uncertainties associated to field measurements and curve fitting (Elgæter et al. 2010). Thereby, piecewise-linear models with approximation error bounded by the degree of uncertainty are suitable to represent the processes.

Several models to approximate non-linear curves with piecewise linear functions are found in the literature. Vielma et al. (2010) compare these models with respect to their theoretical properties and computational performance, including aggregated, disaggregated, and special ordered sets type 2 (SOS2) models. The piecewise linearization model using SOS2 constraints (Keha et al. 2004) has attractive properties for multidimensional applications, since additional binary variables and constraints are not required to be added to the initial formulation—the needed constraints are enforced on demand during the branching process. According to Vielma et al. (2010), the model using SOS2 constraints generates the smallest initial formulation which is solved faster than the formulations that use binary variables, however the former has a larger dual GAP and

thereby generates a larger number of nodes in the branch-and-bound tree. For multidimensional piecewise-linear approximation of non-convex functions, small formulations are desirable because the linear programming (LP) relaxations are solved more expeditiously. For unidimensional piecewise-linear approximation the gain between formulations is not significant.

5.4.1 Piecewise Linearization Applied to Unidimensional Functions

The pressure drops $\Delta p_{i,j}(q^{\mathrm{g}}_{i,j})$, $(i,j) \in \mathcal{S_C} \cup \mathcal{C_C} \cup \mathcal{C_T}$ are unidimensional functions depending only on the flow of gas through the pipelines. Given a set of points $P_{i,j} = \left\{ \left(p^1_{i,j}, q^{\mathrm{g},1}_{i,j}\right), \left(p^2_{i,j}, q^{\mathrm{g},2}_{i,j}\right), \ldots, \left(p^{\kappa(i,j)}_{i,j}, q^{\mathrm{g},\kappa(i,j)}_{i,j}\right) \right\}$, a straightforward piecewise linear approximation for $\Delta p_{i,j}(q^{\mathrm{g}}_{i,j})$ is:

$$(q^{\mathrm{g}}_{i,j}, \tilde{p}_{i,j}) = \sum_{k=1}^{\kappa(i,j)} (q^{\mathrm{g},k}_{i,j}, p^k_{i,j}) \lambda^{\mathrm{g},k}_{i,j}, \tag{5.7a}$$

$$\sum_{k=1}^{\kappa(i,j)} \lambda^{\mathrm{g},k}_{i,j} = 1, \tag{5.7b}$$

$$\lambda^{\mathrm{g},k}_{i,j} \geq 0,\ k = 1, \ldots, \kappa(i,j), \tag{5.7c}$$

$$\left\{ \lambda^{\mathrm{g},k}_{i,j} : k = 1, \ldots, \kappa(i,j) \right\} \text{ is SOS2} \tag{5.7d}$$

Because the flows $\mathbf{q}_{w,m}$ through a pipeline (w,m) from the set $\mathcal{W_M}$ are given by the IPR curves of the related well w, they are expressed as a function of the normalized bottom hole pressure u_w. In turn, the pressure drop $\Delta p_{w,m}(\mathbf{q}_{w,m})$ is also expressed as a function $\Delta p_{w,m}(u_w)$ of u_w, which can be approximated with simpler unidimensional piecewise-linear functions.

The multiphase flow $\mathbf{q}_w(u_w)$, the wellhead pressure $p_w(u_w)$, and the pressure drop $p_{w,m}(u_w)$ from wells to manifolds, $(w,m) \in \mathcal{W_M}$ related to well $w \in \mathcal{W}$ are represented with the following sets of samples, respectively:

- $\mathbf{Q}_w = \left\{ \left(\mathbf{q}^1_w, u^1_w\right), \left(\mathbf{q}^2_w, u^2_w\right), \ldots, \left(\mathbf{q}^{\kappa(w)}_w, u^{\kappa(w)}_w\right) \right\}$,
- $P_w = \left\{ \left(p^1_w, u^1_w\right), \left(p^2_w, u^2_w\right), \ldots, \left(p^{\kappa(w)}_w, u^{\kappa(w)}_w\right) \right\}$, and
- $P_{w,m} = \left\{ \left(p^1_{w,m}, u^1_w\right), \left(p^2_{w,m}, u^2_w\right), \ldots, \left(p^{\kappa(w)}_{w,m}, u^{\kappa(w)}_w\right) \right\}$;

Then, the piecewise-linear approximations are given by the following formulation:

$$(u_w, \tilde{\mathbf{q}}_w, \tilde{p}_w) = \sum_{i=1}^{\kappa(w)} (u_w^i, \mathbf{q}_w^i, p_w^i)\lambda_w^i,\ w \in \mathcal{W} \tag{5.8a}$$

$$\tilde{p}_{w,m} = \sum_{i=1}^{\kappa(w)} p_{w,m}^i \lambda_w^i,\ (w,m) \in \mathcal{W}_{\mathcal{M}}, \tag{5.8b}$$

$$\sum_{i=1}^{\kappa(w)} \lambda_w^i = 1, \tag{5.8c}$$

$$\left\{\lambda_w^i : i \in 1, \ldots, \kappa(w)\right\} \text{ is SOS2} \tag{5.8d}$$

Although the piecewise linear forms described above could have different independent variables (λ), the functions are sampled at the same break points for the sake of simplicity and model compactness.

5.4.2 Multidimensional Piecewise Linearization Applied to Pressure Drop Functions

The pressure drop functions associated with the pipelines from manifolds to separators, $\mathcal{M}_{\mathcal{M}} \cup \mathcal{M}_{\mathcal{S}}$, cannot be generically expressed in terms of the variables u_w related to the upstream wells. The number of upstream wells varies depending on each pipeline, multidimensional piecewise linearization can be practically intractable when several independent variables are considered. To unify the piecewise-linear models for pressure drop functions, the gas, oil, and water rates are taken as independent variables and expressed in terms of the gas-oil ratio (GOR) $q^{\mathrm{g}}/q^{\mathrm{o}}$ (G), water cut (WCUT) $q^{\mathrm{w}}/(q^{\mathrm{o}} + q^{\mathrm{w}})$ (W), and liquid rate (QL) $q^{\mathrm{o}} + q^{\mathrm{w}}$ (L). Let $\mathcal{H} = \{\mathrm{G}, \mathrm{W}, \mathrm{L}\}$. Given the breakpoint set $\mathcal{B}_{i,j}^h = \left\{b_{i,j}^{h,1}, b_{i,j}^{h,2}, \ldots, b_{i,j}^{h,\kappa_{i,j}^h}\right\}$ for each $(i,j) \in \mathcal{M}_{\mathcal{M}} \cup \mathcal{M}_{\mathcal{S}}$ and $h \in \mathcal{H}$,

$$q^{\mathrm{g}}_{i,j} = \sum_{k_{\mathrm{g}}=1}^{\kappa^{\mathrm{G}}_{i,j}} \sum_{k_{\mathrm{w}}=1}^{\kappa^{\mathrm{W}}_{i,j}} \sum_{k_{\mathrm{l}}=1}^{\kappa^{\mathrm{L}}_{i,j}} b^{\mathrm{G},k_{\mathrm{g}}}_{i,j} \left(1 - b^{\mathrm{W},k_{\mathrm{w}}}_{i,j}\right) b^{\mathrm{L},k_{\mathrm{l}}}_{i,j} \lambda^{k_{\mathrm{g}},k_{\mathrm{w}},k_{\mathrm{l}}}_{i,j}, \tag{5.9a}$$

$$q^{\mathrm{o}}_{i,j} = \sum_{k_{\mathrm{g}}=1}^{\kappa^{\mathrm{G}}_{i,j}} \sum_{k_{\mathrm{w}}=1}^{\kappa^{\mathrm{W}}_{i,j}} \sum_{k_{\mathrm{l}}=1}^{\kappa^{\mathrm{L}}_{i,j}} \left(1 - b^{\mathrm{W},k_{\mathrm{w}}}_{i,j}\right) b^{\mathrm{L},k_{\mathrm{l}}}_{i,j} \lambda^{k_{\mathrm{g}},k_{\mathrm{w}},k_{\mathrm{l}}}_{i,j}, \tag{5.9b}$$

$$q^{\mathrm{w}}_{i,j} = \sum_{k_{\mathrm{g}}=1}^{\kappa^{\mathrm{G}}_{i,j}} \sum_{k_{\mathrm{w}}=1}^{\kappa^{\mathrm{W}}_{i,j}} \sum_{k_{\mathrm{l}}=1}^{\kappa^{\mathrm{L}}_{i,j}} b^{\mathrm{W},k_{\mathrm{w}}}_{i,j} b^{\mathrm{L},k_{\mathrm{l}}}_{i,j} \lambda^{k_{\mathrm{g}},k_{\mathrm{w}},k_{\mathrm{l}}}_{i,j}, \tag{5.9c}$$

$$\tilde{p}_{i,j} = \sum_{k_{\mathrm{g}}=1}^{\kappa^{\mathrm{G}}_{i,j}} \sum_{k_{\mathrm{w}}=1}^{\kappa^{\mathrm{W}}_{i,j}} \sum_{k_{\mathrm{l}}=1}^{\kappa^{\mathrm{L}}_{i,j}} \Delta p_{i,j} \left(b^{\mathrm{G},k_{\mathrm{g}}}_{i,j}, b^{\mathrm{W},k_{\mathrm{w}}}_{i,j}, b^{\mathrm{L},k_{\mathrm{l}}}_{i,j}\right) \lambda^{k_{\mathrm{g}},k_{\mathrm{w}},k_{\mathrm{l}}}_{i,j}, \tag{5.9d}$$

$$1 = \sum_{k_{\mathrm{g}}=1}^{\kappa^{\mathrm{G}}_{i,j}} \sum_{k_{\mathrm{w}}=1}^{\kappa^{\mathrm{W}}_{i,j}} \sum_{k_{\mathrm{l}}=1}^{\kappa^{\mathrm{L}}_{i,j}} \lambda^{k_{\mathrm{g}},k_{\mathrm{w}},k_{\mathrm{l}}}_{i,j}, \tag{5.9e}$$

$$\gamma^{\mathrm{G},k_{\mathrm{g}}}_{i,j} = \sum_{k_{\mathrm{w}}=1}^{\kappa^{\mathrm{W}}_{i,j}} \sum_{k_{\mathrm{l}}=1}^{\kappa^{\mathrm{L}}_{i,j}} \lambda^{k_{\mathrm{g}},k_{\mathrm{w}},k_{\mathrm{l}}}_{i,j},\ k_{\mathrm{g}} \in \left\{1, \ldots, \kappa^{\mathrm{G}}_{i,j}\right\}, \tag{5.9f}$$

$$\gamma^{\mathrm{W},k_{\mathrm{w}}}_{i,j} = \sum_{k_{\mathrm{g}}=1}^{\kappa^{\mathrm{G}}_{i,j}} \sum_{k_{\mathrm{l}}=1}^{\kappa^{\mathrm{L}}_{i,j}} \lambda^{k_{\mathrm{g}},k_{\mathrm{w}},k_{\mathrm{l}}}_{i,j},\ k_{\mathrm{w}} \in \left\{1, \ldots, \kappa^{\mathrm{W}}_{i,j}\right\}, \tag{5.9g}$$

$$\gamma^{\mathrm{L},k_{\mathrm{l}}}_{i,j} = \sum_{k_{\mathrm{g}}=1}^{\kappa^{\mathrm{G}}_{i,j}} \sum_{k_{\mathrm{w}}=1}^{\kappa^{\mathrm{W}}_{i,j}} \lambda^{k_{\mathrm{g}},k_{\mathrm{w}},k_{\mathrm{l}}}_{i,j},\ k_{\mathrm{l}} \in \left\{1, \ldots, \kappa^{\mathrm{L}}_{i,j}\right\}, \tag{5.9h}$$

$$\lambda^{k_{\mathrm{g}},k_{\mathrm{w}},k_{\mathrm{l}}}_{i,j} \geq 0,\ k_h \in \left\{1, \ldots, \kappa^{h}_{i,j}\right\},\ h \in \mathcal{H} \tag{5.9i}$$

$$\left\{\gamma^{h,k}_{i,j} : k = 1, \ldots, \kappa^{h}_{i,j}\right\} \text{ is SOS2},\ h \in \mathcal{H} \tag{5.9j}$$

Others works like (Gunnerud et al. 2010a) model the pressure drop functions using piecewise linearization along the fluid rate dimensions, namely oil, gas, and water rates. The piecewise-linear approximation using these dimensions is a straightforward application of the existing models in the literature. However, such strategy for piecewise linearization requires many non-realistic sample points, for instance points with extremely low GOR, combining the maximum oil rate and minimum gas rate breakpoints. From the process point of view, the well IPR curves and the pipeline pressure drop functions are better specified in terms of GOR, WCUT, and QL values, making it easier to generate

sample points that relate to actual operating points, establish tight bounds for breakpoints, and thereby generate tighter formulations.

It is worth remarking that this formulation allows multiple pressure drop solutions for a given multiphase rate, because a three dimensional point given by the flow rates is obtained by convex combination of eight points which are vertices of a cube in the $\mathcal{H}$ space. Misener et al. (2010) show an explicit formulation for three dimensional piecewise-linear functions that yields a unique interpolation solution, which in our case translates into a unique pressure drop solution for a given multiphase rate. While Misener et al. (2010) use SOSX constraints and binary variables, Vielma et al. (2011) propose a formulation with a logarithmic number of binary variables and constraints in the number of breakpoints which also ensures a unique interpolation. A potential drawback is the fact that extra constraints and variables are needed to enforce a unique interpolation solution, which may imply in a larger formulation with slower solution time. It is also worth remarking that the non-unique representation can be conveniently modeled in optimization solvers using SOS2 constraints. Formulations allowing multiple solutions as the one given in equation (5.9) were already proposed by Bieker et al. (2006) and Gunnerud et al. (2010a). In this work, a methodology will be developed in Section 5.5 for generating piecewise-linear approximations of the nonlinear functions that ensure sufficiently accurate approximations, regardless of the multiple interpolation solutions.

5.4.3 Piecewise-Linear Approximation of the Production Optimization Problem

The production optimization problem P is approximated by problem $\tilde{P}$ obtained from (5.6) after making the following modifications:

- Equations (5.1a), (5.4a), and (5.4b) modeling respectively flow rates, pressure drops, and wellhead absolute pressures are removed;
- Equations (5.7), (5.8), and (5.9) with the piecewise-linear approximations are included; and
- the variables $\mathbf{q}_w$, p_w, and $p_{i,j}$ are replaced by their approximations $\tilde{\mathbf{q}}_w$, $\tilde{p}_w$, and $\tilde{p}_{i,j}$, respectively.

5.5 Field Data Integration, Model Validation, and Problem Synthesis

This section proposes a methodology for generating mathematical representations adjusted to existing gathering system models for re-routing purposes. A simplification procedure is developed to obtain representations suitable for real-time optimization by ensuring process representation accuracy.

5.5.1 Field Data Gathering for Real-Time Optimization

Simulators for reservoir and surface facilities are constantly being tuned by field engineers to reflect the prevailing operating conditions. In spite of being independent, these simulators must operate in an integrated manner to account for the dependencies among the processes. For instance, the processing capacity of surface facilities constrains the production from the reservoir imposing simulation ranges, while the fluid properties from the reservoir establish certain operating parameters for surface facilities.

In this work, field simulators are used to generate piecewise-linear representations for the involved processes. Since the simulator parameters are constantly being updated to match field measurements, dependencies must be minimized to reduce model maintenance each time one simulator parameter changes.

When approximating non-linear phenomena by piecewise linear functions for optimization purposes two aspects must be considered:

- Feasible operating ranges must be described. To rule out conditions not within feasible ranges, a comprehensive model considering large operating ranges would be excessively large and complex for real-time optimization. Thus, tight feasible ranges are desirable to keep the search space as small as possible.
- The approximation error should be small enough to capture the process characteristics. High approximation errors may cause convergence to a solution away from the optimal point, whereas overly accurate piecewise-linear models may have too many variables and constraints for real-time optimization purposes.

Figure 5.2 shows how to obtain piecewise-linear pressure-drop functions for pipelines from manifolds to separators and gas pipelines downstream separators: the former are multidimensional functions represented in the space of GOR, WCUT, and QL, whereas the latter are unidimensional in the space of gas flow rate.

The nominal pressure at the pipeline outlet is a parameter estimated by field engineers, which triggers the generation of new approximation functions whenever it changes. A sensitivity analysis justifying this assumption is presented in Section 5.5.2. Fixed an outlet pressure, a high-resolution piecewise-linear model is created considering the following:

- The QL sample range is defined by network constraints, with the upper limit being defined as the sum of the maximum liquid rates allowed for the upstream wells or by the maximum liquid rate for separators.
- The minimum GOR is the well solution gas/oil ratio (Rs) and the minimum WCUT is zero, while the maximums are defined by an operational constraint indicating that no well can produce above shut-in GOR and WCUT.
- In a similar way, the maximum gas rate for gas pipelines is limited by the sum of the maximum capacity of the upstream separators or by the total field capacity.
- The piecewise linear model is created with fixed sample steps.

These sample ranges are sufficiently large to avoid frequent model maintenance. The obtained piecewise-linear models are then fed to the reduction procedure along with an accuracy parameter: breakpoints are eliminated to reduce model size while ensuring that the model error is within the given accuracy. The reduction procedure is described in Section 5.5.3.

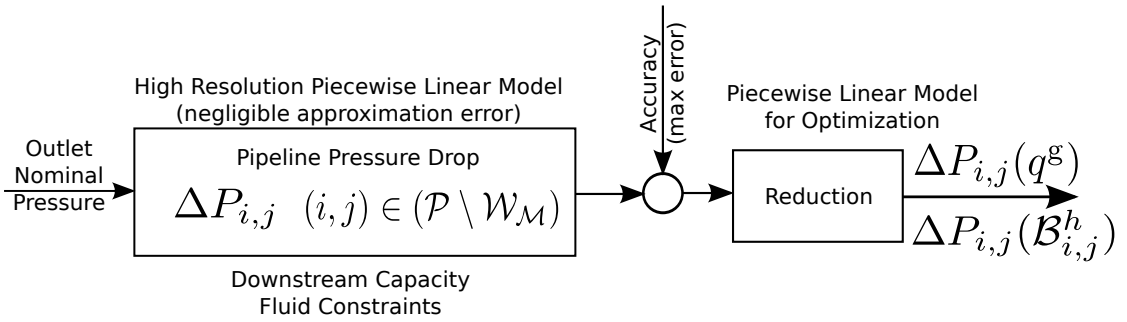

Figure 5.2: Pipeline pressure drop piecewise linear curves obtainment.

Figure 5.3 shows how to obtain piecewise-linear representations of models related to wells, namely IPR, VLP, and pressure drops. To avoid multidimensional representations, all curves are expressed in terms of the normalized bottom hole pressure. However, this artifice entails model maintenance triggered by changes in reservoir parameters identified after well tests. As illustrated in the figure, a high resolution IPR curve is obtained for each well, coupled to the VLP curve and the pressure drop functions for the pipelines connected to the well. The normalized bottom-hole pressure range is set up according to the maximum liquid production allowed for the well. All of the curves are sampled with the same set of normalized bottom-hole pressures. Next, as in the previous case, an accuracy parameter is defined for performing modeling reduction on each curve. However, such reduction is performed under a conciliation restriction that all curves must be sampled on the same set.

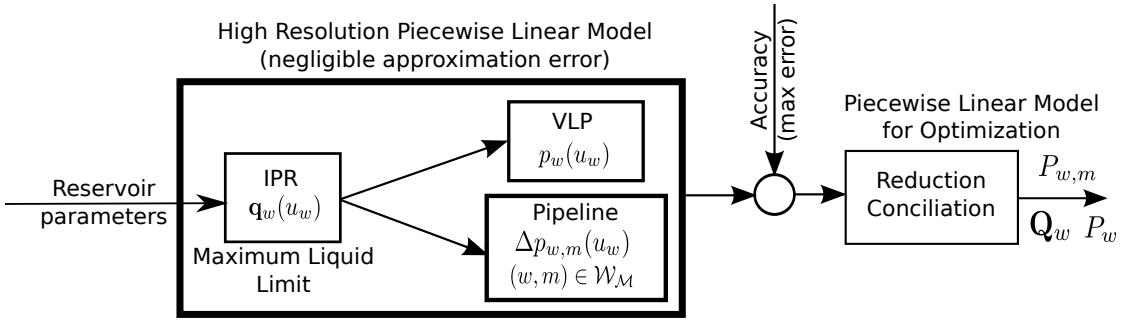

Figure 5.3: Well related piecewise linear curves obtainment.

5.5.2 Pressure Drop Modeling

Pressure drop in pipelines depends on geometries, flow rates, and operating pressures, among other variables (Litvak et al. 1995; Kosmidis et al. 2005; Gunnerud et al. 2010a). For optimization purposes, this work approximates pressure drop curves in pipelines considering the outlet pressure fixed at the nominal pressure, which corresponds to the prevailing field pressure during a production reference day.

For the operating conditions calculated by the optimization algorithm, the actual outlet pressure may not match the nominal pressure assumed during curve generation, thus incurring approximation error.

To assess the validity of this assumption, two pressure drop curves were obtained considering a maximum and minimum operating pressure under the average GOR (2000 sm^3/sm^3) and WCUT (50 %) of the field. The analysis considered a pipeline of 1100 m and elevations varying between -10 m and 20 m, one of the longest in the field, which constitutes a worst-case scenario.

Figure 5.4 shows the pressure drop percentage error for this pipeline assuming a constant outlet pressure. Notice that the percentage error is negligible for low liquid rate. The maximum 4% error reported for the maximum liquid rate is acceptable. The maximum error between the pressure reported by the simulator and field measurements is about 7%. If the fitting data were obtained directly from field measurements instead of being sampled from simulators, then the optimization models would have a maximum error of 4%.

Although the uncertainty is higher for nodes near the wellhead due to the backward pressure calculation, the liquid rate through these nodes is low, typically under 200 m^3/d, rendering the approximation error negligible. Higher rates are found close to the separator nodes, where the absolute pressure estimation is more accurate. Taking into account these remarks, the approximation errors are always much less than 4%.

5.5.3 Pressure Drop Simplification

The effectiveness of the proposed framework for production optimization depends on the approximation quality of the non-linear functions. The accuracy of the approximations with piecewise-linear functions tends to increase as sample points are added to the model description. However, increasing the number of sample points introduces new interpolating variables that, in turn, make the optimization larger and consequently more difficult to be practically solved. Besides this relation between precision and instance size, the increase of sample points cannot improve accuracy beyond the uncertainty inherited from the measurements and model fitting (Elgæter et al. 2010). Thereupon arises the trade-off decision on selecting samples to describe the non-linear curves.

This work assumes that a tight piecewise-linear representation is given for each non-linear function, meaning that each representation approximates the expected non-linear

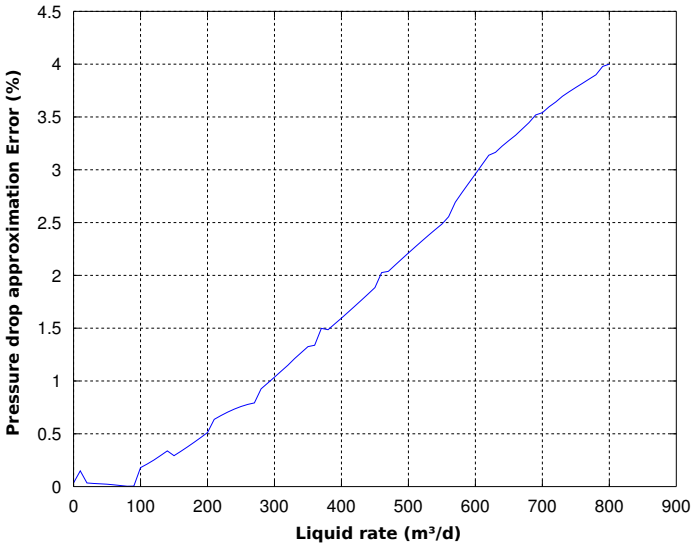

Figure 5.4: Pressure drop approximation for different operating pressures.

function with negligible error using a finite number of sample points. Because this representation may be overly detailed, a greedy heuristic is proposed to reduce the number of sample points, while ensuring a maximum error with respect to the tight piecewise-linear representation. Three different cases are addressed:

- Unidimensional functions, $\Delta p_{i,j}(q^g),\ (i,j) \in \mathcal{S}_\mathcal{C} \cup \mathcal{C}_\mathcal{C} \cup \mathcal{C}_\mathcal{T}$.
- Unidimensional functions with common sample points, $p_w(u_w)$, $q_w(u_w)$ and $p_{w,m}(u_w)$, $w \in \mathcal{W},\ (w,m) \in \mathcal{W}_\mathcal{M}$.
- Multidimensional functions, $\Delta p_{i,j}(g,w,l),\ (i,j) \in \mathcal{M}_\mathcal{M} \cup \mathcal{M}_\mathcal{S}$.

5.5.3.1 Unidimensional Functions

Let $\Delta p(q)$ be an unidimensional function described tightly by the set of sample points $PQ = \left\{\left(p^1, q^1\right), \ldots, \left(p^\kappa, q^\kappa\right)\right\}$, where $Q = \left\{q^1, \ldots, q^\kappa\right\}$. Algorithm 2 iteratively attempts to remove each point in PQ from the piecewise-linear representation, with exception of the end points. A trial point is removed if the approximation error of the resulting piecewise-linear representation with respective to the tight representation is below a given error bound (r), otherwise this point remains in the sample set. The maximum error between a candidate and the tight representation is computed by Algorithm 3, which computes the distance of the missing points to the candidate representation and takes the maximum. Algorithm 3 returns the maximum error introduced to the representation given by $Q_r \setminus \{q\}$, with q being the trial point and Q_r being the current reduced representation. If the approximation error is greater than the bound r for any point in the

tight representation, the algorithm aborts the computation and reports the trial point cannot be removed. Notice that Algorithm 2 runs in $\mathcal{O}(\kappa^2)$ time.

Algorithm 2 Unidimensional representation reduction

input: PQ, Q, r
$Q_r := Q$
for $q \in Q \setminus \{q^1, q^\kappa\}$ **do**
  compute $E(PQ, Q_r, q, r)$, obtaining $e^{\max}$
  if $e^{\max} \leq r$ **then**
    $Q_r := Q_r \setminus \{q\}$
  end if
end for
return Q_r

Algorithm 3 $E(PQ, Q_r, q, r)$. Maximum error introduced when q is removed.

input: PQ, Q_r, q, r
$e^{\max} := 0$
$(p^u, q^u) := \underset{(p^s,q^s)\in PQ}{\operatorname{argmin}} \{q^s : q^s \in Q_r, q^s > q\}$
$(p^l, q^l) := \underset{(p^s,q^s)\in PQ}{\operatorname{argmax}} \{q^s : q^s \in Q_r, q^s < q\}$
for $(p^t, q^t) \in \{(p^s, q^s) \in PQ : q^l < q^s < q^u\}$ **do**
  $p^c := p^l + \frac{p^u - p^l}{q^u - q^l}(q^t - q^l)$
  $e^{\max} := \max\left(|p^c - p^t|, e^{\max}\right)$
  if $e^{\max} > r$ **then**
    return ∞
  end if
end for
return $e^{\max}$

5.5.3.2 Unidimensional Functions with Common Breakpoints

The heuristic for reducing the complexity of the piecewise-linear representation is essentially identical to Algorithm 2, differing only on how the approximation error is computed in Algorithm 3. A sample point is removed if the maximum error introduced after the removal is less than the threshold for all of the involved functions. Notice that the resulting heuristic runs in $\mathcal{O}(\kappa^2 l)$ time where l is the number of unidimensional functions.

5.5.3.3 Multidimensional Functions

Let Δp be a function tightly represented using the formulation given in (5.9) for the set of sample points $P^{\mathcal{H}} = \{(p, g, w, l) \in \mathbb{R}^4 : g \in \mathcal{B}^{\mathrm{G}}, w \in \mathcal{B}^{\mathrm{W}}, l \in \mathcal{B}^{\mathrm{L}}, p = \Delta p(g, w, l)\}$ for a given pipeline (i, j), not indicated here to keep notation simple, where $\mathcal{B}^h = \left\{b^{h,1}, b^{h,2}, \ldots, b^{h,\kappa^h}\right\}$ is the set of breakpoints in each dimension.

The heuristic for breakpoint removal appears in Algorithm 4, which works similarly to the heuristics for the unidimensional cases. The difference is twofold. First, the heuristic for multidimensional functions attempts to remove all sample points for a given breakpoint in one of the dimensions—for instance, if a breakpoint b^{G} is to be removed, then entire set of sample points $\{(b^{\mathrm{G}}, b^{\mathrm{W}}, b^{\mathrm{L}}) : b^{\mathrm{W}} \in \mathcal{B}^{\mathrm{W}}, b^{\mathrm{L}} \in \mathcal{B}^{\mathrm{L}}\}$ is removed. Second, the error incurred by removing a breakpoint must consider all sample points influenced by the removal.

The computation of the error $E_m(P^{\mathcal{H}}, \mathcal{B}^{\mathrm{G}}_r, \mathcal{B}^{\mathrm{W}}_r, \mathcal{B}^{\mathrm{L}}_r, b, h, r)$ caused by the removal of a breakpoint p is computationally intensive, mostly because the formulation (5.9) allows more than one feasible pressure value for each point of the sample set

$$T = \left\{(b^{\mathrm{G}}, b^{\mathrm{W}}, b^{\mathrm{L}}) \in \mathcal{B}^{\mathrm{G}} \times \mathcal{B}^{\mathrm{W}} \times \mathcal{B}^{\mathrm{L}} : b^h = b\right\}.$$

For the flow rates defined by each point $t \in T$, the test solves two MILP problems with constraints given by formulation (5.9), the solution of the first problem yields the minimum pressure drop $\tilde{p}^{\min}(t)$ whereas the second yields the maximum pressure drop $\tilde{p}^{\max}(t)$. This MILP problems can be reduced to LP programs since the interpolating points for the test point p are easily identified, eliminating the need of SOS2 constraints. The breakpoint b^h cannot be removed if there exists at least one sample point $t \in T$ such that $\max(|\tilde{p}^{\max}(t) - \Delta p(t)|, |\tilde{p}^{\min}(t) - \Delta p(t)|) > r$.

5.5.3.4 Linear Functions

In some pipelines, the fluid rate variation is small or their geometrical properties cause small pressure drops. The pressure drop in such pipelines can be represented by a simple linear function:

$$p = p_0 + p_o q_o + p_g q_g + p_w q_w \tag{5.10}$$

provided that there exist parameters p_0, p_o, p_g, and p_w for which the approximation error is within the given accuracy for all the sample points. The existence and obtainment of optimal parameters can be easily determined solving an LP problem.

Algorithm 4 Multidimensional representation reduction

input: $P^{\mathcal{H}}$, $\mathcal{B}^{\mathrm{G}}$, $\mathcal{B}^{\mathrm{W}}$, $\mathcal{B}^{\mathrm{L}}$, r
for $h \in \mathcal{H}$ **do**
  $\mathcal{B}_r^h := \mathcal{B}^h$
  $\mathcal{B}_t^h := \mathcal{B}^h \setminus \{b^{h,1}, b^{h,\kappa^h}\}$
end for
for $h \in \mathcal{H}$ **do**
  for $b \in \mathcal{B}_t^h$ **do**
    solve $E_m(P^{\mathcal{H}}, \mathcal{B}_r^{\mathrm{G}}, \mathcal{B}_r^{\mathrm{W}}, \mathcal{B}_r^{\mathrm{L}}, b, h, r)$, obtaining $e^{\max}$
    if $e^{\max} \leq r$ **then**
      $\mathcal{B}_r^h := \mathcal{B}_r^h \setminus \{b\}$
    end if
  end for
end for
return Q_r

5.6 Computational Performance, Validation, and Applications

This section aims to show that the framework for system production modeling, data gathering, and instance generation is suitable for production optimization of complex oil fields such as Urucu. The implementation of the framework may become an invaluable decision-support tool for field engineers. The following sections describe Urucu's production system, present the application of procedures for data simplification, show results regarding production optimization and solution validation, and finally discuss operational issues on the framework application.

5.6.1 Instance Characteristics

The instance is constructed to reflect LUC field wells and routing degree of freedom for the reference case. In total, 28 wells were producing, among which 15 wells did not have reliable IPR models. Therefore, bottom hole pressure was fixed leaving only the routing for decision making. For the other 13 wells, the bottom hole pressure and routing are the decision variables in the optimization process.

Every well has at least 2 manifold connections (production and test manifold), but in some cases there is a direct connection to a separator passing through a bypass manifold connection. The field has 9 independent separators and 1 gas terminal point. Table 5.1 shows the cardinality of parameter sets related to the problem.

The gathering system of the LUC field is modeled using a commercial network production system analysis software. The black-oil model is used to characterize the field

Table 5.1: Cardinality of sets.

$\mathcal{W}$	$\mathcal{M}$	$\mathcal{S}$	$\mathcal{C}$	$\mathcal{T}$	$\mathcal{W}_{\mathcal{M}}$	$\mathcal{M}_{\mathcal{M}}$	$\mathcal{M}_{\mathcal{S}}$	$\mathcal{S}_{\mathcal{C}}$	$\mathcal{C}_{\mathcal{C}}$	$\mathcal{C}_{\mathcal{T}}$
28	32	9	8	1	61	58	9	9	7	1

fluid, some parameters of this model are depicted in Table 5.2. The simulator must be tuned to represent as accurately as possible field conditions. To this end, a stable production day (without any plant upset or shutdowns) was chosen to become the reference production condition for model tuning and routing comparisons. The surface gathering network model was prepared to reproduce this day. To perform the tuning process the following information is gathered:

- Individual well production rates, which are calculated through a reconciliation process based on the last well test information.
- Routing and status (open/closed, production/test) for each well, as stated by the Technical Instructions.
- Pressure and temperature in equipments and pipeline key locations, obtained in real-time through the Process Information Management System (PIMS).

Rates per well, pressures, temperatures, and routing are input variables for model calibration. The real flow rate and well stream composition are sources of high uncertainty for tuning. The wells with the oldest tests introduce higher errors, mainly the ones whose GOR depend on liquid flow rate (gas coning).

The tuning procedure consists of changing the roughness of pipelines to match the separator and manifold pressures. In this work, the tuned model is the source for piecewise-linear representations.

To obtain tight representations of the curves (IPR, VLP, and pressure drops) related to the wells, a fixed step of 0.01 of the normalized bottom hole pressure was adopted. Similarly, tight representations of the multiphase pressure-drop functions were obtained fixing sampling steps at 25 m^3/day, 200 sm^3/sm^3, and 10% for QL, GOR, and WCUT, respectively. For pressure-drop functions depending only on the gas rate, tight representations were sampled such that the pressure drop between consecutive points is $20kPa$ apart. The accuracy parameter that guides pressure-drop function reduction is set at $20kPa$. On the other hand, the accuracy for the rates is disconsidered because the functions modeling these variables are almost linear, thus the sampling is guided by the error induced by the wellhead pressure and pressure-drop function. The wells have a GOR varying between 200 and $3\,000$ sm^3/sm^3. The upper GOR limit is related to the shut-in of a swing well with subsequent opening of a well with lower GOR. The field WCUT ranges between 0 and 72 %. Table 5.3 summarizes sampling parameters for pressure drop functions.

Table 5.2: Black Oil fluid characterization.

Property[1]	Assumption
Water cut (WCUT)	Variable
Gas-oil ratio (GOR)	Variable
Gas specific gravity	0.75
Water specific gravity	1.02
Oil density	45 ^{o}API
Reservoir gas solubility factor (R_s)	200 sm^3/sm^3
Bubble point pressure (P_b) correlation	Kartoatmodjo
Gas solubility factor (R_s) correlation	Kartoatmodjo
Dead oil viscosity correlation	Beggs & Robinson
Live oil viscosity correlation	Beggs & Robinson
Undersaturated oil viscosity correlation	Vasquez & Beggs
Emulsion viscosity method	Volume ratio of oil and water
Contaminants	No contaminants

[1] Further properties are confidential.

Table 5.3: Pressure drop function sampling.

Variable	Minimum	Maximum	Sampling Step
Liquid rate (QL) sm^3/d	0	1500	25
Gas-oil ratio (GOR) sm^3/sm^3	200	3000	200
Water cut (WCUT) $\%$	0	90	10
Normalized bottom hole pressure	0	1	0.01

With this configuration an instance of the production optimization problem has 145 binary variables, 168 SOS2 constraints, $143\,114$ continuous variables, and $5\,095$ constraints.

5.6.2 Computational Analysis

The production optimization problem was modeled in AMPL and solved with CPLEX 12.3.0.0 on a workstation equipped with 16 GB memory and two processors, each with a six-core AMD Opteron running at 2.4 GHz.

The solver was not able to find a feasible solution for the tight representation with a deadline set to 1 hour. After applying the reduction procedures on the piecewise-linear representations, the solver was able to find feasible solutions but could not prove

optimality within the given deadline. To improve solution quality, we imposed branching priorities for the solver, pruned interpolating variables of the piecewise-linear forms, add cuts on flow rates, and limited the flow rates in pipelines according to network relations, all without cutting off feasible solutions in a preprocessing step.

The branching priority consists of branching first on the routing variables rather than on the SOS2 constraints. The activations of the pipelines (*i.e.*, $z_{i,j}$ variables) impose structural changes in the flow network that have a major impact on the flow rates and, thereby, the pressure drops which are then determined by the interpolating variables. Put another way, the interpolating variables are greatly affected by the routing variables which are hierarchically superior.

The pruning procedure rules out unused variables such as the interpolating variables λ_w^i, $i \in 1, \ldots, \kappa(w)$, which can be fixed at zero and thereby removed because of the bounds on u_w given by restriction (5.2c). Pruning is also applied on the flow rates of the pipelines: the range of GOR (WCUT) for a pipeline (i, j) can be restricted to the minimum and maximum GOR (WCUT) of the upstream wells whose production can be sent to node i; the maximum value for QL can be set to the sum of the maximum liquid rate allowed for all upstream wells or the QL capacity of the downstream facilities.

The pruning procedure also introduces valid inequalities on flow rates to prevent manifolds from acting as separators, *i.e.* linear-relaxation solutions where the fluid phases are separated downstream the node. One such constraint for a pipeline (i, j) is $q_{i,j}^{\mathrm{o}} \leq q_{i,j}^{\mathrm{g}} GOR_i$ with GOR_i being the maximum possible GOR for the pipeline. Similar constraints are introduced for the other phases.

The best solution reported using these techniques within the deadline are shown in Table 5.4. The optimal oil production for the problem instance is $3\,040.77\ m^3/d$, obtained in $45\,969$ s ($\approx$ 13 h), which is obtained using reduction, branching priorities, and pruning. Using these acceleration techniques, a near-optimal solution with an oil production rate of $3\,035.67\ m^3/d$ was found within the deadline.

Table 5.4: Feasible solutions using reduction (R), branching priorities (BP), and pruning (P).

Techniques	Best Solution m^3/d	Absolute MIPGAP m^3/d
R	2 971.46	186.02
R+P	2 997.23	160.25
R+BP	3 015.36	142.13
R+P+BP	3 035.67	121.81

5.6.3 Optimal Solution Validation

The analysis in Section 5.5.2 regarding pressure drop modeling simplification and error bounding was restricted to a single pipeline, thereby not sufficiently representative of the entire network. Other sources of error should be considered such as the error introduced by the reduction procedure and the propagation of pressure drop error across the network.

To this end, the optimal solution pressures found by the optimization process were contrasted against the pressures obtained with the simulator, using the same well rates and routings. The multiphase rates for each well and the routing options are taken from the optimization solution and input to the simulator, which incurs no error in the flow estimation of the nodes because of the mass conservation laws. The approximation errors appear in the absolute pressures and pressure drop estimations.

Table 5.5 shows statistics comparing absolute pressures. Column "Nominal Model vs. Simulator" compares absolute pressures used as nominal points for piecewise-linear representation generation and the absolute pressures given by the simulator under the optimal flows from the wells. Column "Optimization vs. Simulator" compares the absolute pressures given by the piecewise-linear models and the simulator, both considering the optimal flows from the wells.

Table 5.5: Approximation error comparison.

	Nominal Model vs. Simulator		Optimization vs. Simulator	
	Absolute (kPa)	Relative (%)	Absolute (kPa)	Relative (%)
Mean error	262.85	3.89	32.62	0.48
RMSE	288.89	4.26	40.47	0.60
Maximum error	734.48	10.70	68.66	1.02

The data in Table 5.5 elicited the following conclusions:

- High differences between nominal pressures and operational pressures given by the simulator do not significantly affect the quality of the absolute pressures given by the piecewise-linear representations. The pressure-drop functions generated under the assumption of fixed nominal pressure are sufficiently accurate.
- The pressures represented by piecewise-linear models are within the expected precision, as controlled by the accuracy parameter r used during the reduction procedure. The maximum absolute error was 68.66 kPa for the whole network with an accuracy parameter of 20 kPa, which is expected because of the propagation of error for several pressure drop approximations. The accuracy parameter was intentionally set low enough to keep all approximation errors under 100 kPa.
- If the pressure-drop correlations used by the simulator represent accurately the pressure drops in the field, then the real pressure drops are also represented accu-

rately by the piecewise-linear models.

5.6.4 Operational and Gain Analysis

The developed optimization model is intended to be used by field engineers as a decision support tool. Besides calculating optimal operating points, field engineers would like to reduce dynamic transients from the current to the next operating point (not necessarily the global optimum), which is achieved by limiting the number operational switchings. To this end, additional restrictions are enforced: maximum number of alterations of well rates and routing switchings, which are stated as follows:

$$(u_w^{\min} - \overline{u}_w)c_w \leq u_w - \overline{u}_w \leq (u_w^{\max} - \overline{u}_w)\, c_w,\ w \in \mathcal{W} \tag{5.11a}$$

$$\sum_{w \in \mathcal{W}} c_w \leq c^{\max} \tag{5.11b}$$

$$\sum_{(i,j) \in \mathcal{P}} (z_{i,j} - 2z_{i,j}\overline{z}_{i,j} + \overline{z}_{i,j}) \leq z^{\max} \tag{5.11c}$$

where $\overline{u}_w$ is the current normalized bottom hole pressure of well w, $\overline{z}_{i,j}$ is the current state of the pipeline (i,j), $c^{\max}$ and $z^{\max}$ are the maximum number of changes allowed for the wells and pipelines, and c_w is a binary variable taking value 1 if the bottom hole pressure of well w is to be reset.

To test the model solving time with these restrictions, $c^{\max}$ and $z^{\max}$ are set to 3 and 5 respectively and a feasible solution representing the current production of the field ($3\,001.76\ m^3/d$) is input to the system. The current solution is obtained by solving the optimization problem with routing decisions fixed to the actual routings of the field—thus, this is the optimal solution for the given routing configuration. The optimal solution to the production optimization problem additionally subject to the operational constraints (5.11) is reached in 1604 s ($\approx$ 27 min) reporting an oil production rate of $3\,033.18\ m^3/d$. The fact that the current routing is nearly optimal explains why the solution obtained after optimizing under operational constraints yields small production gains. However, oil production was increased by allowing a few operational switchings, a production gain that could not be achieved without the routing degree of freedom.

Despite being limited by constraints on the number of well and routing changes, which avoid large operational changes in the field, the obtained solution yields an oil production rate that is close to the global optimum that would be obtained without such constraints.

5.7 Conclusion

This paper presented an MILP optimization formulation approximating mature oil fields like Urucu. Such production systems have wells producing under gas conning, limited

processing capacity, and complex pipeline network structures with manifold-manifold, manifold-separator, and gas pipeline connections. Due to these degrees of freedom and complex constraints, operational points should be calculated taking into account flow pressures to ensure pressure limits. Therefore, optimization procedures should model pressure constraints across the network.

This work innovates by approximating pressure drop relations with piecewise-linear functions in the space of gas-oil-ratio, water cut, and liquid rate assuming the outlet pipeline pressure constant. With this new representation, better integration with field simulators is attained and tighter formulations are obtained because infeasible rates are not represented. The computational analysis shows that the approximation errors are within the desired accuracy for the application purpose, despite the nominal absolute pressure being significantly away from the operational point determined for the field.

Procedures were developed to synthesize piecewise-linear functions approximating process relations that are then integrated in an optimization tool. Such procedures can be implemented and are sufficiently fast to adjust the models in response to process variations, such as changes in inflow and vertical-lift performance relations. The IPR relations are updated at every well test, triggering the procedures that generate unidimensional piecewise-linear models with low computational cost. On the other hand, the multidimensional pressure-drop functions are obtained considering the limitations of the surface facilities, not the production of the wells, thereby avoiding frequent updates which would consume considerable computational resources. After obtaining representations of the process relations (IPR, VLP, and pressure drop functions) with high resolution, which need a large number of sample points, a procedure is performed to reduce the size of the piecewise-linear approximations without prejudicing significantly the accuracy.

According to our computational analysis, the following strategies were shown to expedite the solution of the production optimization problem:

- the reduction of size of the piecewise-linear approximation, without which feasible solutions could not be found within the deadline;
- branching priorities attributing higher priority to routing variables than interpolating variables used in the piecewise-linear forms (SOS2 constraints);
- valid inequalities ruling out infeasible flows according to network relations.

The optimization framework can be used as decision-support tool to perform daily well scheduling when wells must undergo production test. Further, the optimization framework can handle operating constraints that limit flows and absolute pressures in all network nodes. The optimization algorithm produces solutions along with quality certificates (absolute mixed-integer gap), which upper bounds the gain that is possible to achieve with a better solution if it exists. Such certificates are valuable for field engineers to estimate how much the current production might be improved.

A direction for future research is the modeling of nodes with more than one output, which would allow one well to send its production to more than one separator. The difficulty arises from the fact that such nodes can act as separators, since the downstream flow rates do not necessarily have the same compositions, meaning the same gas-oil ratio and water cut. A simplifying approach implemented in some simulators considers equal the fluid compositions in the pipelines downstream the node. However, the flow modeling under this assumption would require additional nonlinear constraints which may lead to large, multidimensional piecewise-linear approximations.

A second research direction is the dynamic modeling for optimization of daily well scheduling, which would entail representing fluid flow and pressure transients that are triggered by new operational settings.

A third research direction is the design of algorithms to reduce the number of points needed in piecewise-linear functions, possibly based on the dynamic-programming strategies to find the optimal representation complying with the given accuracy requirement, rather than heuristics.

Chapter 6

A two-layer structure for stabilization and optimization of an oil gathering network

This chapter is based on (Codas et al. 2016c):

Codas, A. et al. (2016c). 'A two-layer structure for stabilization and optimization of an oil gathering network'. In: *11th IFAC Symposium on Dynamics and Control of Process Systems, including Biosystems*.

Abstract

In this work, we present the control and optimization of a network consisting of two gas-lifted oil wells, a common pipeline-riser system and a separator. The gas-lifted oil wells may be open-loop unstable. The regulatory layer stabilizes the system by cascade control of wellhead pressure measurements without needing bottom hole sensing devices. An economic Nonlinear Model Predictive Control (NMPC) based on the Multiple Shooting (MS) formulation is applied for optimization of the network operations. The optimization layer thus provides optimal settings for the regulatory controllers. The control structure has been validated by using the realistic OLGA simulator as the process, and using simplified models for Kalman filtering and the NMPC design. The simplified models are implemented in Modelica and fit to the Olga model to represent the main dynamics of the system. The proposed two-layer controller was able to stabilize the system and increase the economical outcome.

6.1 Introduction

In an offshore platform, the flow control of the oil wells is a key to attain good overall operational performance. The control of the producers assisted by gas-lift may be challenging due to oscillatory flow patterns known as *casing heading* and *density wave* (Bin et al. 2003). Moreover, even under stable well operations, oscillations known as *riser slugging* may originate in the pipeline-riser system that transport the production from the wellhead to the platform (Taitel 1986).

The oscillatory flow behavior can be reduced or eliminated by increasing the pipeline back-pressure, *i.e.*, reducing the opening of the choke vale (Schmidt et al. 1980), or by increasing the lift-gas injection rate (Golan et al. 1991). However, these solutions are not necessarily optimal from an economical point of view, and automatic feedback control has emerged as a viable alternative (Havre et al. 2002).

Dynamic multiphase flow models are required to develop, analyze and tune well flow controllers. These models are typically built based on physical assumptions and vary in complexity. Detailed models are implemented in commercial multiphase flow simulators such as OLGA (Schlumberger 2014). However, simplified low-order models are typically preferred for model based controllers (Eikrem et al. 2008; Jahanshahi et al. 2014). Moreover, when appropriately tuned, such models are sufficiently accurate for use in such controllers.

Feedback control solutions for wells assisted by gas-lift and pipeline-riser systems have been studied thoroughly during the last 30 years. Most of these works consider decoupled or independent wells and risers, for instance stabilization of slug flow in wells (Eikrem et al. 2008) or in pipelines/riser systems (Jahanshahi et al. 2014). Wells sharing the same riser may affect a common manifold pressure; hence, it is then required to analyze the dynamics of the sub-systems performing as a whole. Willersrud et al. (2013) addresses control and optimization of an oil gathering network with several wells, risers, a compressors and a separator with nonlinear model predictive control. However, the regulation capability in closed-loop was not studied. Nonlinear predictive control applied for regulatory control to such systems may be prohibitively computationally expensive. Therefore, in this work we assess the applicability of the simplified gas-lifted well and riser models described by Jahanshahi (2013) for dynamic optimization of a coupled system of wells feeding a riser. To this end, Nonlinear Model Predictive Control (NMPC) is applied to steer set-points of a regulatory layer implemented with PI controllers.

It is preferable to use a structured software platform for development and analysis of NMPC. Modelica is a convenient non-proprietary modeling language that assists to generate balanced-complexity models (Elgsæter et al. 2012). The models by Jahanshahi (2013) are translated to independent Modelica sub-models. The boundary conditions of these sub-models, which are given by pressures and flows, can be coupled to other

sub-models or set to a constant. Moreover, Modelica compilers, such as OpenModelica[1], are able to check the consistency of the sub-models, and their interconnections. Therefore, Modelica assists in a bottom-up model development. Modelica compilers generate a *functional mock-up unit* (FMU), which is a standard model component that can be shared with other applications. Subsequently, the resulting model may be imported to CasADi (Andersson 2013) via the integration to the JModelica.org compiler. Casadi implements efficient automatic differentiation techniques and is interfaced to other numerical packages. This enables fast development of NMPC solutions, without needing deep knowledge on the implementation of Nonlinear Programming solvers or Automatic Differentiation tools.

In this work, the control structure is divided into two layers. A regulatory layer is designed after controllability analysis of the unstable system. This consists of cascade controllers for wells and SISO controllers for the pipeline-riser system. Then, the second layer implements production optimization by providing set-points to the lower layer. To this end, the simplified sub-models are parametrized and adjusted to a detailed model in OLGA. An Extended Kalman Filter (EKF) is developed using the simplified models and tuned to track the detailed model. Then, the NMPC is implemented using state feedback. In order to assess the performance of the controller, the network system is steered from an initial predetermined fixed set-point to an optimal point by the NMPC.

The paper is organized as follows. In Section 6.2, the network system is described, and then the simplified models and the modeling fitting are presented in Section 6.3. The control structure and its building blocks are described in Section 6.4. The numerical results are presented in Section 6.5, and finally, the main conclusions and remarks are summarized in Section 6.6.

6.2 System Description

The oil gathering system to be studied is modelled in the OLGA simulator and is represented in Figure 6.1. The network consists of two wells operated by gas-lift which feed a common pipeline-riser to a separator. The network contains 7 control inputs:

- Gas injection controlled by mass flow rate at the annulus top of each well.
- Production choke valve opening of each well.
- Top-side valve opening.
- Two valves downstream to the separator.

The wells are considered to be geometrically identical. These are vertical with tubing and annulus length of 2048 m. The tubing diameters are equal to 0.124 m., the annuli are represented by a cylindrical not-annular pipeline of 0.2 m. diameter, and the roughness coefficients are equal to 4.5E-5 m. The reservoir temperature is equal to 108 °C

[1] www.openmodelica.org

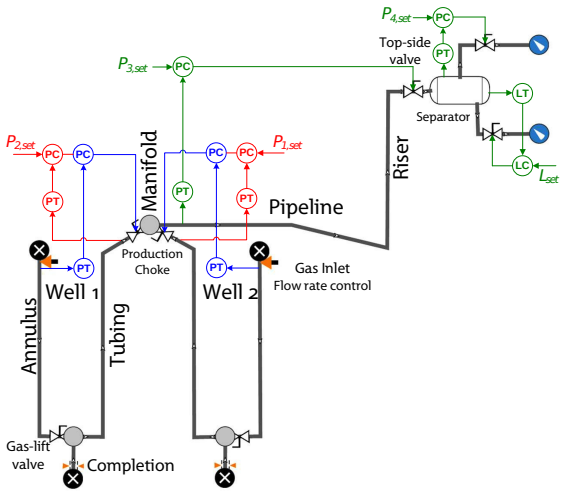

Figure 6.1: OLGA-model: Oil gathering system with low level control structure.

while the well inflow relation is considered linear with a coefficients of 2.47E-6 kg/s/Pa. The produced gas-oil-ratio (GOR) and water fraction (WCUT) are considered negligible. However, the reservoir pressures are different, being 160 bar for well 1 and 170 bar for well 2.

The pipeline length is 4300 m, where the last 2300 m has a negative inclination of 1° to mimic an undulated seabed. The riser has a height of 300 m. The pipeline and riser have a diameter of 0.2 m and a roughness of 2.8E-5 m. The separator is controlled to operate at a constant pressure of 5 bar.

In the OLGA simulator, the fluid properties can be specified by a black-oil model or can be supplied as PVT Tables. We use the PVT option in this work. The PVT tables are generated by PVTSim©. These tables store the fluid properties such as gas density (ROG), oil density (API), and gas mass fraction (RS) as functions of the pressure and temperature. The viscosity of the fluid model ranges from 0.2 to 1 cP, which is not sufficient to classify the fluid as heavy oil. The produced fluid is saturated and does not have free gas in a wide range of pressures. Due to this fluid conditions and the low reservoir pressure, the wells considered in this work are not *naturally flowing*. Therefore, gas-lift is required to assist the production.

6.3 Simplified Models and Fitting

The OLGA model described in Section 6.2 acts as the real system and is treated as a black-box model. However, we assume that some commonly available parameters of the system are given, such as the geometry and fluid properties at a given pressure and temperature.

Simplified models are built using representative parameters and first principles. We choose the models developed by Jahanshahi (2013) since these were successfully fit to the OLGA model. However, parameters of the simplified model had to be modified due to changes in the boundary conditions and the fluid model. Hence, in this section we present and discuss the simplified model parametrization and suitability to control the OLGA model.

6.3.1 Generalized sub-model

We treat the gas-lift well and pipeline-riser as independent building components of the gathering network system. From a general perspective, any of these subsystems can be represented by the following ODE structure:

$$\dot{x}_s = f_s\left(x_s, u_s\right) \tag{6.1a}$$

$$y_s = h_s\left(x_s, u_s\right) \tag{6.1b}$$

where the subscript s refers to any subsystem in $\mathcal{S} = \{w_1, w_2, r_1\}$ which contains a reference to the wells and pipeline-riser. The separator is assumed to be operating at a constant pressure, which is the usual and reasonable assumption. The differential states x_s represent the mass of the phases liquid and gas contained in the subsystem s which evolve according to f_s. The function h_s defines the variables y_s which gather the input pressures and output mass flow rate variables for each phase.

The physical assumptions on each sub-model are similar. The liquid phase is considered incompressible and the gas phase is modeled assuming the ideal gas law, with constant temperature and gas molecular weight.

6.3.2 Gas-lift well sub-model

The annulus is modeled as a vertical cylindrical tank filled with gas at a constant temperature. The state of the annulus is fully defined by the contained mass of gas,

$$\left(\dot{m}_{\mathrm{G}}\right)_a = \left(w_{\mathrm{G},in}\right)_a - \left(w_{\mathrm{G}}\right)_{inj}, \tag{6.2}$$

where $\left(w_{\mathrm{G},in}\right)_a$ is the inlet gas flow rate to the annulus which is used as a control input and $\left(w_{\mathrm{G}}\right)_{inj}$ is the injection rate from the annulus to the bottom of the tubing. The pressure at the annulus top, where the measurement is taken, is calculated based on the ideal gas law while the pressure at the injection point is considered to be the pressure at the top plus the pressure due to gas gravity.

The well tubing is modeled by two states, the mass of the gas and liquid in the well,

$$\left(\dot{m}_{\mathrm{G}}\right)_w = \left(\frac{\eta}{\eta + 1}\right) w_{res} + \left(w_{\mathrm{G}}\right)_{inj} - \left(w_{\mathrm{G}}\right)_{wh} \tag{6.3a}$$

$$(\dot{m}_{\mathrm{L}})_w = \left(\frac{1}{\eta+1}\right) w_{res} - (w_{\mathrm{L}})_{wh}\,, \tag{6.3b}$$

where η is the average mass ratio of gas and liquid produced from the reservoir which is assumed to be a known constant parameter of the well. $(w_{\mathrm{G}})_{wh}$ and $(w_{\mathrm{L}})_{wh}$ are the mass flow rates of gas and liquid at the well-head. The production mass rate w_{res} [kg/s] from the reservoir to the well is assumed to be described by a linear Inflow Performance Relationship (IPR). Similar to the annulus the pressure at the top of the well is calculated assuming the ideal gas law. Then, the gravity of the two-phase mixture and the friction in the tuning are taken into account to get the bottom-hole pressure. See (Jahanshahi 2013) for the complete formulation.

6.3.3 Pipeline-riser sub-model

The pipeline-riser is modeled by four states which are the masses of the gas and liquid phases inside the pipeline and the riser sections. The four state equations of this sub-model are:

$$(\dot{m}_{\mathrm{G}})_p = (w_{\mathrm{G},in})_p - (w_{\mathrm{G}})_{rb} \tag{6.4a}$$

$$(\dot{m}_{\mathrm{L}})_p = (w_{\mathrm{L},in})_p - (w_{\mathrm{L}})_{rb} \tag{6.4b}$$

$$(\dot{m}_{\mathrm{G}})_r = (w_{\mathrm{G}})_{rb} - (w_{\mathrm{G},out})_r \tag{6.4c}$$

$$(\dot{m}_{\mathrm{L}})_r = (w_{\mathrm{L}})_{rb} - (w_{\mathrm{L},out})_r \tag{6.4d}$$

Here, the subscripts 'in', 'rb' and 'out' stand for 'inlet', 'riser base' and 'outlet' respectively. The mass flow rates at the riser base are calculated by valve equations, and there are four tuning parameters in the pipeline-riser model which are used to fit the model to a real system or a detailed OLGA model. The model equations and the model-fitting procedure are given by Jahanshahi et al. (2014).

6.3.4 Coupling sub-models

Submodel equations represented by eq. (6.1) are coupled with mass and pressure balances. Moreover, every sub-model has at the output boundary a valve equation:

$$|w^{\mathrm{o}}|_1 = k\sqrt{\rho^{\mathrm{o}} \max\left(p^{\mathrm{o}} - p^{\mathrm{i}}\right)} \tag{6.5}$$

where $w^{\mathrm{o}} = (w^{\mathrm{o}}_{\mathrm{G}}, w^{\mathrm{o}}_{\mathrm{L}})$ are the mass flow of gas phase and liquid phase, respectively, and ρ^{o} is the estimated mixture density at the output. The pressures upstream and downstream the valves are p^{o} and p^{i}, respectively. The parameter k should be tuned following a procedure described in (Jahanshahi 2013; Jahanshahi et al. 2014).

6.3.5 Model fitting

The simplified models include tuning parameters which are fit to the process. The tuning parameters must be chosen to match both the steady-state and dynamic behavior of the system. A good matching of the steady-state behavior of pressures and flow rates are necessary to find correct optimal settings. Moreover, the dynamic behavior (*e.g.*, stability regions) is required to design the regulatory layer. We followed the model fitting procedure described by Jahanshahi et al. (2014).

6.4 Closed-loop control

This work is focused on the control and automation layer of a multi-level offshore control hierarchy (Foss 2012) and on the production optimization layer. Our suggested control structure is represented in Figure 6.2.

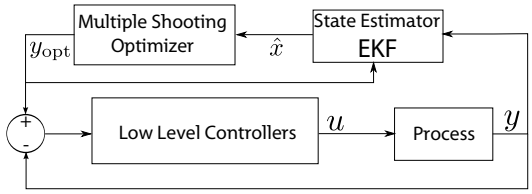

Figure 6.2: Control structure

The controller can be separated in three main building components:

- Low level controller: The wells are controlled by cascade controllers which inner-loop measures the pressure at the top of the annulus and the outer-loop the pressure at the wellhead. The pressure at the inlet of the pipeline is controlled by a PI control loop which manipulates the valve at the top of the riser. Finally, for the separator, the liquid level is measured and controlled by a PI controller manipulating a liquid output valve; in the same way, the pressure is measured and controlled by a PI controller manipulating a gas output valve. The pressure and level set-points are 5 bar and 20% of the separator height, respectively.
- State-estimator: The process measurements y are used to correct estimated dynamical states $\hat{x}$ of the system. This operation is performed on-line with an Extended Kalman Filter (EKF). The EKF uses the simplified models of the wells and risers coupled to the low level controllers. Thus, the states being estimated correspond to the states of the simplified models and the state of the controllers
- Multiple Shooting (MS) optimizer: The MS optimizer takes as input the estimated states $\hat{x}$ of the EKF and computes an optimal trajectory y_{opt} for the pressure set points and an input flow rate for gas. The objective function considers the oil

being produced and the gas being injected over a certain period, and penalizes the control effort being applied.

6.4.1 Low level control

Optimal gas-lift operating points under high lift-gas injection price are located in an unstable region where the casing-heading instability occurs. Therefore, low level controllers are required for stabilization. The gas-lift well has two degrees of freedom for control, the gas injection rate and the production choke valve. In this work we use the production choke for stabilization, see *e.g.*, (Jahanshahi 2013).

Downhole pressure measurements can be used for stabilizing flow. A simpler alternative are instruments placed on the wellhead and topside. In this work we combine wellhead pressure measurements in a cascade structure. In an earlier controllability analysis (Jahanshahi 2013), it has been shown that the pressure measurement at the top of the tubing is not a suitable controlled variable in a SISO structure. The reason is the RHP (Right Half-Plane) zero dynamics associated with the pressure at the top of the tubing. With a SISO controller, this measurement reacts with an inverse response to input changes (Skogestad et al. 2005), that imposes unavoidable large peaks in the sensitivity transfer functions. However, when the tubing pressure is combined with other measurements, such as the annulus pressure, it is possible to design a controller with a low peak in its sensitivity transfer function (Jahanshahi 2013). In the cascade control structure used in this work, the annulus pressure measurement is controlled by the valve and its set-point comes from the master control loop controlling the tubing pressure at a given set-point.

6.4.2 State estimation

The EKF is implemented in discrete time as in (Simon 2006, p. 409). The model used within the filter consists of coupling the sub-models described in Section 6.3 and models for the low level controllers in Section 6.4.1.

The low level controllers are implemented within the OLGA-model, and their state variables are not available. Therefore, similar low level controllers are coupled with the simplified models and their states are estimated in the EKF.

All models are written in continuous time and discretized using the CVODES (Hindmarsh et al. 2005) integrators and CasADi (Andersson 2013) for Automatic differentiation of the system equations. The EKF receives measurements every 10 sec., hence CVODES integrates the system and find the required sensitivities for this period of time.

The measurements used for state estimation are the wellhead pressures and the pipeline inlet pressure. Although more measurements are available, only measurements which are control variables in the regulatory layer are considered. The reason is that the regulatory layer forces these variables to track the same set-points in the model and in

the plant. Thus, these measurements are unbiased in steady-state and therefore suitable for the Kalman filter algorithm. Additional measurements which contain steady-state bias deteriorate the estimation. Here, the estimation relies on a good model rather than on aggressive corrections due to measurements.

6.4.3 Multiple Shooting optimizer

The MS optimizer solves the following problem:

$$\min_{\Theta} \sum_{k\in\mathcal{K}} \left(-q_{\text{o}}(\mathbf{x}_k,\mathbf{u}_k)+\alpha_{\text{g}}q_{\text{inj}}(\mathbf{x}_k,\mathbf{u}_k)\right)+ \tag{6.6a}$$

$$\sum_{k\in\mathcal{K}} \left(\mathbf{u}_{k-1}-\mathbf{u}_k\right)^{\top} R_{\text{u}} \left(\mathbf{u}_{k-1}-\mathbf{u}_k\right)+ \tag{6.6b}$$

$$\left(\mathbf{u}_K-\mathbf{u}_{\text{opt}}\right)^{\top} R_{\text{u}}^{\text{f}} \left(\mathbf{u}_K-\mathbf{u}_{\text{opt}}\right)+ \tag{6.6c}$$

$$\text{s.t.}: \quad \mathbf{x}_{k+1}=F\left(\mathbf{x}_k,\mathbf{u}_k\right), \quad k\in\mathcal{K}, \tag{6.6d}$$

$$\mathbf{y}_k=Y\left(\mathbf{x}_{k+1},\mathbf{u}_k\right), \quad k\in\mathcal{K} \tag{6.6e}$$

$$\mathbf{b}_l^{\text{x}}\le\mathbf{x}\le\mathbf{b}_u^{\text{x}} \tag{6.6f}$$

$$\mathbf{b}_l^{\text{y}}\le\mathbf{y}\le\mathbf{b}_u^{\text{y}} \tag{6.6g}$$

$$\mathbf{b}_l^{\text{u}}\le\mathbf{u}\le\mathbf{b}_u^{\text{u}}, \tag{6.6h}$$

where the set of variables to be optimized Θ is composed of the state variables at the end of the shooting periods $(\mathbf{x}_2,\ldots,\mathbf{x}_{K+1})$ and the control variables $\mathbf{u}_k, k\in\mathcal{K}$. Hence, the problem is divided in K shooting periods ($\mathcal{K}=\{1,\ldots,K\}$), which are coupled by the MS state constraints (6.6d). The function F represents a simulation of the simplified models over a discretization period, which is chosen equal to 1 hour. The states $\mathbf{x}_{k+1}, k\in\mathcal{K}$ contains the state of the simplified models at the end of the corresponding shooting period. The initial state $\mathbf{x}_1$ is not a decision variable and it is estimated by the EKF. The objective function aims to maximize an economical value, given by the oil production and the gas injection at a given price α_{g}. Moreover, a penalty term that penalizes control changes is included in (6.6b) which can be tuned with the positive semi-definite matrix R_{u}. To this end, $\mathbf{u}_0$ is equal to the current set-points being applied to the process. Finally, the objective implements a final stage cost (6.6c), which penalizes the mismatch between the final inputs $\mathbf{u}_K$ and the steady-state optimal input $\mathbf{u}_{\text{opt}}$. With this aim, optimal input $\mathbf{u}_{\text{opt}}$ is computed off-line and the positive semi-definite matrices R_{u}^{f} is tuned. Output constraints are implemented as bounds on the states (6.6f) and with bounds on the output variables $\mathbf{y}$ in the equations (6.6e) and (6.6g). Finally, input bounds are set in (6.6h).

Output constraints are required to keep the optimizer inside the physical limits of the system and away of unstable regions. Therefore, many constraints are implemented to provide robustness to the optimization method. These include bounds on wellhead

pressures, flow rates and mass fractions within the pipelines. The requirement of a large-set of output constraints makes the MS formulation the preferable choice as opposed to the most compact Single Shooting formulation. The cost of an iteration of the MS formulation is dictated by the number of state variables, which is low in this example. However, the cost of an iteration of the Single Shooting formulation depends on the number of output constraints being considered.

Problem (6.6) is solved with IPOPT (Wächter et al. 2005). Observe that fulfilling tight tolerances of the optimality conditions for problem (6.6) can be computationally very expensive. Therefore the solver was limit to make 60 major iterations or to process during 30 minutes.

6.5 Controller Performance

We apply the controller suggested in section 6.4 to control the OLGA model. We start the NMPC after 1 hour when the regulatory layer has settled and the Kalman filter has converged. The prediction horizon is set to forecast 16 hours and the discretization period of each shooting interval is 1 hour. We optimize 16 shooting intervals ($K = 16$), each containing 20 variables, corresponding to 5 controls and 15 states. However, the MS algorithm returns only the optimal control inputs for the next 1 hour. The optimal inputs consist of the gas injection rates of the two wells and the optimal set-points for the regulatory controllers.

The performance of the pressure controller for well #1 is shown in Fig. 6.3. The performance of the controller related to well #2 is similar. These are cascade controllers where the set-points for the master loops (tubing pressure) are given by the optimization layer and the slave loops manipulate the production choke valve openings. The production valves are opening gradually to increase the oil production rates. Nevertheless, they respect the constraints imposed for the controllability purpose. Since the wellhead pressures are used for the state estimation and they follow the optimal set-points, the measurements and estimates are very close. However, the modeling mismatch causes estimation errors for the annulus pressures and the openings of the valves.

Fig. 6.4 and Fig. 6.5 show the gas injection rates and oil production rates for the two wells. The optimal gas injection rates are calculated by the NMPC. As shown in the figures, the optimizer injects more gas to the wells to reach the optimal operation point which is dependent on the oil and gas prices. The estimation error is caused by process/model mismatch. Here, the normalized price of oil is 1 and the normalized price of gas equals 2.5, for each kg/s.

Fig. 6.6 shows the control of the pressure at the pipeline inlet. This controller manipulates the top-side valve and the optimal set-points are given by the NMPC. The estimation error of the inlet pressure is negligible because its measurement is used for state estimation and it is directly controlled by the regulatory layer. Nevertheless, the valve

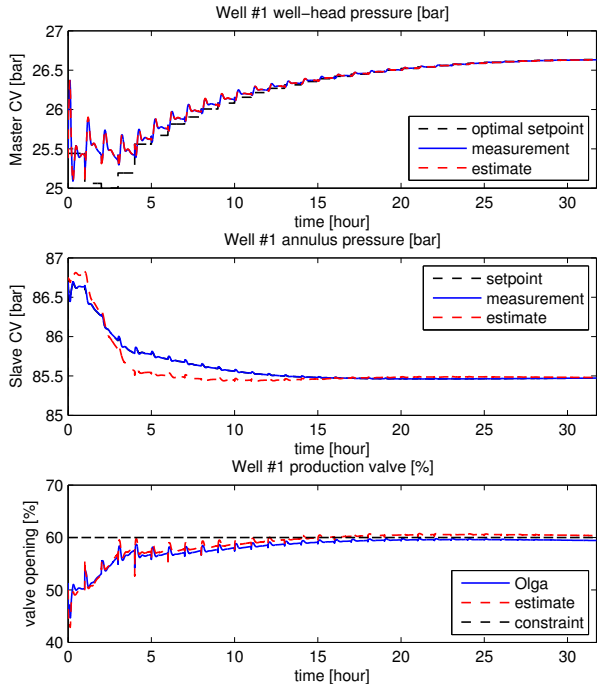

Figure 6.3: Well-head pressure of well #1

opening estimation suffers due to modeling error. Moreover, we observe a constraint violation in the transient response because the optimization algorithm was halted (CPU-time limit) before and optimal solution is reached. However, this constraint is satisfied in steady-state. The proposed low level control structure and the EKF computational times are negligible compared to the sampling time of the plant. Hence, these are suitable for on-line applications. However, the NMPC solution is not solved to the default tolerances in IPOPT and it is halted after 30 minutes of execution, therefore a sub-optimal solution is used. Moreover, in order to keep the controller performance assessment independent of this computational time, the process simulator is paused during this computation. Nevertheless, observe that IPOPT is a general purpose solver and does not exploit structure of the MS formulation. Therefore, appropriate solvers may solve this problem in a feasible time for a closed-loop application (Diehl et al. 2009).

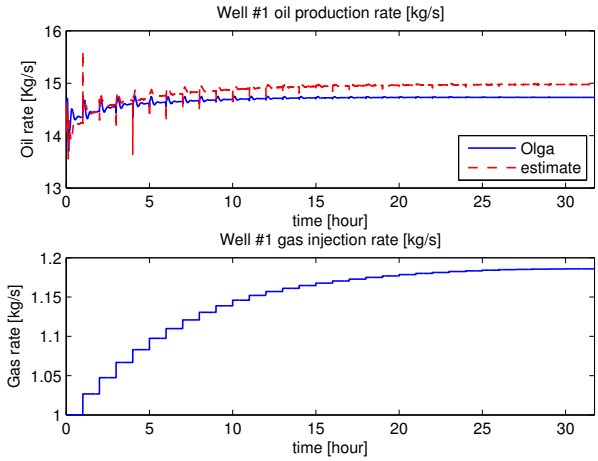

Figure 6.4: Oil production rate of well #1

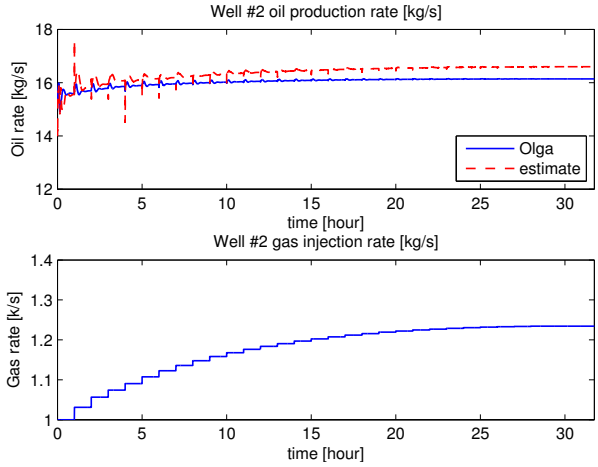

Figure 6.5: Oil production rate of well #2

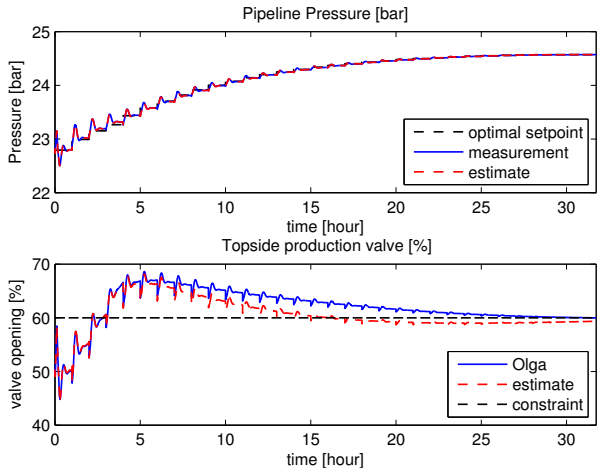

Figure 6.6: Pressure at pipeline inlet

6.6 Conclusion

To our knowledge, this paper is the first publication considering regulatory control of a multiple well system and riser steered by an NMPC optimization layer. The structure work well by jointly calculating dynamic set-point trajectories and ensuring stable flow conditions on a realistic simulator. Thus, it is a promising approach.

However, the optimization algorithm for NMPC is not fast enough to be used in closed-loop, therefore, further research developments should be carried out to exploit the structure of the Multiple Shooting formulation with specialized Nonlinear Programming solvers.

Chapter 7

Concluding Remarks

This chapter concludes the thesis and defines relevant topics for future work. Since there is a specific conclusion included at the end of each chapter, the intention here is to provide a global perspective on the work and to recap the most important findings.

7.1 Conclusion

This thesis covers different optimization methods for oil production. The common aim is to maximize the economic return of the oil field operation. Moreover, all the presented methods rely on mathematical models describing the production process and optimization methods to find optimal operation policies. However, the considered models rely on principles that make them suitable for different time-scales. In addition, the characteristics of the models motivate the use of different optimization tools. Therefore, the integration of these tools to meet the common objective is a formidable challenge.

The considered time-scales are the long-term, the middle-term, and the short-term, which capture the main characteristics of the reservoir control optimization problem, the daily-production optimization problem, and the low-level regulatory control problem, respectively. The models used in the long-term problem represent the fluids flowing through the reservoir. These models are important to design schedules for recovery strategies such as waterflooding. However, the long-term models disregard a detailed gathering network. A detailed gathering network is taken into account in the daily-production optimization problem. The main objective of the daily-production optimization problem is to find the optimal allocation of the production facilities. In this middle-term, the reservoir inflow performance is considered constant and all the gathering network facilities at steady-state. Therefore, the middle-term models are not appropriated for long-term production forecasting. Finally, the low-level control problem considers the dynamics of the production facilities. The low-level controller aims to maintain the stability of the process while it is steered and maintained at the optimal operational

point dictated by the upper layers.

The goals of the long-term and the middle-term optimization layers are conflicting. On the one hand, the middle-term optimization approach is greedy and seeks to optimize the present cash-flow regardless of the future consequences. On the other hand, the long-term optimization approach aims at the field Net Present Value (NPV) at the expense of the present cash-flow. Therefore, Van Essen et al. (2011), Chen et al. (2012) and Hasan et al. (2013) suggest alternative methods to prioritize the daily cash-flow objective in the long-term optimization problem. However, the previous methods disregard the gathering network, hence, the feasibility of the strategy is not ensured. Rahmawati et al. (2012) suggest a solution for the coupled model, however the optimization algorithms are not able to deliver solutions in real-time. Thus, an optimization algorithm that is capable to handle coupled problems efficiently is necessary. The Multiple Shooting (MS) formulation together with tailored optimization solvers is a candidates to tackle this problem.

The application of the MS to the long-term optimization problem is motivated by computationally costly simulators and output constraints:

- MS uses computational parallelization to expedite the execution of simulators. MS divides the prediction horizon in time frames which can be evaluated in parallel. Moreover, the output constraints can be evaluated in parallel to the reservoir simulator. In addition, Albersmeyer et al. (2010) show that even without parallelization MS can have faster local convergence than Single Shooting (SS).
- MS handles output constraints as bounds in the optimizer. The MS formulation defines additional variables associated to the output constraints. The feasibility of these variables with respect to the bounds is maintained during the execution of the optimizer. However, the equality constraints are relaxed and possibly violated during optimization. Therefore, the proposed algorithm computes a correction term using a single forward gradient propagation. The trade-off between feasibility and optimality is handled by a line-search algorithm.

This thesis provides case examples to illustrate the flexibility of MS to handle a large number of output constraints. This feature is a key to deal with coupled sub-surface and surface models efficiently. A publication describing the application of MS to the coupled model is in preparation.

The models for the process play a key role in optimization. Chapter 6 shows the application of MS for control and optimization of an oil gathering network. Like in most real applications, the plant model and the controller model are different, and therefore there is modeling error. Although, there are techniques to compensate for this type of errors, the presented method disregards such techniques. Hence, the model used for the Nonlinear Model Predictive Control (NMPC) is unable to predict correctly the output flow-rate of oil and gas in steady-state. Although this steady-state prediction is calculated with the simplified models used for NMPC, it can also be computed by a more accurate

daily-production optimization tool. Nevertheless, observe that the use of more advanced models for steady-state calculations will not eliminate the modeling errors completely. Thus, future work must address automatic model calibration with feedback.

The key to the efficiency of the MS formulation is the tailored Reduced Sequential Quadratic (rSQP) algorithm. The solution of the MS formulation with a general purpose sparse NLP solver such as IPOPT (Wächter et al. 2005) requires the construction of the Jacobian for the equality constraints coordinating the predictions. This Jacobian requires a prohibitive amount of memory and linear algebra operations to find a solution to the corresponding linear systems. Nevertheless, MS and IPOPT are used together to tackle the problem in Chapter 6 and the solver is not able to deliver solutions in real-time. A similar approach applied to the reservoir problem is impossible with contemporary desktop computers as shown in Chapter 2. However, the algorithms can be adapted for real-time applications by performing heavy computations off-line and light computations right after new measurements are available. These algorithms are discussed in the feedback control literature, see *e.g.*, (Biegler et al. 2015).

Chapter 2 includes an experimental comparison between SS and MS. This comparison is not conclusive because there are cases where either SS or MS have the best performance, see *e.g.*, (Albersmeyer et al. 2010) for simple examples. There are several indicators for comparison including iteration speed, final solution quality, local convergence, initialization flexibility, and execution robustness. These formulations are compared with respect to these indicators in the following items:

- The iteration speed depends on the implementation of the optimization algorithm. For MS using the rSQP method, the speed depends on how the computations related to the nullspace matrix are performed, see Chapter 1.4.2. For SS, the Augmented Lagrangian algorithm requires one forward and one adjoint simulation only, however, the dual variables and the quadratic penalty must be estimated too. Alternatively, it is discussed in Chapter 2 that SNOPT (Gill et al. 2005) is unable to tackle a large number of constraints due to memory limits. However, an active-set strategy to prevent the computation of all the adjoint simulations in SS should be investigated. Finally, it must be emphasized that the iteration speed can be improved for MS with the use of parallelization.

- The final solution quality in terms of the attained objective value is the same for both algorithms. Observe that any feasible solution for SS is also feasible for MS and vice versa. Moreover, neither of the considered algorithms provides an upper bound for the maximum possible objective value. Thus, if any of the algorithms converge, then only local optimality can be ensured with additional second-order derivative evaluations. Therefore, the comparison of optimal solutions computed by the SS and MS algorithms depend on the given initial solution guess and the path to convergence. Further, MS and SS deal with the constraints differently. MS respects all the inequality constraints at every step but allows violations of the

equality constraints, whereas SS has the opposite behavior. Thus, if the algorithms are aborted before convergence, SS will provide accurate state predictions which probably do not respect the output constraints, whereas MS will provide an approximation of the simulation which respects the output constraints.

- Albersmeyer et al. (2010) present a comparative study of the local convergence and conclude that no formulation is superior. However, the simplified study indicates that MS perform better if the simulator preserves curvature. Moreover, it is obvious that there is no difference in local convergence if the involved functions are linear.
- The MS formulation has more flexibility for initialization. MS receives a guess of the optimal state variables and control variables, whereas SS receives a guess of the control variables only. However, the numerical experiments dealing with MS are always initialized with the states from a simulation. Thus, this thesis does not investigate the potential benefits of this feature.
- MS is known to be numerically more robust than SS. Biegler (2010, Chapter 9.4) recommends MS for unstable dynamic systems and to deal with problems that suffer from ill-conditioning. Although it is not reported in Chapter 6, SS was explored but replaced by MS due to repeated simulation failures during optimization. Moreover, observe that the bounds on the states that are readily available in MS can be used to keep the simulation profile away from undefined regions.

The numerical robustness of MS motivates its application to reservoir problems dealing with more complex physics. However, it is not evident how to extend MS to black-oil problems including miscible fluids. The reason is that Chapter 2 suggests the oil pressure and the water saturation as grid-block state variables, but these variables together with the gas saturation are not sufficient for problems including miscible gas. Moreover, a change of simulation primary variables to tackle the bubble point problem (Chen et al. 2006, Chapter 8.2.2) hinders the application of MS. Thus, Chapter 3 develops a transformation of the state variables to tackle the aforementioned problems. The advantages of this transformation are:

- The transformation and its inverse are explicit functions, therefore they are efficient.
- It uses the minimal number of parameters to represent the fluid state.
- It only requires bounds on the primary variables to define the feasible state space.
- It does not require any modification to the reservoir simulator.

However, a disadvantage of this transformation is related to the state representation of grid-blocks with only water. For this particular case the new representation must use a convention. This issue may lead to discontinuities in the representation. Therefore, this formulation is not recommended for reservoirs that can contain grid-blocks full of water.

This thesis considers the extension of MS to robust reservoir control optimization under constraints on coherent risk measures. Typically, a robust control input maximizes the expected value of the field operation (Van Essen et al. 2009). Moreover, output constraints are enforced on all the plausible scenarios (Chen et al. 2012; Liu et al. 2015a). Since these solutions can lead to overly conservative control inputs, constraints on coherent risk measures are imposed instead. Chapter 4 tailors the rSQP algorithm for this problem:

- Parallelization can be applied for the simulation of different scenarios and different prediction time steps.
- The algorithm requires adjoint gradient computations of the active constraints only.
- The implementation of the functional AV@R instantiating the coherent risk measures does not need extra variables as in other algorithms (Rockafellar et al. 2000; Hanssen et al. 2015)

Finally, Chapter 4 demonstrates how output constraints can be applied to diminish the total water production on a waterflooding benchmark case.

Chapter 5 deals with the daily production optimization problem of a field example with diverse routing possibilities. It is a challenge to optimize the gathering network simulator together with the integer variables introduced by the routing degrees of freedom. In contrast to simulators, structured surrogate models are very efficient for optimization. The reason is that the structure of the surrogate models is tailored for state-of-the-art optimization algorithms. Chapter 5 proposes piecewise linear models to represent nonlinear pressures drops in pipelines. Although this concept has been previously explored, this work innovates by approximating these functions in the space of gas-oil-ratio, water cut, and liquid rate. Instead of the typical representation in standard flow rates of oil, water, and gas, this new representation allows for a direct coupling of the simulator output and prevents sampling on infeasible flow rates. The main criticism of the surrogate models is the introduction of new approximations compared to the process simulator. For that reason, this work proposes heuristic procedures to reduce the size of high resolution pressure drop models while keeping the maximum approximation error within a predefined tolerance. This tolerance is chosen tight enough so that the optimal solution found with the surrogate models has modeling errors within acceptable bounds.

Finally, this project produced open-source code to motivate the application of MS to reservoir control optimization problems. The implementation of the algorithms and the problem instances related to chapters 2-4 are available in (Codas 2014).

7.2 Future Work

This thesis considered optimization tools to tackle the integrated control problem efficiently. Future work should address the full integration of the control layers. To this end,

it is suggested two strategies to integrate the control layers two-by-two:

1. The low-level controllers steered by the coupled reservoir and gathering system optimization strategy.
2. The low-level controllers steered by a pure steady-state optimizer.

Observe that this thesis does not investigate how to calibrate the process models. Besides the requirement of models matching the actual process, the models used for optimization must match each other. In particular, the set-point given by the upper-layer controller must be a stable steady-state solution for the models used within the low-level controllers. Thus, it is required an additional calibration procedure to ensure this condition.

Note that this thesis does not investigate mixed-integer methods for the long-term reservoir control optimization problem. It is not known how to combine the efficient daily-production optimization methods based on surrogate models with the reservoir models. Thus, the first integration strategy considered above requires additional work to include binary variables efficiently. However, the second strategy can handle binary variables but the long-term objective is disregarded.

The Brugge case (Peters et al. 2010), the Norne case (Rwechungura et al. 2012), and the Egg model (Jansen et al. 2013) are benchmark problems that motivate the development of many solutions for the reservoir management problem. Unfortunately, these benchmark cases do not consider the gathering network facilities. Thus, it is recommended to extend these models so that the value of integrated control strategies can be illustrated. Such experiment has the potential to demonstrate the value of Integrated Operations (Stenhouse 2006; Ringstad et al. 2007; Campos et al. 2010), *i.e.*, the value aggregated by a multidisciplinary team operating a virtual field with the available technology.

7.2.1 Future work related to Chapter 2

Many aspects of the proposed rSQP algorithms can be further studied and improved. Chapter 2 shows the application of MS to reservoir control optimization with a simple NLP algorithm. Therefore, future work includes:

- Study of a better approximation of the reduced Hessian. To this end, evaluate the inclusion of the cross-term (Biegler et al. 1997) and alternative Quasi-Newton algorithms to deal with ill-conditioning.
- Study the advantage of alternative globalization strategies such as the filter methods or merit functions based on the Augmented Lagrangian.
- Evaluate the inclusion of trust-regions, see (Ternet et al. 1998).
- Investigate an alternative to the active-set method proposed for the solution of the Quadratic Programming problems.

- Tailor Interior Point and Augmented Lagrangian methods for MS.
- Derive theoretical results indicating whether MS or SS have better local convergence in the context of reservoir control optimization.

Chapter 2 deals with fairly simple output constraints. Thus, to demonstrate the power of MS, it is recommended to show applications on coupled surface and subsurface models.

7.2.2 Future work related to Chapter 3

MS may expedite the optimization of reservoir models with more complex physics. Therefore, it is recommended to extend the MS formulation to general compositional reservoir simulators, see (Kourounis et al. 2014).

Chapter 3 shows rather simple test cases, therefore, the convergence of the algorithm in larger field cases should be investigated.

The proposed state transformation has limitations if grid-blocks contain only water. Thus, it remains as future work to investigate how to deal with this case.

7.2.3 Future work related to Chapter 4

Chapter 4 deals only with one piece of the closed-loop reservoir management strategy. It is important to analyze how the data-assimilation algorithms can work efficiently together with the MS control optimizer. In particular, there are many calculations that can be performed off-line as proposed in the feedback control literature (Biegler et al. 2015).

The control parametrization for the robust control optimization problem are usually predefined. Thus, it is suggested to verify other control structures that are possibly less sensitive to disturbances or uncertainty. Therefore, the study of self-optimizing control (Skogestad 2004) is a good start for this direction.

The typical formulations for robust control optimization disregard the fact that future measurements will be available. This consideration leads to a multistage stochastic optimization problem, see (Shapiro et al. 2009b; Pflug et al. 2014). Therefore, it is recommended to develop optimization algorithms to tackle the scenario trees generated by such formulations.

7.2.4 Future work related to Chapter 5

The formulation developed in Chapter 5 did not consider flow splitting. However, flow splitting is actively used in the Urucu field by the production engineers. Silva et al. (2015) propose Mixed-Integer Linear models to deal with this problem.

The computational efficiency of the Mixed-Integer Linear Programming (MILP) solvers can be improved by reducing the resolution of the piecewise-linear models. Therefore, it

is recommended to develop algorithms to obtain optimal sampling grids for the pressure drop functions.

The formulation in Chapter 5 considered only Special-Ordered-Sets to enforce branching conditions. Since then, other models and algorithms were already investigated in (Silva et al. 2012; Silva et al. 2014).

Unfortunately, the application of this optimization algorithm to the Urucu field is not reported. Therefore, the actual impact of the strategy in the field is not known. However, Petrobras (Teixeira et al. 2013) has shown the economic gain of such strategies in practice.

7.2.5 Future work related to Chapter 6

The low-level control structure in Chapter 6 considers the riser inlet pressure and the pressure at the wellheads as controlled variables. However, output constraints are imposed on the valve opening to prevent oscillations. A future work considers alternative low-level control structures that eliminate the need of these output constraints.

The NMPC method in Chapter 6 has steady-state model/plant prediction mismatch. Thus, a future work must consider a correction of the model parameters through feedback.

Bibliography

Acs, G., Doleschall, S. and Farkas, E. (1985). 'General Purpose Compositional Model'. In: *Society of Petroleum Engineers Journal* 25.04, pp. 543–553. ISSN: 0197-7520. DOI: 10.2118/10515-PA.

Aguiar, M. A. (2013). 'Optimal oil production network control using Modelica'. Final project work. Federal University of Santa Catarina.

Aguiar, M. A., Codas, A. and Camponogara, E. (2015). 'Systemwide Optimal Control of Offshore Oil Production Networks with Time Dependent Constraints'. In: *2nd IFAC Workshop on Automatic Control in Offshore Oil and Gas Production*. Vol. 48. 6. Elsevier Ltd., pp. 200–207. DOI: 10.1016/j.ifacol.2015.08.032.

Aitokhuehi, I. and Durlofsky, L. J. (2005). 'Optimizing the performance of smart wells in complex reservoirs using continuously updated geological models'. In: *Journal of Petroleum Science and Engineering* 48.3-4, pp. 254–264. ISSN: 09204105. DOI: 10.1016/j.petrol.2005.06.004.

Alarcón, G. A., Torres, C. F. and Gomez, L. E. (2002). 'Global Optimization of Gas Allocation to a Group of Wells in Artificial Lift Using Nonlinear Constrained Programming'. In: *Journal of Energy Resources Technology* 124.4, pp. 262–268. DOI: 10.1115/1.1488172.

Albersmeyer, J. (2010). 'Adjoint-based algorithms and numerical methods for sensitivity generation and optimization of large scale dynamic systems'. PhD thesis. Heidelberg. URL: http://www.ub.uni-heidelberg.de/archiv/11651 (visited on 01/12/2015).

Albersmeyer, J. and Diehl, M. (2010). 'The Lifted Newton Method and Its Application in Optimization'. In: *SIAM Journal on Optimization* 20.3, pp. 1655–1684. ISSN: 1052-6234. DOI: 10.1137/080724885.

Alhuthali, A. H., Datta-Gupta, A., Yuen, B. and Fontanilla, J. P. (2010). 'Optimizing smart well controls under geologic uncertainty'. In: *Journal of Petroleum Science and Engineering* 73.1-2, pp. 107–121. ISSN: 09204105. DOI: 10.1016/j.petrol.2010.05.012.

Alhuthali, A., Oyerinde, A. and Datta-Gupta, A. (2007). 'Optimal Waterflood Management Using Rate Control'. In: *SPE Reservoir Evaluation & Engineering* 10.05, pp. 539–551. ISSN: 1094-6470. DOI: 10.2118/102478-PA.

Alveberg, L.-J. and Melberg, E. V., eds. (2013). *Facts 2013 - The Norwegian petroleum sector*. URL: http://www.npd.no/en/publications/facts/facts-2013/ (visited on 01/12/2015).

Amestoy, P. R., Duff, I. S., L'Excellent, J.-Y. and Koster, J. (2001). 'A Fully Asynchronous Multifrontal Solver Using Distributed Dynamic Scheduling'. In: *SIAM Journal on Matrix Analysis and Applications* 23.1, pp. 15–41. ISSN: 0895-4798. DOI: 10.1137/S0895479899358194.

Amestoy, P. R., Guermouche, A., L'Excellent, J.-Y. and Pralet, S. (2006). 'Hybrid scheduling for the parallel solution of linear systems'. In: *Parallel Computing* 32.2, pp. 136–156. ISSN: 01678191. DOI: 10.1016/j.parco.2005.07.004.

Andersson, J. (2013). 'A General-Purpose Software Framework for Dynamic Optimization'. PhD thesis. Department of Electrical Engineering (ESAT/SCD) and Optimization in Engineering Center, Kasteelpark Arenberg 10, 3001-Heverlee, Belgium: Arenberg Doctoral School, KU Leuven. ISBN: 978-94-6018-750-6. URL: https://lirias.kuleuven.be/handle/123456789/418048 (visited on 01/12/2015).

Artzner, P., Delbaen, F., Eber, J.-M. and Heath, D. (1999). 'Coherent Measures of Risk'. In: *Mathematical Finance* 9.3, pp. 203–228. DOI: 10.1111/1467-9965.00068.

Bailey, W. J. and Couet, B. (2005). 'Field Optimization Tool for Maximizing Asset Value'. In: *SPE Reservoir Evaluation & Engineering* 8.01, pp. 7–21. ISSN: 1094-6470. DOI: 10.2118/87026-PA.

Basova, H. G., Rockafellar, R. T. and Royset, J. O. (2011). 'A computational study of the buffered failure probability in reliability-based design optimization'. In: *Proceedings of the 11th International Conference on Application of Statistics and Probability in Civil Engineering*. Ed. by Faber, M., Koehler, J. and Nishijima, K. Zurich, Switzerland: Taylor & Francis. ISBN: 9780415669863. URL: http://www.math.washington.edu/~rtr/papers/rtr214-CompuStudyBufferedProb.pdf (visited on 01/12/2015).

Bertsekas, D. P. (1996). *Constrained Optimization and Lagrange Multiplier Methods*. 2nd ed. Belmont, Massachusetts: Athena Scientific, p. 395. ISBN: 1886529043.

— (1999). *Nonlinear Programming*. 2nd ed. Belmont, Massachusetts: Athena Scientific, p. 777. ISBN: 1886529000.

Biegler, L. T. (2010). *Nonlinear Programming: Concepts, Algorithms, and Applications to Chemical Processes*. Ed. by Liebling, T. MPS-Siam Series on Optimization. Society for Industrial and Applied Mathematics (SIAM, 3600 Market Street, Floor 6, Philadelphia, PA 19104), p. 415. ISBN: 9780898717020.

Biegler, L. T., Yang, X. and Fischer, G. A. G. (2015). 'Advances in sensitivity-based nonlinear model predictive control and dynamic real-time optimization'. In: *Journal of Process Control* 30, pp. 104–116. ISSN: 0959-1524. DOI: 10.1016/j.jprocont.2015.02.001.

Biegler, L. T., Nocedal, J. and Schmid, C. (1995). 'A Reduced Hessian Method for Large-Scale Constrained Optimization'. In: *SIAM Journal on Optimization* 5.2, pp. 314–347. ISSN: 1052-6234. DOI: 10.1137/0805017.

Biegler, L. T., Nocedal, J., Schmid, C. and Ternet, D. (2000). 'Numerical Experience with a Reduced Hessian Method for Large Scale Constrained Optimization'. In: *Computational Optimization and Applications* 15.1, pp. 45–67. DOI: 10.1023/A:1008723031056.

Biegler, L. T., Schmid, C. and Ternet, D. (1997). 'A Multiplier-Free, Reduced Hessian Method for Process Optimization'. In: *Large-Scale Optimization with Applications*. Ed. by Biegler, L. T., Coleman, T. F., Conn, A. R. and Santosa, F. N. Vol. 93. The IMA Volumes in Mathematics and its Applications. Springer New York, pp. 101–127. ISBN: 978-1-4612-7356-1. DOI: 10.1007/978-1-4612-1960-6_6.

Bieker, H. P., Slupphaug, O. and Johansen, T. A. (2006). 'Global Optimization of Multiphase Flow Networks in Oil and Gas Production Systems'. In: *American Institute of Chemical Engineers Annual Meeting*. URL: http://folk.ntnu.no/torarnj/AIChE-paper.pdf (visited on 01/12/2015).

Bieker, H. P., Slupphaug, O. and Johansen, T. A. (2007). 'Real-Time Production Optimization of Oil and Gas Production Systems: A Technology Survey'. In: *SPE Production & Operations* 22.04, pp. 382–391. ISSN: 1930-1855. DOI: 10.2118/99446-PA.

Bin, H. and Golan, M. (2003). 'Gas-lift Instability Resulted Production Loss and Its Remedy by Feedback Control: Dynamical Simulation Results'. In: *SPE International Improved Oil Recovery Conference in Asia Pacific*. Society of Petroleum Engineers. DOI: 10.2118/84917-MS.

Binder, T., Blank, L., Bock, H. G., Bulirsch, R., Dahmen, W., Diehl, M., Kronseder, T., Marquardt, W., Schlöder, J. P. and Stryk, O. (2001). 'Introduction to Model Based Optimization of Chemical Processes on Moving Horizons'. In: *Online Optimization of Large Scale Systems*. Ed. by Grötschel, M., Krumke, S. and Rambau, J. Springer Berlin Heidelberg. Chap. 3, pp. 295–339. ISBN: 978-3-642-07633-6. DOI: 10.1007/978-3-662-04331-8_18.

Bischof, C., Guertler, N., Kowarz, A. and Walther, A. (2008). 'Parallel Reverse Mode Automatic Differentiation for OpenMP Programs with ADOL-C'. In: *Advances in Automatic Differentiation*. Ed. by Bischof, C. H., Bücker, H. M., Hovland, P., Naumann, U. and Utke, J. Vol. 64. Lecture Notes in Computational Science and Engineering. Berlin,

Heidelberg: Springer Berlin Heidelberg, pp. 163–173. ISBN: 978-3-540-68935-5. DOI: 10.1007/978-3-540-68942-3_15.

Bock, H. G., Diehl, M., Kühl, P., Kostina, E., Schiöder, J. P. and Wirsching, L. (2007). 'Numerical methods for efficient and fast nonlinear model predictive control'. In: *Assessment and Future Directions of Nonlinear Model Predictive Control*. Ed. by Findeisen, R., Allgöwer, F. and Biegler, L. T. Springer, pp. 163–179. ISBN: 978-3-540-72699-9. DOI: 10.1007/978-3-540-72699-9_13.

Bock, H. and Plitt, K. (1984). 'A multiple shooting algorithm for direct solution of optimal control problems'. In: *9th IFAC World Congress*. Budapest, Hungary: Pergamon Press, pp. 242–247.

Brouwer, D. R. and Jansen, J. D. (2004). 'Dynamic Optimization of Waterflooding With Smart Wells Using Optimal Control Theory'. In: *SPE Journal* 9.04, pp. 391–402. ISSN: 1086-055X. DOI: 10.2118/78278-PA.

Buitrago, S., Rodriguez, E. and Espin, D. (1996). 'Global Optimization Techniques in Gas Allocation for Continuous Flow Gas Lift Systems'. In: *SPE Gas Technology Symposium*. Society of Petroleum Engineers. ISBN: 9781555634285. DOI: 10.2118/35616-MS.

Byrd, R. H. (1985). 'An example of irregular convergence in some constrained optimization methods that use the projected Hessian'. In: *Mathematical Programming* 32.2, pp. 232–237. ISSN: 0025-5610. DOI: 10.1007/BF01586093.

Byrd, R. H. and Nocedal, J. (1990). 'An analysis of reduced Hessian methods for constrained optimization'. In: *Mathematical Programming* 49.1-3, pp. 285–323. ISSN: 0025-5610. DOI: 10.1007/BF01588794.

Camponogara, E. and Nakashima, P. (2006). 'Optimizing gas-lift production of oil wells: piecewise linear formulation and computational analysis'. In: *IIE Transactions* 38.2, pp. 173–182. ISSN: 0740-817X. DOI: 10.1080/07408170500327345.

Camponogara, E., Plucenio, A., Teixeira, A. F. and Campos, S. R. V. (2009). 'An automation system for gas-lifted oil wells: Model identification, control, and optimization'. In: *Journal of Petroleum Science and Engineering* 70.3-4, pp. 157–167. ISSN: 09204105. DOI: 10.1016/j.petrol.2009.11.003.

Campos, S. R. V., Teixeira, A. F., Vieira, L. F. and Sunjerga, S. (2010). 'Urucu Field Integrated Production Model'. In: *SPE Intelligent Energy Conference and Exhibition*. 2010. Society of Petroleum Engineers, pp. 1–21. ISBN: 9781555632847. DOI: 10.2118/128742-MS.

Capolei, A., Foss, B. and Jørgensen, J. B. (2015a). 'Profit and Risk Measures in Oil Production Optimization'. In: *2nd IFAC Workshop on Automatic Control in Offshore Oil and Gas Production*. DOI: http://dx.doi.org/10.1016/j.ifacol.2015.08.034.

Capolei, A., Suwartadi, E., Foss, B. and Jørgensen, J. B. (2015b). 'A mean-variance objective for robust production optimization in uncertain geological scenarios'. In: *Journal of Petroleum Science and Engineering* 125, pp. 23–37. ISSN: 09204105. DOI: 10.1016/j.petrol.2014.11.015.

Cardoso, M. A. and Durlofsky, L. J. (2010). 'Use of Reduced-Order Modeling Procedures for Production Optimization'. In: *SPE Journal* 15.02, pp. 426–435. ISSN: 1086-055X. DOI: 10.2118/119057-PA.

Cardoso, M. A. (2009). 'Development and Application of Reduced-Order Modeling Procedures for Reservoir Simulation'. PhD thesis. Stanford, p. 134. URL: http://gradworks.umi.com/33/51/3351430.html (visited on 01/12/2015).

Chamberlain, R. M., Powell, M. J. D., Lemarechal, C. and Pedersen, H. C. (1982). 'The watchdog technique for forcing convergence in algorithms for constrained optimization'. In: *Algorithms for Constrained Minimization of Smooth Nonlinear Functions*. Ed. by Buckley, A. G. and Goffin, J. L. Vol. 16. Mathematical Programming Studies. Springer Berlin Heidelberg, pp. 1–17. ISBN: 978-3-642-00812-2. DOI: 10.1007/BFb0120945.

Chen, C., Li, G. and Reynolds, A. (2012). 'Robust Constrained Optimization of Short- and Long-Term Net Present Value for Closed-Loop Reservoir Management'. In: *SPE Journal* 17.03, pp. 849–864. ISSN: 1086-055X. DOI: 10.2118/141314-PA.

Chen, C., Wang, Y., Li, G. and Reynolds, A. C. (2010). 'Closed-loop reservoir management on the Brugge test case'. In: *Computational Geosciences* 14.4, pp. 691–703. ISSN: 1420-0597. DOI: 10.1007/s10596-010-9181-7.

Chen, Y., Oliver, D. S. and Zhang, D. (2009). 'Efficient Ensemble-Based Closed-Loop Production Optimization'. In: *SPE Journal* 14.04, pp. 634–645. ISSN: 1086-055X. DOI: 10.2118/112873-PA.

Chen, Z., Huan, G. and Ma, Y. (2006). *Computational Methods for Multiphase Flows in Porous Media*. Society for Industrial and Applied Mathematics. ISBN: 978-0-89871-606-1. DOI: 10.1137/1.9780898718942.

Codas, A. (2014). *Reservoir Multiple Shooting Optimization Code and Cases*. URL: https://github.com/iocenter/remso (visited on 01/12/2015).

Codas, A., Aguiar, M. A., Nalum, K. and Foss, B. (2013). 'Differentiation Tool Efficiency Comparison for Nonlinear Model Predictive Control Applied to Oil Gathering Systems'. In: *9th IFAC Symposium on Nonlinear Control Systems, 2013*. Ed. by Tarbouriech, S., pp. 821–826. DOI: 10.3182/20130904-3-FR-2041.00069.

Codas, A. and Camponogara, E. (2012a). 'Mixed-integer linear optimization for optimal lift-gas allocation with well-separator routing'. In: *European Journal of Operational Research* 217.1, pp. 222–231. ISSN: 03772217. DOI: 10.1016/j.ejor.2011.08.027.

Codas, A., Campos, S., Camponogara, E., Gunnerud, V. and Sunjerga, S. (2012b). 'Integrated Production Optimization of Oil Fields with Pressure and Routing Constraints: The Urucu Field'. In: *Computers & Chemical Engineering* 46, pp. 178–189. ISSN: 00981354. DOI: 10.1016/j.compchemeng.2012.06.016.

Codas, A., Foss, B. and Camponogara, E. (2015). 'Output-Constraint Handling and Parallelization for Oil-Reservoir Control Optimization by Means of Multiple Shooting'. In: *SPE Journal* 20.04, pp. 856–871. ISSN: 1086-055X. DOI: 10.2118/174094-pa.

Codas, A., Foss, B., Camponogara, E. and Krogstad, S. (2016a). 'Black-oil minimal fluid state parametrization for constrained reservoir control optimization'. In: *Journal of Petroleum Science and Engineering* 143, pp. 35–43. ISSN: 0920-4105. DOI: 10.1016/j.petrol.2016.01.034.

Codas, A., Hanssen, K. G., Foss, B., Capolei, A. and Jørgensen, J. B. (2016b). 'Multiple Shooting applied to robust reservoir control optimization including output constraints on coherent risk measures.' To be submitted.

Codas, A., Jahanshahi, E. and Foss, B. (2016c). 'A two-layer structure for stabilization and optimization of an oil gathering network'. In: *11th IFAC Symposium on Dynamics and Control of Process Systems, including Biosystems*.

Conejo, A. J., Castillo, E., Minguez, R. and Garcia-Bertrand, R. (2006). *Decomposition Techniques in Mathematical Programming*. 1st ed. Berlin/Heidelberg: Springer-Verlag. ISBN: 3-540-27685-8. DOI: 10.1007/3-540-27686-6.

da Silva, D. V. A. and Jansen, J. D. (2015). 'A Review of Coupled Dynamic Well-Reservoir Simulation'. In: *2nd IFAC Workshop on Automatic Control in Offshore Oil and Gas Production*. Vol. 48. 6. Elsevier Ltd., pp. 236–241. DOI: 10.1016/j.ifacol.2015.08.037.

Danesh, A. (1998). *PVT and phase behaviour of petroleum reservoir fluids*. Elsevier. ISBN: 978-0-444-82196-6.

Davidson, J. and Beckner, B. (2003). 'Integrated optimization for rate allocation in reservoir simulation'. In: *SPE Reservoir Evaluation & Engineering* 6.6, pp. 426–432. ISSN: 1094-6470. DOI: 10.2118/87309-PA.

de Montleau, P., Cominelli, A., Neylon, K., Rowan, D., Pallister, I., Tesaker, O. and Nygard, I. (2006). 'Production Optimization under Constraints Using Adjoint Gradients'. In: *10th European Conference on the Mathematics of Oil Recovery*. Amsterdam. DOI: 10.3997/2214-4609.201402506.

Diehl, M., Ferreau, H. J. and Haverbeke, N. (2009). 'Efficient Numerical Methods for Nonlinear MPC and Moving Horizon Estimation'. In: *Nonlinear Model Predictive Control*. Ed. by Magni, L., Raimondo, D. M. and Allgöwer, F. Springer, pp. 391–417. ISBN: 978-3-642-01093-4. DOI: 10.1007/978-3-642-01094-1_32.

Diehl, M., Walther, A., Bock, H. G. and Kostina, E. (2010). 'An adjoint-based SQP algorithm with quasi-Newton Jacobian updates for inequality constrained optimization'. In: *Optimization Methods and Software* 25.4, pp. 531–552. ISSN: 1055-6788. DOI: 10.1080/10556780903027500.

Dutta-Roy, K. and Kattapuram, J. (1997). 'A New Approach to Gas-Lift Allocation Optimization'. In: *Proceedings of SPE Western Regional Meeting*. Society of Petroleum Engineers. ISBN: 9781555634025. DOI: 10.2118/38333-MS.

Eikrem, G., Aamo, O. and Foss, B. (2008). 'On Instability in Gas Lift Wells and Schemes for Stabilization by Automatic Control'. In: *SPE Production & Operations* 23.2. ISSN: 1930-1855. DOI: 10.2118/101502-PA.

Elgæter, S. M., Slupphaug, O. and Johansen, T. A. (2010). 'A structured approach to optimizing offshore oil and gas production with uncertain models'. In: *Computers & Chemical Engineering* 34.2, pp. 163–176. ISSN: 0098-1354. DOI: 10.1016/j.compchemeng.2009.07.011.

Elgsæter, S. M., Kittilsen, P. and Hauger, S. O. (2012). 'Designing Large-Scale Balanced-Complexity Models for Online Use'. In: *2012 IFAC Workshop on Automatic Control in Offshore Oil and Gas Production*. Ed. by Imsland, L. 2010, pp. 157–162. DOI: 10.3182/20120531-2-NO-4020.00011.

Evensen, G. (1994). 'Sequential data assimilation with a nonlinear quasi-geostrophic model using Monte Carlo methods to forecast error statistics'. In: *Journal of Geophysical Research* 99, p. 10143. ISSN: 0148-0227. DOI: 10.1029/94JC00572.

Fang, W. Y. and Lo, K. K. (1996). 'A Generalized Well Management Scheme for Reservoir Simulation'. In: *SPE Reservoir Engineering* 11.02, pp. 116–120. ISSN: 0885-9248. DOI: 10.2118/29124-PA.

Fathi, Z. and Ramirez, F. (1984). 'Optimal Injection Policies for Enhanced Oil Recovery: Part 2-Surfactant Flooding'. In: *Society of Petroleum Engineers Journal* 24.3. ISSN: 07411146. DOI: 10.2118/12814-PA.

Fathi, Z. and Ramirez, W. F. (1986). 'Use of optimal control theory for computing optimal injection policies for enhanced oil recovery'. In: *Automatica* 22.1, pp. 33–42. ISSN: 00051098. DOI: 10.1016/0005-1098(86)90103-2.

Fetkovich, M. J. (1973). 'The Isochronal Testing of Oil Wells'. In: *Fall Meeting of the Society of Petroleum Engineers of AIME*. Society of Petroleum Engineers. ISBN: 978-1-55563-773-6. DOI: 10.2118/4529-MS.

Fevang, Ø., Singh, K. and Whitson, C. H. (2000). 'Guidelines for Choosing Compositional and Black-Oil Models for Volatile Oil and Gas-Condensate Reservoirs'. In: *SPE Annual Technical Conference and Exhibition*. Society of Petroleum Engineers, pp. 1–20. DOI: 10.2118/63087-MS.

Fonseca, R. M., Kahrobaei, S. S., Van Gastel, L. J. T., Leeuwenburgh, O. and Jansen, J. D. (2015). 'Quantification of the Impact of Ensemble Size on the Quality of an Ensemble Gradient Using Principles of Hypothesis Testing'. In: *SPE Reservoir Simulation Symposium*. DOI: 10.2118/173236-MS.

Fonseca, R. M., Stordal, A. S., Leeuwenburgh, O., Van Den Hof, P. M. J. and Jansen, J. D. (2014). 'Robust Ensemble-based Multi-objective Optimization'. In: *14h European Conference on Mathematics of Oil Recovery*. September 2014. Catania, Sicily, Italy, pp. 1–14. DOI: 10.3997/2214-4609.20141895.

Foss, B. (2012). 'Process control in conventional oil and gas fields — Challenges and opportunities'. In: *Control Engineering Practice* 20.10, pp. 1058–1064. ISSN: 09670661. DOI: 10.1016/j.conengprac.2011.11.009.

Foss, B., Grimstad, B. and Gunnerud, V. (2015). 'Production Optimization — Facilitated by Divide and Conquer Strategies'. In: *IFAC-PapersOnLine* 48.6, pp. 1–8. ISSN: 24058963. DOI: 10.1016/j.ifacol.2015.08.001.

Gill, P. E., Murray, W. and Saunders, M. A. (2005). 'SNOPT: An SQP Algorithm for Large-Scale Constrained Optimization'. In: *SIAM Review* 47.1, pp. 99–131. ISSN: 0036-1445. DOI: 10.1137/S0036144504446096.

Golan, M. and Whitson, C. H. (1991). *Well performance*. Prentice Hall. ISBN: 978-0-139-46609-0.

Griewank, A. and Walther, A. (2008). *Evaluating Derivatives*. Society for Industrial and Applied Mathematics. ISBN: 978-0-89871-659-7. DOI: 10.1137/1.9780898717761.

Grimstad, B., Foss, B., Heddle, R. and Woodman, M. (2016). 'Global optimization of multiphase flow networks using spline surrogate models'. In: *Computers & Chemical Engineering* 84, pp. 237–254. ISSN: 00981354. DOI: 10.1016/j.compchemeng.2015.08.022.

Gringarten, A. C. (2006). 'From straight lines to deconvolution: the evolution of the state-of-the art in well test analysis'. In: *SPE Annual Technical Conference and Exhibition*. Society of Petroleum Engineers. DOI: 10.2118/102079-MS.

Grothey, A. and McKinnon, K. (2000). *Decomposing the Optimization of a Gas Lifted Oil Well Network*. Tech. rep. Department of Mathematics and Statistics. University of Edinburgh. URL: www.maths.ed.ac.uk/mckinnon/MS/00-005/paper.pdf (visited on 01/12/2015).

Gunnerud, V. and Foss, B. (2010a). 'Oil production optimization – A piecewise linear model, solved with two decomposition strategies'. In: *Computers & Chemical Engineering* 34.11, pp. 1803–1812. ISSN: 00981354. DOI: 10.1016/j.compchemeng.2009.10.019.

Gunnerud, V., Foss, B. and Torgnes, E. (2010b). 'Parallel Dantzig – Wolfe decomposition for real-time optimization—Applied to a complex oil field'. In: *Journal of Process Control* 20.9, pp. 1019–1026. ISSN: 09591524. DOI: 10.1016/j.jprocont.2010.06.003.

Han, C., Wallis, J., Sarma, P., Li, G., Schrader, M. and Chen, W. H. (2012). 'Adaptation of the CPR Preconditioner for Efficient Solution of the Adjoint Equation'. In: *SPE Journal* 18.02, pp. 207–213. ISSN: 1086-055X. DOI: 10.2118/141300-PA.

Hanssen, K. G., Foss, B. and Teixeira, A. (2015). 'Production Optimization under Uncertainty with Constraint Handling'. In: *2nd IFAC Workshop on Automatic Control in Offshore Oil and Gas Production*. DOI: 10.1016/j.ifacol.2015.08.011.

Hasan, A., Gunnerud, V., Foss, B., Teixeira, A. F. and Krogstad, S. (2013). 'Decision Analysis for Long-term and Short-term Production Optimization Applied to the Voador Field'. In: *SPE Reservoir Characterization and Simulation Conference and Exhibition*. DOI: 10.2118/166027-ms.

Havre, K. and Dalsmo, M. (2002). 'Active Feedback Control as a Solution to Severe Slugging'. In: *SPE Production & Facilities* 17.03, pp. 138–148. ISSN: 1064-668X. DOI: 10.2118/79252-PA.

Heirung, T. A. N., Wartmann, M. R., Jansen, J. D., Ydstie, B. E. and Foss, B. A. (2011). 'Optimization of the Water-Flooding Process in a Small 2D Horizontal Oil Reservoir by Direct Transcription'. In: *Proceedings of the 18th IFAC World Congress*. 9. Milano, Italy, pp. 10863–10868. DOI: 10.3182/20110828-6-IT-1002.03503.

Hesse, H. K. (2008). 'Multiple Shooting and Mesh Adaptation for PDE Constrained Optimization Problems'. PhD thesis. University of Heidelberg. URL: http://www.ub.uni-heidelberg.de/archiv/8518 (visited on 01/12/2015).

Hindmarsh, A. C., Brown, P. N., Grant, K. E., Lee, S. L., Serban, R., Shumaker, D. E. and Woodward, C. S. (2005). 'SUNDIALS: Suite of Nonlinear and Differential/Algebraic Equation Solvers'. In: *ACM Transactions on Mathematical Software* 31.3, pp. 363–396. ISSN: 00983500. DOI: 10.1145/1089014.1089020.

Hou, J., Zhou, K., Zhang, X.-S., Kang, X.-D. and Xie, H. (2015). 'A review of closed-loop reservoir management'. In: *Petroleum Science* 12.1, pp. 114–128. ISSN: 1672-5107. DOI: 10.1007/s12182-014-0005-6.

IEA (2013). *Resources to Reserves 2013*. OECD Publishing. ISBN: 9789264083547. DOI: 10.1787/9789264090705-en.

— (2014). *Key World Energy Statistics 2014*. Key World Energy Statistics. OECD Publishing, p. 82. ISBN: 9789264223998. DOI: 10.1787/key_energ_stat-2014-en.

Jahanshahi, E. (2013). 'Control Solutions for Multiphase Flow Linear: Linear and nonlinear approaches to anti-slug control'. PhD thesis. Norwegian University of Science and

Technology. ISBN: 9788247146705. URL: http://hdl.handle.net/11250/248593 (visited on 01/12/2015).

Jahanshahi, E. and Skogestad, S. (2014). 'Simplified Dynamic Models for Control of Riser Slugging in Offshore Oil Production'. In: *Oil and Gas Facilities* 3.06, pp. 080–088. ISSN: 2224-4514. DOI: 10.2118/172998-PA.

Jahn, F., Cook, M. and Graham, M. (2008). *Hydrocarbon Exploration & Production*. 2nd ed. Developments in Petroleum Science. Elsevier Science. ISBN: 9780080568836.

Jansen, B., Høydalsvik, H., Nordtvedt, J.-E. and Moe, H. I. (2006). *Potential value of Integrated Operations on the Norwegian Shelf*. Tech. rep. April. Stavanger, p. 31.

Jansen, J. D. (2011). 'Adjoint-based optimization of multi-phase flow through porous media: A review'. In: *Computers & Fluids* 46.1, pp. 40–51. ISSN: 00457930. DOI: 10.1016/j.compfluid.2010.09.039.

— (2013). *A systems description of flow through porous media*. Springer. ISBN: 978-3-319-00260-6. DOI: 10.1007/978-3-319-00260-6.

Jansen, J. D., Bosgra, O. H. and Van den Hof, P. M. J. (2008). 'Model-based control of multiphase flow in subsurface oil reservoirs'. In: *Journal of Process Control* 18.9, pp. 846–855. ISSN: 09591524. DOI: 10.1016/j.jprocont.2008.06.011.

Jansen, J. D., Brouwer, D. R., Nævdal, G. and Van Kruijsdijk, C. P. J. W. (2005). 'Closed-loop reservoir management'. In: *First Break* 23.1, pp. 43–48. DOI: 10.3997/1365-2397.2005002.

Jansen, J. D., Brouwer, R. and Douma, S. (2009). 'Closed Loop Reservoir Management'. In: *Proceedings of SPE Reservoir Simulation Symposium*. The Woodlands, Texas, USA: Society of Petroleum Engineers. ISBN: 9781555632090. DOI: 10.2118/119098-MS.

Jansen, J. D., Fonseca, R. M., Kahrobaei, S., Siraj, M., Van Essen, G. and Van Den Hof, P. (2013). *The Egg Model*. Tech. rep. Research note and data set. The Netherlands: Delft University of Technology, pp. 1–8. URL: http://repository.tudelft.nl/view/ir/uuid:1b85ee17-3e58-4fa4-be79-8328945a4491 (visited on 01/12/2015). Data: http://data.3tu.nl/repository/uuid:916c86cd-3558-4672-829a-105c62985ab2.

Keha, A. B., de Farias, I. R. and Nemhauser, G. L. (2004). 'Models for representing piecewise linear cost functions'. In: *Operations Research Letters* 32.1, pp. 44–48. ISSN: 01676377. DOI: 10.1016/S0167-6377(03)00059-2.

Kenyon, D. and Alda Behie, G. (1987). 'Third SPE Comparative Solution Project: Gas Cycling of Retrograde Condensate Reservoirs'. In: *Journal of Petroleum Technology* 39.8, pp. 981–997. ISSN: 0149-2136. DOI: 10.2118/12278-PA.

Kirches, C., Bock, H. G., Schlöder, J. P. and Sager, S. (2011). 'A factorization with update procedures for a KKT matrix arising in direct optimal control'. In: *Mathematical Programming Computation* 3.4, pp. 319–348. ISSN: 1867-2949. DOI: 10.1007/s12532-011-0030-z.

Kosmidis, V. D., Perkins, J. D. and Pistikopoulos, E. N. (2004). 'Optimization of Well Oil Rate Allocations in Petroleum Fields'. In: *Industrial & Engineering Chemistry Research* 43.14, pp. 3513–3527. ISSN: 0888-5885. DOI: 10.1021/ie034171z.

Kosmidis, V. D., Perkins, J. D. and Pistikopoulos, E. N. (2005). 'A mixed integer optimization formulation for the well scheduling problem on petroleum fields'. In: *Computers & Chemical Engineering* 29.7, pp. 1523–1541. ISSN: 00981354. DOI: 10.1016/j.compchemeng.2004.12.003.

Kourounis, D., Durlofsky, L. J., Jansen, J. D. and Aziz, K. (2014). 'Adjoint formulation and constraint handling for gradient-based optimization of compositional reservoir flow'. In: *Computational Geosciences* 18.2, pp. 117–137. ISSN: 1420-0597. DOI: 10.1007/s10596-013-9385-8.

Kraaijevanger, J. F. B. M., Egberts, P. J. P., Valstar, J. R. and Buurman, H. W. (2007). 'Optimal Waterflood Design Using the Adjoint Method'. In: *SPE Reservoir Simulation Symposium*. Society of Petroleum Engineers. DOI: 10.2118/105764-MS.

Krogstad, J. A. (2015). 'Control-Switching Strategies for Reservoir Water-Flooding Management'. Master thesis. Norwegian University of Science and Technology. URL: http://hdl.handle.net/11250/2352548 (visited on 01/12/2015).

Krogstad, S., Nilsen, H. M. and Raynaud, X. (2014). 'Reservoir Management Optimization Using Calibrated Transmissibility Upscaling'. In: *14th European Conference on the Mathematics of Oil Recovery*. September 2014. Catania, Sicily, Italy, pp. 1–11. DOI: 10.3997/2214-4609.20141864.

Krogstad, S., Raynaud, X., Nilsen, H. M., Lie, K.-A., Møyner, O. and Skaflestad, B. (2015). 'MRST-AD, an Open-Source Framework for Rapid Prototyping and Evaluation of Reservoir Simulation Problems'. In: *SPE Reservoir Simulation Symposium*. DOI: 10.2118/173317-MS.

Kwok, W. H. F. (2007). 'Scalable linear and nonlinear algorithms for multiphase flow in porous media'. PhD thesis. Stanford. URL: https://icme.stanford.edu/sites/icme/icme-common/files/people/thesis-files/Kwok-2007.pdf (visited on 01/12/2015).

Leemhuis, A. P., Nennie, E., Belfroid, S., Alberts, G., Peters, L. and Joosten, G. J. P. (2008). 'Gas Coning Control for Smart Wells Using a Dynamic Coupled Well-Reservoir Simulator'. In: *Intelligent Energy Conference and Exhibition*. Society of Petroleum Engineers, pp. 1–10. DOI: 10.2118/112234-MS.

Leeuwenburgh, O., Egberts, P. J. P. and Alin G., C. (2015). 'An Ensemble-Based Method for Constrained Reservoir Life-Cycle Optimization'. In: *EUROPEC 2015*. Society of Petroleum Engineers. ISBN: 978-1-61399-405-4. DOI: 10.2118/174318-MS.

Leineweber, D. B. (1998). 'Efficient Reduced SQP Methods for the Optimization of Chemical Processes Described by Large Sparse DAE Models'. PhD thesis. University of Heidelberg. ISBN: 9783183613038. URL: http://www.iwr.uni-heidelberg.de/groups/agbock/USER_PAGES/LEINEWEBER_DANIEL/WWW/phddiss.pdf (visited on 01/12/2015).

Leineweber, D. B., Bauer, I., Bock, H. G. and Schlöder, J. P. (2003). 'An efficient multiple shooting based reduced SQP strategy for large-scale dynamic process optimization. Part 1: theoretical aspects'. In: *Computers & Chemical Engineering* 27.2, pp. 157–166. ISSN: 00981354. DOI: 10.1016/S0098-1354(02)00158-8.

Li, R., Reynolds, A. C. and Oliver, D. S. (2003). 'History Matching of Three-Phase Flow Production Data'. In: *SPE Journal* 8.4, pp. 328–340. ISSN: 1086-055X. DOI: 10.2118/87336-PA.

Lie, K.-A. (2014). *An Introduction to Reservoir Simulation Using MATLAB*. SINTEF ICT, Departement of Applied Mathematics. URL: http://www.sintef.no/projectweb/mrst/publications/ (visited on 01/12/2015).

Lie, K.-A., Krogstad, S., Ligaarden, I. S., Natvig, J. R., Nilsen, H. M. and Skaflestad, B. (2011). 'Open-source MATLAB implementation of consistent discretisations on complex grids'. In: *Computational Geosciences* 16.2, pp. 297–322. ISSN: 1420-0597. DOI: 10.1007/s10596-011-9244-4.

Litvak, M. L., Clark, A. J., Fairchild, J. W., Fossum, M. P., Macdonald, C. J. and Wood, A. R. O. (1997). 'Integration of Prudhoe Bay Surface Pipeline Network and Full Field Reservoir Models'. In: *Proceedings of SPE Annual Technical Conference and Exhibition*. Society of Petroleum Engineers. ISBN: 9781555633998. DOI: 10.2118/38885-MS.

Litvak, M. L. and Darlow, B. L. (1995). 'Surface Network and Well Tubinghead Pressure Constraints in Compositional Simulation'. In: *SPE Reservoir Simulation Symposium*. Society of Petroleum Engineers, pp. 325–337. ISBN: 9781555634582. DOI: 10.2118/29125-MS.

Litvak, M., Hutchins, L., Skinner, R., Darlow, B., Wood, R. and Kuest, L. (2002). 'Prudhoe Bay E-Field Production Optimization System Based on Integrated Reservoir and Facility Simulation'. In: *Proceedings of SPE Annual Technical Conference and Exhibition*. Society of Petroleum Engineers. ISBN: 9781555631536. DOI: 10.2118/77643-MS.

Liu, X. and Reynolds, A. C. (2015a). 'Multiobjective Optimization for Maximizing Expectation and Minimizing Uncertainty or Risk with Application to Optimal Well Control'.

In: *SPE Reservoir Simulation Symposium*. 2014. Society of Petroleum Engineers. DOI: 10.2118/173216-MS.

— (2015b). 'Pareto Optimal Solutions for Minimizing Risk and Maximizing Expected Value of Life-Cycle NPV of Production under Nonlinear Constraints'. In: *SPE Reservoir Simulation Symposium*. 2014. Society of Petroleum Engineers. DOI: 10.2118/173274-MS.

Lund, T. (2014). 'Non-linear model predictive control for an oil production network based on gas-lift'. Master thesis. Norwegian University of Science and Technology. URL: http://hdl.handle.net/11250/261237 (visited on 01/12/2015).

Mattax, C. C. and Dalton, R. L. (1990). *Reservoir Simulation*. SPE Monograph. Society of Petroleum Engineers, p. 187. ISBN: 978-1-55563-028-7.

Ministry of Petroleum and Energy Norway (2011). *An industry for the future — Norway's petroleum activities*. Tech. rep. Norges regjering. URL: https://www.regjeringen.no/en/dokumenter/meld.-st.-28-20102011/id649699/ (visited on 01/12/2015).

Misener, R. and Floudas, C. A. (2010). 'Piecewise-linear approximations of multidimensional functions'. In: *Journal of Optimization Theory and Applications* 145.1, pp. 120–147. ISSN: 00223239. DOI: 10.1007/s10957-009-9626-0.

Misener, R., Gounaris, C. E. and Floudas, C. A. (2009). 'Global Optimization of Gas Lifting Operations: A Comparative Study of Piecewise Linear Formulations'. In: *Industrial & Engineering Chemistry Research* 48.13, pp. 6098–6104. ISSN: 0888-5885. DOI: 10.1021/ie8012117.

Naevdal, G., Johnsen, L. M., Aanonsen, S. I. and Vefring, E. H. (2005). 'Reservoir Monitoring and Continuous Model Updating Using Ensemble Kalman Filter'. In: *SPE Journal* 10.01, pp. 66–74. ISSN: 1086-055X. DOI: 10.2118/84372-PA.

Nalum, K. (2013). 'Modeling and Dynamic Optimization in Oil Production'. Master thesis. Norwegian University of Science and Technology. URL: http://hdl.handle.net/11250/260881 (visited on 01/12/2015).

Nennie, E., Alberts, G., Belfroid, S., Peters, L. and Joosten, G. (2007). 'An Investigation Into the Need of a Dynamic Coupled Well-Reservoir Simulator'. In: *Proceedings of SPE Annual Technical Conference and Exhibition*. Society of Petroleum Engineers. ISBN: 9781604239263. DOI: 10.2523/110316-MS.

Nennie, E., Alberts, G., Peters, L. and van Donkelaar, E. (2008). 'Using a Dynamic Coupled Well-Reservoir Simulator to Optimize Production of a Horizontal Well in a Thin Oil Rim.' In: *Abu Dhabi International Petroleum Exhibition and Conference*. Society of Petroleum Engineers, pp. 1–8. DOI: 10.2118/118173-MS.

Nennie, E., Savanko, S., Alberts, G. J. N., Cargnelutti, M. F. and Van Donkelaar, E. (2009). 'Comparing the Benefits: Use of Various Wellhead Gas Coning Control Strate-

gies To Optimize Production of a Thin Oil Rim'. In: *SPE Annual Technical Conference and Exhibition*. Society of Petroleum Engineers. DOI: 10.2118/125050-MS.

Nocedal, J. and Overton, M. L. (1985). 'Projected Hessian Updating Algorithms for Nonlinearly Constrained Optimization'. In: *SIAM Journal on Numerical Analysis* 22.5, pp. 821–850. ISSN: 0036-1429. DOI: 10.1137/0722050.

Nocedal, J. and Wright, S. J. (2006). *Numerical Optimization*. 2nd ed. Springer Series in Operations Research and Financial Engineering. Springer New York, p. 664. ISBN: 978-0-387-30303-1. DOI: 10.1007/978-0-387-40065-5.

Norwegian Petroleum Directorate (2014). *Petroleum on the Norwegian Continental Shelf 2014 Fields and Discoveries*. Tech. rep., p. 42. URL: http://www.npd.no/en/Publications/Resource-Reports/2014/ (visited on 01/12/2015).

Odeh, A. (1981). 'Comparison of Solutions to a Three-Dimensional Black-Oil Reservoir Simulation Problem'. In: *Journal of Petroleum Technology* 33.1. ISSN: 0149-2136. DOI: 10.2118/9723-PA.

Oliver, D. S., Reynolds, A. C. and Liu, N. (2008). *Inverse theory for petroleum reservoir characterization and history matching*. Cambridge University Press, p. 394. ISBN: 9780521881517.

Ordonez, B., Codas, A. and Moreno, U. F. (2009). 'Improving the operational conditions for the sucker-rod pumping system'. In: *2009 IEEE International Conference on Control Applications*. IEEE, pp. 1259–1264. ISBN: 978-1-4244-4601-8. DOI: 10.1109/CCA.2009.5281122.

Osborne, M. R. (1969). 'On shooting methods for boundary value problems'. In: *Journal of Mathematical Analysis and Applications* 27.2, pp. 417–433. ISSN: 0022247X. DOI: 10.1016/0022-247X(69)90059-6.

Peaceman, D. W. (1983). 'Interpretation of Well-Block Pressures in Numerical Reservoir Simulation With Nonsquare Grid Blocks and Anisotropic Permeability'. In: *Society of Petroleum Engineers Journal* 23.3, pp. 531–543. ISSN: 0197-7520. DOI: 10.2118/10528-PA.

Peters, L., Arts, R., Brouwer, G., Geel, C., Cullick, S., Lorentzen, R. J., Chen, Y., Dunlop, N., Vossepoel, F. C., Xu, R., Sarma, P., Alhuthali, A. H. H. and Reynolds, A. (2010). 'Results of the Brugge Benchmark Study for Flooding Optimization and History Matching'. In: *SPE Reservoir Evaluation & Engineering* 13.03, pp. 391–405. ISSN: 1094-6470. DOI: 10.2118/119094-PA.

Pflug, G. C. and Pichler, A. (2014). 'Multistage Stochastic Optimization'. In: *Springer Series in Operations Research and Financial Engineering*. ISSN: 2197-1773. DOI: 10.1007/978-3-319-08843-3.

Powell, M. J. D. (1978). 'A fast algorithm for nonlinearly constrained optimization calculations'. In: *Numerical Analysis*. Ed. by Watson, G. A. Vol. 630. Lecture Notes in Mathematics. Springer Berlin Heidelberg, pp. 144–157. ISBN: 978-3-540-08538-6. DOI: 10.1007/BFb0067703.

Rahmawati, S. D. (2012). 'Integrated Field Modeling and Optimization'. PhD thesis. Norwegian University of Science and Technology. ISBN: 978-82-471-3309-5. URL: http://folk.ntnu.no/bjarnean/pubs/others/thesis-Rahmawati.pdf (visited on 01/12/2015).

Rahmawati, S. D., Whitson, C. H., Foss, B. and Kuntadi, A. (2012). 'Integrated field operation and optimization'. In: *Journal of Petroleum Science and Engineering* 81, pp. 161–170. ISSN: 09204105. DOI: 10.1016/j.petrol.2011.12.027.

Ramirez, W. F. (1987). *Application of optimal control theory to enhanced oil recovery*. Ed. by Chilingarian, G. V. Elsevier Science, p. 242. ISBN: 0444428356.

Ringstad, A. J. and Andersen, K. (2006). 'Integrated Operations and HSE - Major Issues and Strategies'. In: *SPE International Health, Safety & Environment Conference*. Society of Petroleum Engineers. DOI: 10.2118/98530-MS.

— (2007). 'Integrated operations and the need for a balanced development of people, technology and organisation'. In: *International Petroleum Technology Conference*. 7. International Petroleum Technology Conference. DOI: 10.2523/11668-MS.

Rockafellar, R. T. and Royset, J. O. (2010). 'On buffered failure probability in design and optimization of structures'. In: *Reliability Engineering & System Safety* 95.5, pp. 499–510. ISSN: 09518320. DOI: 10.1016/j.ress.2010.01.001.

Rockafellar, R. T. (2007). 'Coherent Approaches to Risk in Optimization Under Uncertainty'. In: *INFORMS Tutorials in Operations Research*, pp. 38–61. DOI: 10.1287/educ.1073.0032.

Rockafellar, R. T. and Uryasev, S. (2000). 'Optimization of conditional value-at-risk'. In: *Journal of risk* 2, pp. 21–42. URL: http://www.math.washington.edu/~rtr/papers/rtr179-CVaR1.pdf (visited on 01/12/2015).

Rockafellar, R. T., Uryasev, S. and Zabarankin, M. (2002). *Deviation Measures in Risk Analysis and Optimization*. Tech. rep. Gainesville: Department of Industrial and Systems Engineering, University of Florida, pp. 1–27.

Rwechungura, R., Bhark, E., Miljeteig, O., Suman, A., Kourounis, D., Foss, B., Hoier, L. and Kleppe, J. (2012). 'Results of the First Norne Field Case on History Matching and Recovery Optimization Using Production and 4D Seismic Data'. In: *SPE Annual Technical Conference and Exhibition*. San Antonio, Texas, USA. DOI: 10.2118/157112-MS.

Saputelli, L., Nikolaou, M. and Economides, M. J. (2006). 'Real-time reservoir management: A multiscale adaptive optimization and control approach'. In: *Computational Geosciences* 10.1, pp. 61–96. ISSN: 1420-0597. DOI: 10.1007/s10596-005-9011-5.

Sarma, P., Chen, W. H., Durlofsky, L. J. and Aziz, K. (2008). 'Production Optimization With Adjoint Models Under Nonlinear Control-State Path Inequality Constraints'. In: *SPE Reservoir Evaluation & Engineering* 11.02, pp. 326–339. ISSN: 1094-6470. DOI: 10.2118/99959-PA.

Schäfer, A., Kühl, P., Diehl, M., Schlöder, J. and Bock, H. G. (2007). 'Fast reduced multiple shooting methods for nonlinear model predictive control'. In: *Chemical Engineering and Processing: Process Intensification* 46.11, pp. 1200–1214. ISSN: 02552701. DOI: 10.1016/j.cep.2006.06.024.

Schlumberger (2009). *PIPESIM - Steady-State Multiphase Flow Simulator*.

— (2011). *ECLIPSE reservoir simulation software: Technical Description Manual*.

— (2014). *OLGA - Dynamic Multiphase Flow Simulator*.

Schmidt, Z., Brill, J. and Beggs, H. (1980). 'Experimental Study of Severe Slugging in a Two-Phase-Flow Pipeline - Riser Pipe System'. In: *Society of Petroleum Engineers Journal* 20.05, pp. 407–414. ISSN: 0197-7520. DOI: 10.2118/8306-PA.

Schulz, V. H. (1996). 'Reduced SQP Methods for Large-Scale Optimal Control Problems in DAE with Application to Path Planning Problems for Satellite Mounted Robots'. PhD thesis. University of Heidelberg. URL: http://citeseerx.ist.psu.edu/viewdoc/download?doi=10.1.1.50.4710&rep=rep1&type=pdf (visited on 01/12/2015).

— (1998). 'Solving discretized optimization problems by partially reduced SQP methods'. In: *Computing and Visualization in Science* 1.2, pp. 83–96. ISSN: 1432-9360. DOI: 10.1007/s007910050008.

Shapiro, A., Dentcheva, D. and Ruszczynski, A. (2009a). *Lectures on stochastic programming: modeling and theory*, p. 447. ISBN: 089871687X. DOI: http://dx.doi.org/10.1137/1.9780898718751.

Shapiro, A., Dentcheva, D. and Ruszczyński, A. (2009b). 'Lectures on Stochastic Programming'. In: DOI: 10.1137/1.9780898718751.

Shapiro, A. and Philpott, A. (2007). 'A tutorial on stochastic programming'. URL: www.isye.gatech.edu/people/faculty/Alex_Shapiro/TutorialSP.pdf (visited on 01/12/2015).

Silva, T. L. and Camponogara, E. (2014). 'A computational analysis of multidimensional piecewise-linear models with applications to oil production optimization'. In: *European Journal of Operational Research* 232.3, pp. 630–642. ISSN: 0377-2217. DOI: 10.1016/j.ejor.2013.07.040.

Silva, T. L., Camponogara, E., Teixeira, A. F. and Sunjerga, S. (2015). 'Modeling of flow splitting for production optimization in offshore gas-lifted oil fields: Simulation validation and applications'. In: *Journal of Petroleum Science and Engineering* 128, pp. 86–97. ISSN: 0920-4105. DOI: 10.1016/j.petrol.2015.02.018.

Silva, T. L., Codas, A. and Camponogara, E. (2012). 'A Computational Analysis of Convex Combination Models for Multidimensional Piecewise-Linear Approximation in Oil Production Optimization'. In: *2012 IFAC Workshop on Automatic Control in Offshore Oil and Gas Production*. Ed. by Imsland, L. DOI: 10.3182/20120531-2-no-4020.00006.

Simon, D. (2006). *Optimal State Estimation*, pp. 1–526. ISBN: 0471708585. DOI: 10.1002/0470045345.

Siraj, M., Van den Hof, P. and Jansen, J. D. (2015). 'Model and Economic Uncertainties in Balancing Short-Term and Long-Term Objectives in Water-Flooding Optimization'. In: *SPE Reservoir Simulation Symposium*. DOI: 10.2118/173285-MS.

Skjerve, A. B. and Rindahl, G. (2010). 'Promoting trust between members of distributed teams'. In: *2010 IEEE International Conference on Systems, Man and Cybernetics*, pp. 1650–1658. ISSN: 1062-922X. DOI: 10.1109/ICSMC.2010.5642403.

Skogestad, S. (2004). 'Near-optimal operation by self-optimizing control: from process control to marathon running and business systems'. In: *Computers & Chemical Engineering* 29.1, pp. 127–137. ISSN: 0098-1354. DOI: 10.1016/j.compchemeng.2004.07.011.

Skogestad, S. and Postlethwaite, I. (2005). *Multivariable feedback control: analysis and design*. Second. West Sussex, UK: Wiley-Interscience, p. 592. ISBN: 9780470011683.

Standing, M. B. (1952). *Volumetric and phase behavior of oil field hydrocarbon systems*. Reinhold.

Stenhouse, B. J. (2006). 'Towards Close-Loop Optimisation - The Valhall Optimiser Field Trial'. In: *Intelligent Energy Conference and Exhibition*. DOI: 10.2118/99828-ms.

Strasunskas, D., Tomasgard, A. and Nystad, A. N. (2012). 'A Framework to Assess Value of Intelligent Petroleum Fields and Integrated Operations'. In: *SPE Intelligent Energy International*. Society of Petroleum Engineers. ISBN: 9781613991916. DOI: 10.2118/150253-MS.

Suwartadi, E., Krogstad, S. and Foss, B. (2010). 'Second-order adjoint-based control for multiphase flow in subsurface oil reservoirs'. In: *49th IEEE Conference on Decision and Control (CDC)*. IEEE, pp. 1866–1871. ISBN: 978-1-4244-7745-6. DOI: 10.1109/CDC.2010.5716930.

Suwartadi, E., Krogstad, S. and Foss, B. (2011). 'Nonlinear output constraints handling for production optimization of oil reservoirs'. In: *Computational Geosciences* 16.2, pp. 499–517. ISSN: 1420-0597. DOI: 10.1007/s10596-011-9253-3.

Taitel, Y. (1986). 'Stability of severe slugging'. In: *International Journal of Multiphase Flow* 12.2, pp. 203–217. ISSN: 03019322. DOI: 10.1016/0301-9322(86)90026-1.

Teixeira, A. F., de Campos, M. C. M. M., Barreto, F. P., Rosa, V. R., Arraes, F. F. and Stender, A. S. (2013). 'Model Based Production Optimization Applied to Offshore Fields'. In: *OTC Brasil*. October. Offshore Technology Conference, pp. 29–31. ISBN: 9781613992876. DOI: 10.4043/24301-MS.

Ternet, D. J. and Biegler, L. T. (1998). 'Recent improvements to a multiplier-free reduced Hessian successive quadratic programming algorithm'. In: *Computers & Chemical Engineering* 22.7-8, pp. 963–978. ISSN: 00981354. DOI: 10.1016/S0098-1354(98)00009-X.

The World Bank (2015). *Sustainable Energy for All 2015 : Progress Toward Sustainable Energy*. ISBN: 9781464802003. DOI: 10.1596/978-1-4648-0690.

Tormodsgard, Y., ed. (2014). *Facts 2014 - The Norwegian petroleum sector*. URL: http://www.npd.no/en/Publications/Facts/Facts-2014/ (visited on 01/12/2015).

Tosserams, S., Etman, L. F. P., Papalambros, P. Y. and Rooda, J. E. (2006). 'An augmented Lagrangian relaxation for analytical target cascading using the alternating direction method of multipliers'. In: *Structural and Multidisciplinary Optimization* 31, pp. 176–189. ISSN: 1615147X. DOI: 10.1007/s00158-005-0579-0.

Tosserams, S., Etman, L. F. P. and Rooda, J. E. (2009). 'Multi-modality in augmented Lagrangian coordination for distributed optimal design'. In: *Structural and Multidisciplinary Optimization* 40.1-6, pp. 329–352. ISSN: 1615-147X. DOI: 10.1007/s00158-009-0371-7.

Trangenstein, J. A. and Bell, J. B. (1989). 'Mathematical Structure of the Black-Oil Model for Petroleum Reservoir Simulation'. In: *SIAM Journal on Applied Mathematics* 49.3, pp. 749–783. ISSN: 0036-1399. DOI: 10.1137/0149044.

Van Doren, J. F. M., Markovinović, R. and Jansen, J. D. (2006). 'Reduced-order optimal control of water flooding using proper orthogonal decomposition'. In: *Computational Geosciences* 10.1, pp. 137–158. ISSN: 1420-0597. DOI: 10.1007/s10596-005-9014-2.

Van Essen, G., Van Den Hof, P. and Jansen, J. D. (2012). 'A Two-Level Strategy to Realize Life-Cycle Production Optimization in an Operational Setting'. In: *SPE Intelligent Energy ...* April, pp. 1–11. ISSN: 1086055X. DOI: 10.2118/149736-MS.

Van Essen, G., Van den Hof, P. and Jansen, J. D. (2011). 'Hierarchical Long-Term and Short-Term Production Optimization'. In: *SPE Journal* 16.1, pp. 4–7. ISSN: 1086-055X. DOI: 10.2118/124332-PA.

Van Essen, G., Zandvliet, M., Van den Hof, P., Bosgra, O. and Jansen, J. D. (2009). 'Robust Waterflooding Optimization of Multiple Geological Scenarios'. In: *SPE Journal* 14.01, pp. 202–210. ISSN: 1086-055X. DOI: 10.2118/102913-PA.

Vielma, J. P., Ahmed, S. and Nemhauser, G. (2010). 'Mixed-Integer Models for Nonseparable Piecewise-Linear Optimization: Unifying Framework and Extensions'. In: *Operations Research* 58.2, pp. 303–315. ISSN: 0030-364X. DOI: 10.1287/opre.1090.0721.

Vielma, J. P. and Nemhauser, G. L. (2011). 'Modeling disjunctive constraints with a logarithmic number of binary variables and constraints'. In: *Mathematical Programming* 128.1-2, pp. 49–72. ISSN: 0025-5610. DOI: 10.1007/s10107-009-0295-4.

Wächter, A. and Biegler, L. T. (2005). 'On the implementation of an interior-point filter line-search algorithm for large-scale nonlinear programming'. In: *Mathematical Programming* 106.1, pp. 25–57. ISSN: 0025-5610. DOI: 10.1007/s10107-004-0559-y.

Wallis, J. R. (1983). 'Incomplete Gaussian Elimination as a Preconditioning for Generalized Conjugate Gradient Acceleration'. In: *Proceedings of SPE Reservoir Simulation Symposium*. 2. Society of Petroleum Engineers. DOI: 10.2523/12265-MS.

Wallis, J. R., Kendall, R. P. and Little, T. E. (1985). 'Constrained Residual Acceleration of Conjugate Residual Methods'. In: *Proceedings of SPE Reservoir Simulation Symposium*. 1. Society of Petroleum Engineers. DOI: 10.2523/13536-MS.

Wang, P., Litvak, M. and Aziz, K. (2002a). 'Optimization of Production from Mature Fields'. In: *Proc. 17th World Petroleum Congress*. Rio de Janeiro, Brazil. URL: https://www.onepetro.org/conference-paper/WPC-32152 (visited on 01/12/2015).

Wang, P., Litvak, M. and Aziz, K. (2002b). 'Optimization of Production Operations in Petroleum Fields'. In: *Proceedings of SPE Annual Technical Conference and Exhibition*. Society of Petroleum Engineers. DOI: 10.2523/77658-MS.

Willersrud, A., Imsland, L., Hauger, S. O. and Kittilsen, P. (2013). 'Short-term production optimization of offshore oil and gas production using nonlinear model predictive control'. In: *Journal of Process Control* 23.2, pp. 215–223. ISSN: 09591524. DOI: 10.1016/j.jprocont.2012.08.005.

Yasari, E. and Pishvaie, M. R. (2015). 'Pareto-based robust optimization of water-flooding using multiple realizations'. In: *Journal of Petroleum Science and Engineering* 132, pp. 18–27. ISSN: 09204105. DOI: 10.1016/j.petrol.2015.04.038.

Yeten, B., Durlofsky, L. J. and Aziz, K. (2003). 'Optimization of Nonconventional Well Type, Location, and Trajectory'. In: *SPE Journal* 8.03, pp. 200–210. ISSN: 1086-055X. DOI: 10.2118/86880-PA.

Younis, R. and Aziz, K. (2007). 'Parallel Automatically Differentiable Data-Types for Next-Generation Simulator Development'. In: *SPE Reservoir Simulation Symposium*. Society of Petroleum Engineers. DOI: 10.2118/106493-MS.

Zakirov, I., Aanonsen, S. I., Zakirov, E. S. and Palatnik, B. M. (1996). 'Optimizing Reservoir Performance by Automatic Allocation of Well Rates'. In: *5th European Conference on the Mathematics of Oil Recovery*. Leoben, Austria, pp. 375–384. DOI: 10.3997/2214-4609.201406895.